Application of finite element nodal model to multigroup diffusion theory

by

Masoud Feiz

A Thesis Submitted to the
Graduate Faculty in Partial Fulfillment of the
Requirements for the Degree of
MASTER OF SCIENCE

Major: Nuclear Engineering

Iowa State University
Ames, Iowa

1983

TABLE OF CONTENTS

LIST OF FIGURES

LIST OF TABLES

I. INTRODUCTION

One of the important parameters which is required in fuel management analysis is the calculation of power distributions within a reactor. Although power calculations are important, the power distributions may not need to be as detailed as other parameters in the design calculations. Therefore, diffusion theory is adapted as the basis for calculating the flux and the power distributions.

Several techniques have been developed to solve the diffusion equation [1]. Of these, fine mesh diffusion theory is usually used for detailed power calculations. Several coarse mesh calculations have also been developed which are better adapted to the requirements of fuel management power distribution analysis [1]. The finite element method is based upon expansion of the flux by polynomials. Nodal methods are based upon dividing the reactor into a number of large nodes and assuming the average flux and the outgoing currents at each surface of the nodal volume are functions of the properties within the volume and the current entering each node [1].

The purpose of this research is to develop and test a finite element nodal model that can be used to determine power distributions in an operating reactor. The technique is based upon polynomial expansion of the neutron flux within the node. Second, third, and fourth order polynomials have proven to be adequate depending on the geometry and the region of the reactor. The model is first

developed using two group diffusion theory, and then an extension is made to a multigroup analysis.

The interface fluxes and average node neutronic properties are used to evaluate the polynomial coefficients. Using these coefficients, one can calculate new fluxes. Since the fluxes are calculated from the coefficients and the coefficients in turn from the fluxes, the technique requires an iterative process. As a result, convergence and stability of the solutions become a problem. However, basic developmental work on the one dimensional model has shown that these problems can be handled by appropriate numerical techniques [2].

II. LITERATURE REVIEW

The representation of the flux within a subregion of a core have been considered extensively as an alternative to the finite difference solutions of the diffusion equation. The primary attraction of this method is the accuracy by which the flux is determined using few mesh points. One of the advantages of using an alternative to finite difference method was explained by Henry [3]. Spatial mesh points 15 or 20 centimeters apart are too large to be used as the intervals in the conventional finite difference method for solving group diffusion equations. Henry explains the problem further and suggests a way to solve it.

> "Thus the numerical problem here is how to take advantage of the fact that very few (rather than very many) mesh points are needed to describe the geometry.
>
> A class of approximation procedures called finite-element methods are particularly well suited for problems of this type. An essential characteristic of finite-element methods is the representation of the function to be determined by a sum of polynomials in its arguments, each polynomial in the sum being defined over only limited ranges of the arguments."

The importance of using nodal models in reactor analysis was well stated by Askew in the summary of a recent international meeting on nodal methods [4].

> "Coarse mesh methods have demonstrated to be a reliable and useful tool for both reactor designers and operators in predicting the assembly to assembly variations of rating for operating reactors. The most advanced models

> appear to be capable of doing this with a RMS error of the order of ±2%. There is scope for further refinement in the modeling of reflectors and shrouds, and in the representation of variations of burnup within an assembly, especially at the core edge or following shuffling of edge assemblies. With improvements of this kind, the models will be capable, given good nuclear data and lattice calculations, of a predictive accuracy of the same order as that of the measurements."

Askew also commented upon the need for pin power models. "It is important, however, that further data on pin power is obtained, and that there is still scope for improving the ways in which this is deduced from the coarse mesh reactor solution."

Similar comments were made by Wagner in the summary of an earlier conference on static reactor calculations [5].

> "With the reactors becoming even larger and requirements for safety and economy getting more stringent, it is generally felt that improved and more consistent mathematical models are needed, that rely less on empirical fitting.... The primary quantities obtained from coarse mesh nodal solutions are node average fluxes and power. Though average reaction rates are also the primary quantities needed for reactivity balances and depletion calculations, the fact that spatial detail within nodes is lost, is certainly a serious drawback of the conventional nodal method."

To date, most of the emphasis have been on the development of the nodal method or finite element method seperately. The finite element nodal model which is the subject of this research, resembles both methods.

III. THEORETICAL DEVELOPMENT OF THE ONE DIMENSIONAL FINITE ELEMENT NODAL MODEL FOR THE TWO GROUP NEUTRON DIFFUSION EQUATIONS

In this chapter the development of the one dimensional model is considered. The technique used in this model is based upon polynomial expansion of the neutron flux within the node. The model is developed using two group theory as an example and the extension to a multigroup analysis is then considered.

The multigroup diffusion equation for a given node has the following form [1]:

$$-\nabla.[D_g \nabla\phi_g(r)] + \Sigma_{\tau g}\phi_g(r) = \frac{\chi_g}{\lambda} \sum_{g'=1}^{G} \nu\Sigma_{fg'}\phi_{g'}(r)$$

$$+ \sum_{\substack{g'=1 \\ g' \neq g}}^{G} \Sigma_{gg'}\Phi_{g'}(r) \qquad (3\text{-}1)$$

where:

$\Phi_g(r)$ = Scaler neutron flux per unit volume at position r for group g.

D_g = Neutron diffusion coefficient for group g.

$\Sigma_{\tau g}$ = Total macroscopic cross section including capture, fission, and removal by scattering in group g.

$\nu\Sigma_{fg'}$ = Neutrons per fission times macroscopic fission cross section in group g'.

$\Sigma_{gg'}$ = Macroscopic scattering cross section of neutrons from group g' to group g.

χ_g = Fraction of fission neutrons produced in group g.

λ = Eigenvalue of equation (3-1). Physically λ is the neutron multiplication constant of the reactor.

For one dimensional steady state conditions with only two neutron groups, the diffusion equation for a given node becomes

$$D_1 \frac{d^2\phi_1}{dx^2} - (\Sigma_{a1} + \Sigma_{1\to2})\,\phi_1 + \frac{1}{\lambda}(\nu\Sigma_{f1}\phi_1 + \nu\Sigma_{f2}\phi_2) = 0 \qquad (3\text{-}2)$$

$$D_2 \frac{d^2\phi_2}{dx^2} - \Sigma_{a2}\phi_2 + \Sigma_{1\to2}\phi_1 = 0 \qquad (3\text{-}3)$$

It is assumed that there is no upscattering. The diffusion equations (3-2) and (3-3) are rewritten for a homogeneous region as the following:

$$\frac{d^2\phi_1}{dx^2} + \alpha_1\phi_1 + \alpha_2\phi_2 = 0 \qquad (3\text{-}4)$$

$$\frac{d^2\phi_2}{dx^2} + B_2\phi_2 + B_1\phi_1 = 0 \qquad (3\text{-}5)$$

where:

$$\alpha_1 = \frac{\frac{1}{\lambda}\nu\Sigma_{f1} - \Sigma_{a1} - \Sigma_{1\to 2}}{D_1}$$

$$\alpha_2 = \frac{1}{\lambda}\frac{\nu\Sigma_{f2}}{D_1}$$

$$B_1 = \frac{\Sigma_{1\to 2}}{D_2}$$

$$B_2 = -\frac{\Sigma_{a2}}{D_2}$$

The assumed flux profile for the finite element nodal model is shown in Figure 3-1. A coordinate system is located at the center of each node. The flux is expanded in this coordinate system for each node.

A. Second-Order Polynomial

The assumption is that the flux in each node can be expressed in the form of a second order polynomial. Since only two group neutrons are used in this chapter, the fluxes in these two groups are approximated by

$$\phi_1(x) = a_0 + a_1x + a_2x^2 \qquad \text{Group I} \qquad (3\text{-}6)$$

$$\phi_2(x) = b_0 + b_1x + b_2x^2 \qquad \text{Group II} \qquad (3\text{-}7)$$

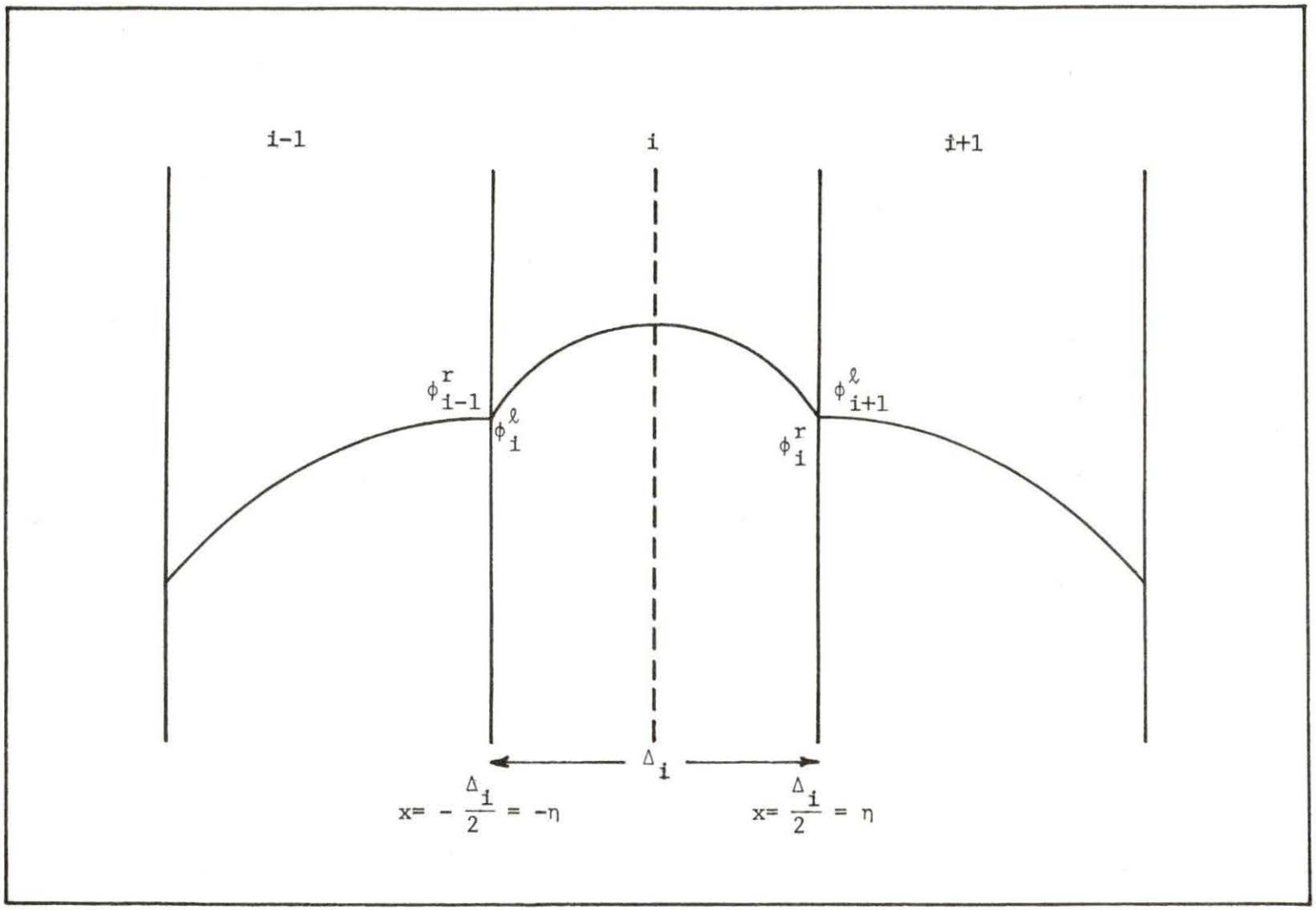

Figure 3-1 Assumed flux profile in one dimensional model

Each one of the polynomials in equations (3-6) and (3-7) has three unknowns namely a_0, a_1, a_2, b_0, b_1, and b_2. Therefore, six conditions are needed to find these six unknowns.

The first assumption is that the fluxes at the right and left of a given node for the two groups are known. Therefore, as it is shown in Figure 3-1, the following four equations would result from this assumption

$$\phi_1^{\ell} = \phi_1(-\eta) = a_0 - a_1 \eta + a_2 \eta^2 \tag{3-8}$$

$$\phi_1^{r} = \phi_1(\eta) = a_0 + a_1 \eta + a_2 \eta^2 \tag{3-9}$$

$$\phi_2^{\ell} = \phi_2(-\eta) = b_0 - b_1 \eta + b_2 \eta^2 \tag{3-10}$$

$$\phi_2^{r} = \phi_2(\eta) = b_0 + b_1 \eta + b_2 \eta^2 \tag{3-11}$$

Equations (3-8) and (3-9) as well as (3-10) and (3-11) are then added and subtracted as follows:

$$\frac{\phi_1^{r} + \phi_1^{\ell}}{2} = a_0 + a_2 \eta^2 \tag{3-12}$$

$$\frac{\phi_1^{r} - \phi_1^{\ell}}{2} = a_1 \eta \tag{3-13}$$

$$\frac{\phi_2^r + \phi_2^\ell}{2} = b_0 + b_2 \eta^2 \tag{3-14}$$

$$\frac{\phi_2^r - \phi_2^\ell}{2} = b_1 \eta \tag{3-15}$$

The coefficients a_0, a_1, b_0, and b_1 are found using equations (3-12) through (3-15), respectively.

$$a_0 = \frac{\phi_1^r + \phi_1^\ell}{2} - a_2 \eta^2 \tag{3-16}$$

$$a_1 = \frac{\phi_1^r - \phi_1^\ell}{2\eta} \tag{3-17}$$

$$b_0 = \frac{\phi_2^r + \phi_2^\ell}{2} - b_2 \eta^2 \tag{3-18}$$

$$b_1 = \frac{\phi_2^r - \phi_2^\ell}{2\eta} \tag{3-19}$$

But a_2 and b_2 are still unknown to completely define the polynomials, therefore, another condition is needed.

The second derivatives of equations (3-6) and (3-7) are:

$$\frac{d^2\phi_1}{dx^2} = 2a_2 \tag{3-20}$$

$$\frac{d^2\phi_2}{dx^2} = 2b_2 \tag{3-21}$$

Equations (3-6) and (3-7) as well as (3-20) and (3-21) are then inserted into equations (3-4) and (3-5). Since the polynomial solutions are only approximations, the equations are not equal to zero. Therefore, let

$$2a_2 + \alpha_1 (\tilde{a}_0 + \tilde{a}_1 x + \tilde{a}_2 x^2) + \alpha_2 (\tilde{b}_0 + \tilde{b}_1 x + \tilde{b}_2 x^2) = g_1(x) \quad (3\text{-}22)$$

$$2b_2 + \beta_1 (\tilde{a}_0 + \tilde{a}_1 x + \tilde{a}_2 x^2) + \beta_2 (\tilde{b}_0 + \tilde{b}_1 x + \tilde{b}_2 x^2) = g_2(x) \quad (3\text{-}23)$$

where $g_1(x)$ and $g_2(x)$ are assumed to be functions of x and are defined by the left hand side of equations (3-22) and (3-23). Now, rewrite equations (3-22) and (3-23) as

$$2a_2 + f_1(x) = g_1(x) \quad (3\text{-}24)$$

$$2b_2 + f_2(x) = g_2(x) \quad (3\text{-}25)$$

where

$$f_1(x) = \alpha_1 (\tilde{a}_0 + \tilde{a}_1 x + \tilde{a}_2 x^2) + \alpha_2 (\tilde{b}_0 + \tilde{b}_1 x + \tilde{b}_2 x^2)$$

$$f_2(x) = \beta_1 (\tilde{a}_0 + \tilde{a}_1 x + \tilde{a}_2 x^2) + \beta_2 (\tilde{b}_0 + \tilde{b}_1 x + \tilde{b}_2 x^2)$$

and are known from a previous iterate.

One requires a minimization of the following integrals

$$\int_{-\eta}^{\eta} g_1^2(x)dx \tag{3-26}$$

$$\int_{-\eta}^{\eta} g_2^2(x)dx \tag{3-27}$$

The idea behind this condition would be more clear if one looks at Figure 3-2, which shows a second order fit to the flux (constant fit on a second derivative). It is desired to minimize the differences shown by the dashed area in Figure 3-2 by the integrals in equations (3-26) and (3-27). The functions $g_1(x)$ and $g_2(x)$ are squared so that the area differences are all positive. It is also assumed that $f_1(x)$ and $f_2(x)$ are independent of a_2 and b_2, respectively, for the purpose of the minimization process.

To minimize equations (3-26) and (3-27), one differentiates them with respect to a_2 and b_2, respectively, and then sets the results equal to zero. By the use of Leibnitz rule, one has

$$\frac{\partial}{\partial a_2}\int_{-\eta}^{\eta} g_1^2(x)dx = 2\int_{-\eta}^{\eta} g_1(x)\,\frac{\partial g_1(x)}{\partial a_2}\,dx = 0 \tag{3-28}$$

$$\frac{\partial}{\partial b_2}\int_{-\eta}^{\eta} g_2^2(x)dx = 2\int_{-\eta}^{\eta} g_2(x)\,\frac{\partial g_2(x)}{\partial b_2}\,dx = 0 \tag{3-29}$$

$\frac{\partial g_1(x)}{\partial a_2}$ and $\frac{\partial g_2(x)}{\partial b_2}$ are found from equations (3-24) and (3-25)

$$\frac{\partial g_1(x)}{\partial a_2} = 2$$

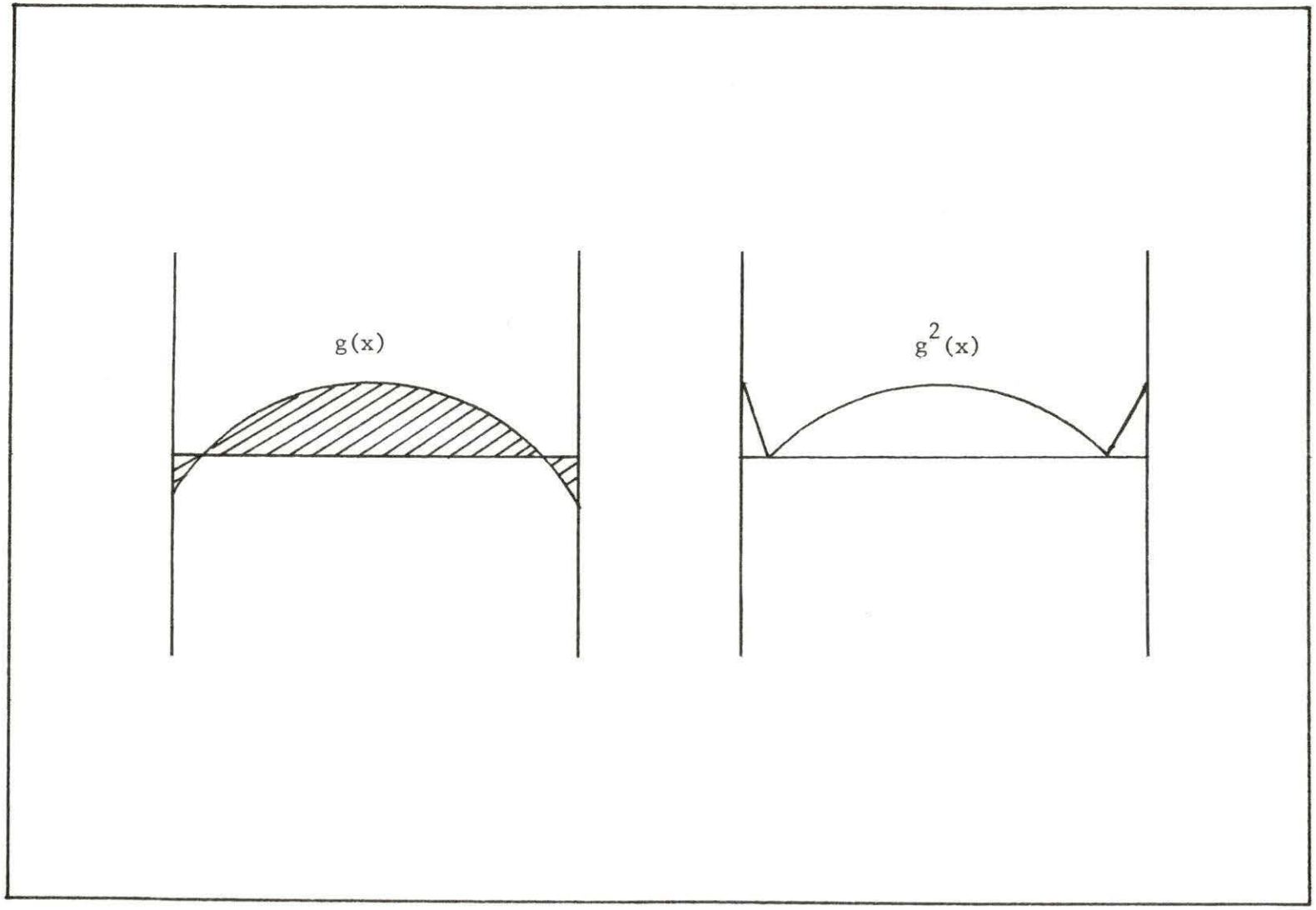

Figure 3-2 Spatial neutron balance approximation for a constant fit

$$\frac{\partial g_2(x)}{\partial b_2} = 2$$

Therefore, equations (3-28) and (3-29) become

$$4 \int_{-\eta}^{\eta} g_1(x)dx = 0$$

$$4 \int_{-\eta}^{\eta} g_2(x)dx = 0$$

$$\int_{-\eta}^{\eta} g_1(x)dx = 0 \qquad (3\text{-}30)$$

$$\int_{-\eta}^{\eta} g_2(x)dx = 0 \qquad (3\text{-}31)$$

Substituting for $g_1(x)$ and $g_2(x)$ from equations (3-22) and (3-23) into equations (3-30) and (3-31), one has the following results

$$\int_{-\eta}^{\eta} [2a_2 + \alpha_1 (\tilde{a}_0 + \tilde{a}_1 x + \tilde{a}_2 x^2) + \alpha_2 (\tilde{b}_0 + \tilde{b}_1 x + \tilde{b}_2 x^2)]dx = 0 \qquad (3\text{-}32)$$

$$\int_{-\eta}^{\eta} [2b_2 + \beta_1 (\tilde{a}_0 + \tilde{a}_1 x + \tilde{a}_2 x^2) + \beta_2 (\tilde{b}_0 + \tilde{b}_1 x + \tilde{b}_2 x^2)]dx = 0 \qquad (3\text{-}33)$$

If equations (3-32) and (3-33) are integrated and evaluated between (η) and $(-\eta)$, the expressions for a_2 and b_2 can be found

$$a_2 = -\frac{1}{2}(\alpha_1 \tilde{a}_0 + \alpha_2 \tilde{b}_0) - \frac{\eta^2}{6}(\alpha_1 \tilde{a}_2 + \alpha_2 \tilde{b}_2) \tag{3-34}$$

$$b_2 = -\frac{1}{2}(\beta_1 \tilde{a}_0 + \beta_2 \tilde{b}_0) - \frac{\eta^2}{6}(\beta_1 \tilde{a}_2 + \beta_2 \tilde{b}_2) \tag{3-35}$$

where the terms on the right hand side are evaluated from a previous iterate.

In summary, for the two group neutrons using a second order polynomial, the following equations were used

$$\phi_1(x) = a_0 + a_1 x + a_2 x^2 \tag{3-6}$$

$$\phi_2(x) = b_0 + b_1 x + b_2 x^2 \tag{3-7}$$

where the coefficients are found using the following equations

$$a_0 = \frac{\phi_1^r + \phi_1^\ell}{2} - a_2 \eta^2 \tag{3-16}$$

$$a_1 = \frac{\phi_1^r - \phi_1^\ell}{2\eta} \tag{3-17}$$

$$a_2 = -\frac{1}{2}(\alpha_1 \tilde{a}_0 + \alpha_2 \tilde{b}_0) - \frac{\eta^2}{6}(\alpha_1 \tilde{a}_2 + \alpha_2 \tilde{b}_2) \tag{3-34}$$

$$b_0 = \frac{\phi_2^r + \phi_2^\ell}{2} - b_2 \eta^2 \tag{3-18}$$

$$b_1 = \frac{\phi_2^r - \phi_2^\ell}{2\eta} \tag{3-19}$$

$$b_2 = -\frac{1}{2}(\beta_1 \tilde{a}_0 + \beta_2 \tilde{b}_0) - \frac{\eta^2}{6}(\beta_1 \tilde{a}_2 + \beta_2 \tilde{b}_2) \qquad (3\text{-}35)$$

The whole process requires an iterative technique in which α_1, α_2, β_1, and β_2 are nuclear data and are known. At the beginning of the process, ϕ_1^r, ϕ_1^ℓ, ϕ_2^r, ϕ_2^ℓ, a_0, a_1, a_2, b_0, b_1, and b_2 are assumed to be known. New polynomial coefficients are calculated using equations (3-16) through (3-19), and equations (3-34) through (3-35). New ϕ_1^r, ϕ_1^ℓ, ϕ_2^r, and ϕ_2^ℓ are found using the boundary conditions (see Figure 3-1). Using the new ϕ_1^r, ϕ_1^ℓ, ϕ_2^r, and ϕ_2^ℓ values, a set of new polynomial coefficients are calculated and the process, is continued until convergence occurs.

B. Third-Order Polynomial

The extension of the polynomial analysis to third order polynomial is the assumption that the flux in each node can be expressed in the form of a third order polynomial. Since only two group neutrons are used in this chapter, the fluxes in these two groups are approximated by

$$\phi_1(x) = a_0 + a_1 x + a_2 x^2 + a_3 x^3 \qquad \text{Group I} \qquad (3\text{-}36)$$

$$\phi_2(x) = b_0 + b_1 x + b_2 x^2 + b_3 x^3 \qquad \text{Group II} \qquad (3\text{-}37)$$

Each one of the polynomials in equations (3-36) and (3-37) has four unknowns, namely a_0, a_1, a_2, a_3, b_0, b_1, b_2, and b_3. Therefore,

eight conditions are needed to find these eight unknowns. As it was observed in the second-order polynomial, the form of the coefficients for the two polynomials are similar. Therefore, the coefficients for the first group would be found here and the coefficients for the second group could be developed in a similar manner.

The first assumption is that again the fluxes at the right and left of a given node for the group are known. Therefore, as it is shown in Figure 3-1, the following equations would result from this assumption

$$\phi_1^{\ell} = \phi_1(-\eta) = a_0 - a_1\eta + a_2\eta^2 - a_3\eta^3 \tag{3-38}$$

$$\phi_1^{r} = \phi_1(\eta) = a_0 + a_1\eta + a_2\eta^2 + a_3\eta^3 \tag{3-39}$$

Equations (3-38) and (3-39) are added and subtracted and the coefficients a_0, and a_1 are found.

$$a_0 = \frac{\phi_1^{r} + \phi_1^{\ell}}{2} - a_2\eta^2 \tag{3-40}$$

$$a_1 = \frac{\phi_1^{r} - \phi_1^{\ell}}{2\eta} - a_3\eta^2 \tag{3-41}$$

But a_2 and a_3 are still unknown, therefore, two other conditions are needed.

The second derivative of equation (3-36) is

$$\frac{d^2\phi_1}{dx^2} = 2a_2 + 6a_3x \tag{3-42}$$

Equation (3-42) as well as (3-36) and (3-37) are then inserted into equation (3-4). Again, since the polynomial solution is only an approximation, the equation is not equal to zero. Therefore, let

$$2a_2 + 6a_3x + \alpha_1 (\tilde{a}_0 + \tilde{a}_1x + \tilde{a}_2x^2 + \tilde{a}_3x^3)$$

$$+ \alpha_2 (\tilde{b}_0 + \tilde{b}_1x + \tilde{b}_2x^2 + \tilde{b}_3x^3) = g_1(x) \tag{3-43}$$

where $g_1(x)$ is assumed to be a function of x and is defined by the left hand side of equation (3-43). Now rewrite equation (3-43) as

$$2a_2 + 6a_3x + f_1(x) = g_1(x) \tag{3-44}$$

where

$$f_1(x) = \alpha_1 (\tilde{a}_0 + \tilde{a}_1x + \tilde{a}_2x^2 + \tilde{a}_3x^3) + \alpha_2 (\tilde{b}_0 + \tilde{b}_1x + \tilde{b}_2x^2$$

$$+ \tilde{b}_3x^3)$$

and again is assumed known from a previous iterate.

One requires a minimization of the following integral with respect to a_2 and a_3 to determine these respective coefficients:

$$\int_{-\eta}^{\eta} g_1^2(x)dx \tag{3-45}$$

Again, the idea behind this condition would be more clear if one looks at Figure 3-3, which shows a third order fit to the flux (first order fit on a second derivative). It is desired to minimize the differences shown by the dashed area in Figure 3-3, by the integral in equation (3-45). The function $g_1(x)$ is squared so that the area differences are all positive. It is also assumed that $f_1(x)$ is independent of both a_2 and a_3 for the purpose of the minimization process.

To minimize equation (3-45), one differentiates it with respect to a_2 and a_3, respectively, and then sets the results equal to zero. By the use of Leibnitz rule one has

$$\frac{\partial}{\partial a_2}\int_{-\eta}^{\eta} g_1^2(x)dx = 2\int_{-\eta}^{\eta} g_1(x)\,\frac{\partial g_1(x)}{\partial a_2}\,dx = 0 \tag{3-46}$$

$$\frac{\partial}{\partial a_3}\int_{-\eta}^{\eta} g_1^2(x)dx = 2\int_{-\eta}^{\eta} g_1(x)\,\frac{\partial g_1(x)}{\partial a_3}\,dx = 0 \tag{3-47}$$

$\frac{\partial g_1(x)}{\partial a_2}$ and $\frac{\partial g_1(x)}{\partial a_3}$ are found from equation (3-44)

$$\frac{\partial g_1(x)}{\partial a_2} = 2$$

$$\frac{\partial g_1(x)}{\partial a_3} = 6x$$

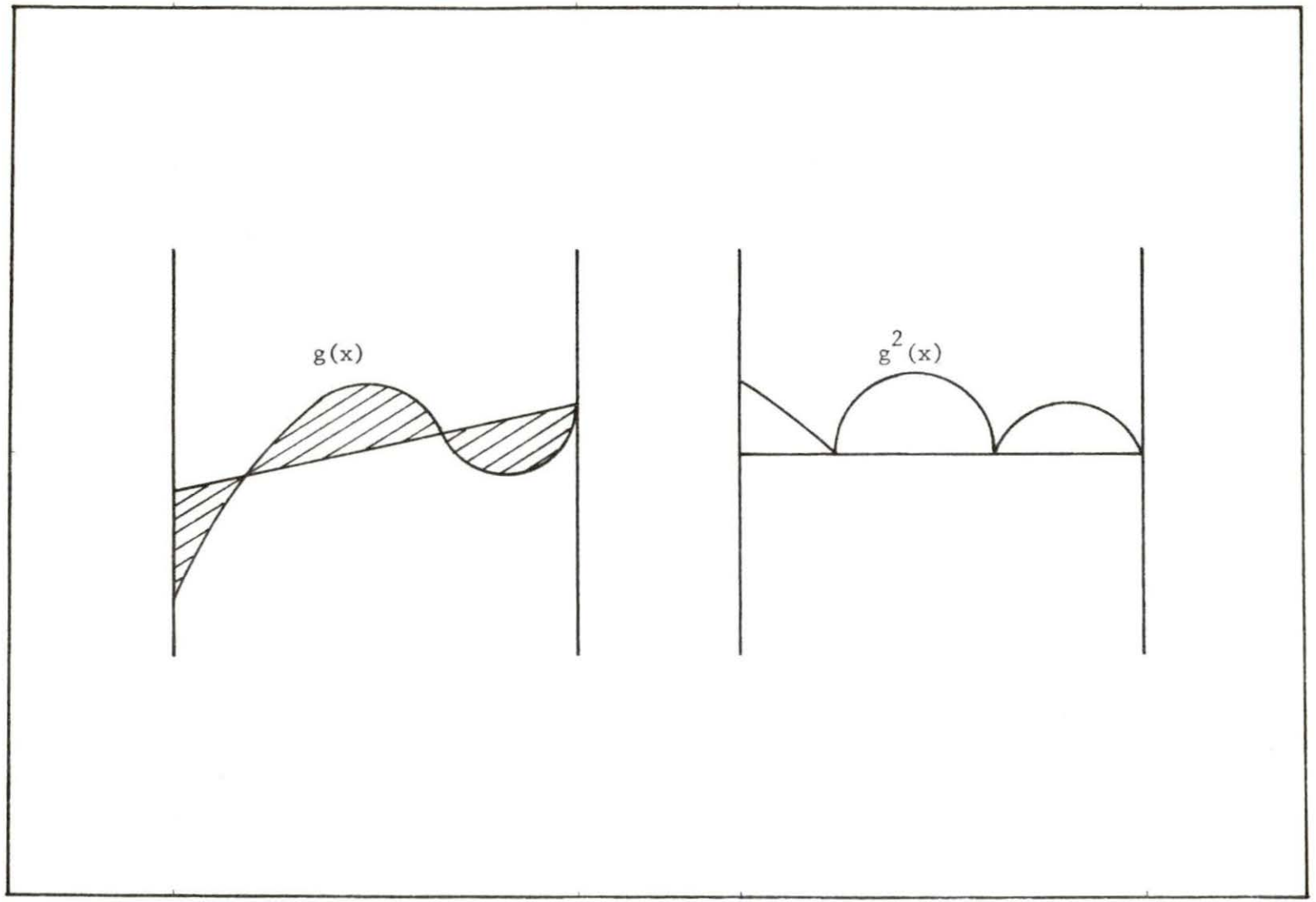

Figure 3-3 Spatial neutron balance approximation for a first order fit

Therefore, equations (3-46) and (3-47) become

$$\int_{-\eta}^{\eta} g_1(x)dx = 0 \tag{3-48}$$

$$\int_{-\eta}^{\eta} xg_1(x)dx = 0 \tag{3-49}$$

Substituting for $g_1(x)$ from equation (3-43) into equations (3-48) and (3-49), one has the following results

$$\int_{-\eta}^{\eta} [2a_2 + 6a_3x + \alpha_1 (\tilde{a}_0 + \tilde{a}_1x + \tilde{a}_2x^2 + \tilde{a}_3x^3) + \alpha_2 (\tilde{b}_0 + \tilde{b}_1x + \tilde{b}_2x^2 + \tilde{b}_3x^3)]dx = 0 \tag{3-50}$$

$$\int_{-\eta}^{\eta} x[2a_2 + 6a_3x + \alpha_1 (\tilde{a}_0 + \tilde{a}_1x + \tilde{a}_2x^2 + \tilde{a}_3x^3) + \alpha_2 (\tilde{b}_0 + \tilde{b}_1x + \tilde{b}_2x^2 + \tilde{b}_3x^3)]dx = 0 \tag{3-51}$$

If equations (3-50) and (3-51) are integrated and evaluated between (η) and ($-\eta$), the expressions for a_2 and a_3 can be found

$$a_2 = -\frac{1}{2} (\alpha_1 \tilde{a}_0 + \alpha_2 \tilde{b}_0) - \frac{\eta^2}{6} (\alpha_1 \tilde{a}_2 + \alpha_2 \tilde{b}_2) \tag{3-52}$$

$$a_3 = -\frac{1}{6} (\alpha_1 \tilde{a}_1 + \alpha_2 \tilde{b}_1) - \frac{\eta^2}{10} (\alpha_1 \tilde{a}_3 + \alpha_2 \tilde{b}_3) \tag{3-53}$$

where the terms on the right hand side are evaluated from a previous iterate.

Similar expressions could be found for the coefficients of the second group by applying the same procedure. If this is done, one has the following results

$$b_0 = \frac{\phi_2^r + \phi_2^\ell}{2} - b_2\eta^2 \tag{3-54}$$

$$b_1 = \frac{\phi_2^r - \phi_2^\ell}{2\eta} - b_3\eta^2 \tag{3-55}$$

$$b_2 = -\frac{1}{2}(\beta_1\tilde{a}_0 + \beta_2\tilde{b}_0) - \frac{\eta^2}{6}(\beta_1\tilde{a}_2 + \beta_2\tilde{b}_2) \tag{3-56}$$

$$b_3 = -\frac{1}{6}(\beta_1\tilde{a}_1 + \beta_2\tilde{b}_1) - \frac{\eta^2}{10}(\beta_1\tilde{a}_3 + \beta_2\tilde{b}_3) \tag{3-57}$$

The iterative process is carried out the same as the one mentioned for the second order polynomial with the exception that initial values for a_3 and b_3 should also be specified.

C. Fourth-Order Polynomial

The extension of the polynomial analysis to fourth order polynomial is the assumption that the flux in each node can be expressed in the form of a fourth order polynomial. Since only two group neutrons are used in this chapter, the fluxes in these two groups are approximated by

$$\phi_1(x) = a_0 + a_1x + a_2x^2 + a_3x^3 + a_4x^4 \qquad \text{Group I} \tag{3-58}$$

$$\phi_2(x) = b_0 + b_1x + b_2x^2 + b_3x^3 + b_4x^4 \qquad \text{Group II} \tag{3-59}$$

Each one of the polynomials in equations (3-58) and (3-59) has five unknowns, namely a_0, a_1, a_2, a_3, a_4, b_0, b_1, b_2. b_3, and b_4. Therefore, ten conditions are needed to find these ten unknowns. As it was observed in the second-order polynomial, the form of the coefficients for the two polynomials is similar. Therefore, the coefficients for the first group would be found here and the coefficients for the second group could be developed in a similar manner.

The first assumption is that again the fluxes at the right and left of a given node for the group are known. Therefore, as it is shown in Figure 3-1, the following equations would result from this assumption

$$\phi_1^{\ell} = \phi_1(-\eta) = a_0 - a_1\eta + a_2\eta^2 - a_3\eta^3 + a_4\eta^4 \tag{3-60}$$

$$\phi_1^{r} = \phi_1(\eta) = a_0 + a_1\eta + a_2\eta^2 + a_3\eta^3 + a_4\eta^4 \tag{3-61}$$

Equations (3-60) and (3-61) are added and subtracted and the coefficients a_0 and a_1 are found.

$$a_0 = \frac{\phi_1^{r} + \phi_1^{\ell}}{2} - a_2\eta^2 - a_4\eta^4 \tag{3-62}$$

$$a_1 = \frac{\phi_1^{r} - \phi_1^{\ell}}{2\eta} - a_3\eta^2 \tag{3-63}$$

But a_2, a_3, and a_4 are still unknown. Therefore, three other conditions are needed.

The second derivative of equation (3-58) is

$$\frac{d^2\phi_1}{dx^2} = 2a_2 + 6a_3x + 12a_4x^2 \tag{3-64}$$

Equation (3-64) as well as (3-58) and (3-59) are then inserted into equation (3-4). Again, since the polynomial solution is only an approximation, the equation is not equal to zero. Therefore, let

$$2a_2 + 6a_3x + 12a_4x^2 + \alpha_1 (\tilde{a}_0 + \tilde{a}_1x + \tilde{a}_2x^2 + \tilde{a}_3x^3 + \tilde{a}_4x^4)$$

$$+ \alpha_2 (\tilde{b}_0 + \tilde{b}_1x + \tilde{b}_2x^2 + \tilde{b}_3x^3 + \tilde{b}_4x^4) = g_1(x) \tag{3-65}$$

where $g_1(x)$ is assumed to be a function of x and is defined by the left hand side of equation (3-65). Now rewrite equation (3-65) as

$$2a_2 + 6a_3x + 12a_4x^2 + f_1(x) = g_1(x) \tag{3-66}$$

where

$$f_1(x) = \alpha_1 (\tilde{a}_0 + \tilde{a}_1x + \tilde{a}_2x^2 + \tilde{a}_3x^3 + \tilde{a}_4x^4) + \alpha_2 (\tilde{b}_0 + \tilde{b}_1x + \tilde{b}_2x^2$$

$$+ \tilde{b}_3x^3 + \tilde{b}_4x^4)$$

and again is assumed known from a previous iterate.

One requires a minimization of the following integral with respect to a_2, a_3, and a_4 to determine these respective coefficients:

$$\int_{-\eta}^{\eta} g_1^2 (x)dx \tag{3-67}$$

Again, the idea behind this condition would be more clear if one looks at Figure 3-4, which shows a fourth order fit to the flux (second order fit on a second derivative). It is desired to minimize the differences shown by the dashed area in Figure 3-4, by the integral in equation (3-67). The function $g_1(x)$ is squared so that the area differences are all positive. It is also assumed that $f_1(x)$ is independent of a_2, a_3, and a_4 for the purpose of the minimization process.

To minimize equation (3-67), one differentiates it with respect to a_2, a_3, and a_4, respectively, and then sets the results equal to zero. By the use of Leibnitz rule one has

$$\frac{\partial}{\partial a_2}\int_{-\eta}^{\eta} g_1^2 (x)dx = 2\int_{-\eta}^{\eta} g_1(x) \frac{\partial g_1(x)}{\partial a_2} dx = 0 \tag{3-68}$$

$$\frac{\partial}{\partial a_3}\int_{-\eta}^{\eta} g_1^2 (x)dx = 2\int_{-\eta}^{\eta} g_1(x) \frac{\partial g_1(x)}{\partial a_3} dx = 0 \tag{3-69}$$

$$\frac{\partial}{\partial a_4}\int_{-\eta}^{\eta} g_1^2 (x)dx = 2\int_{-\eta}^{\eta} g_1(x) \frac{\partial g_1(x)}{\partial a_4} dx = 0 \tag{3-70}$$

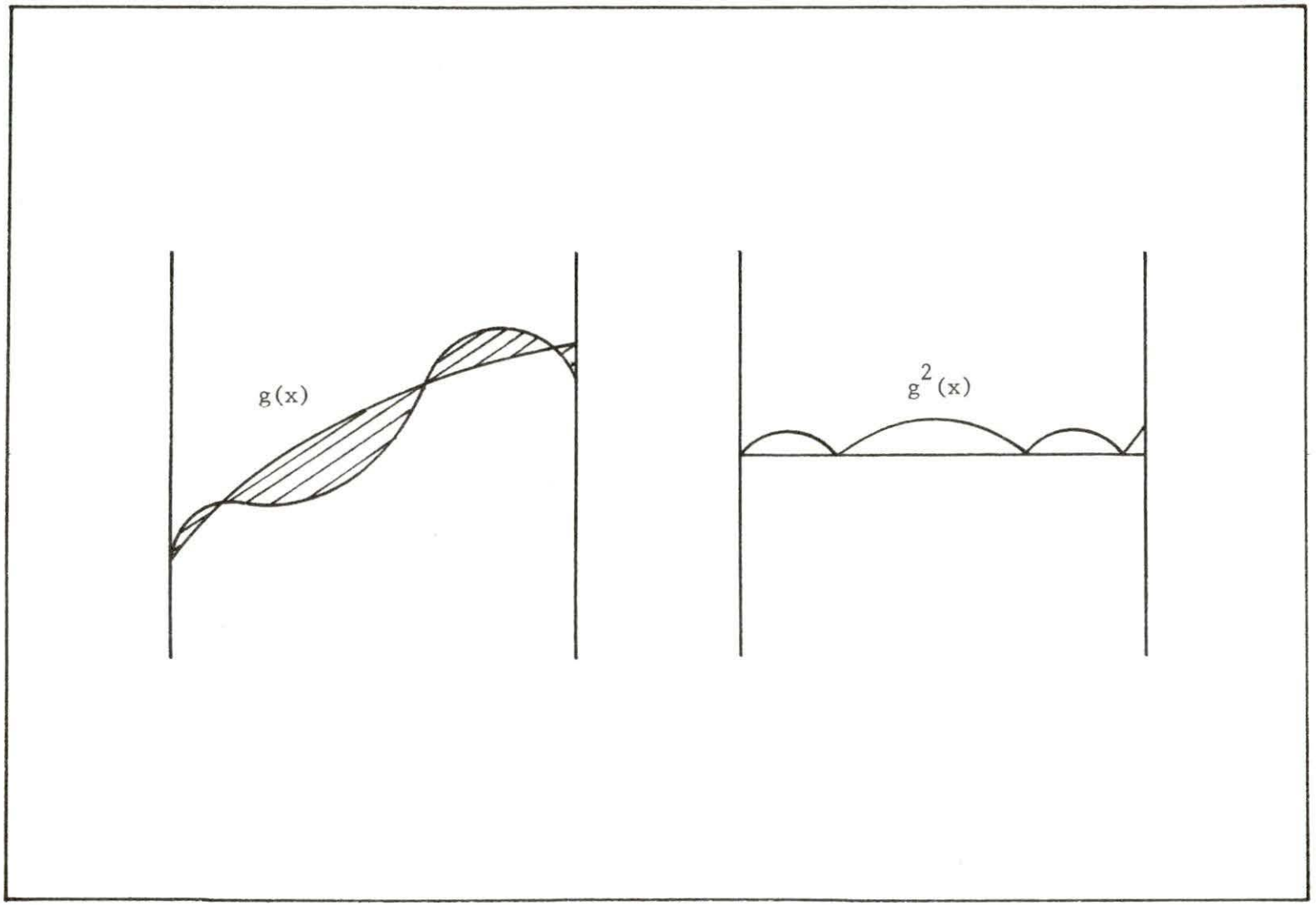

Figure 3-4 Spatial neutron balance approximation for a second order fit

$\frac{\partial g_1(x)}{\partial a_2}$, $\frac{\partial g_1(x)}{\partial a_3}$, and $\frac{\partial g_1(x)}{\partial a_4}$ are found from equation (3-66)

$$\frac{\partial g_1(x)}{\partial a_2} = 2$$

$$\frac{\partial g_1(x)}{\partial a_3} = 6x$$

$$\frac{\partial g_1(x)}{\partial a_4} = 12x^2$$

Therefore, equations (3-68) through (3-70) become

$$\int_{-\eta}^{\eta} g_1(x)dx = 0 \tag{3-71}$$

$$\int_{-\eta}^{\eta} xg_1(x)dx = 0 \tag{3-72}$$

$$\int_{-\eta}^{\eta} x^2 g_1(x)dx = 0 \tag{3-73}$$

Substituting for $g_1(x)$ from equation (3-65) into equations (3-71) through (3-73), one has the following results

$$\int_{-\eta}^{\eta} [2a_2 + 6a_3x + 12a_4x^2 + \alpha_1(\tilde{a}_0 + \tilde{a}_1x + \tilde{a}_2x^2 + \tilde{a}_3x^3 + \tilde{a}_4x^4)$$

$$+ \alpha_2(\tilde{b}_0 + \tilde{b}_1x + \tilde{b}_2x^2 + \tilde{b}_3x^3 + \tilde{b}_4x^4)]dx = 0 \tag{3-74}$$

$$\int_{-\eta}^{\eta} x[2a_2 + 6a_3x + 12a_4x^2 + \alpha_1(\tilde{a}_0 + \tilde{a}_1x + \tilde{a}_2x^2 + \tilde{a}_3x^3 + \tilde{a}_3x^4)$$

$$+ \alpha_2(\tilde{b}_0 + \tilde{b}_1x + \tilde{b}_2x^2 + \tilde{b}_3x^3 + \tilde{b}_4x^4)]dx = 0 \qquad (3\text{-}75)$$

$$\int_{-\eta}^{\eta} x^2[2a_2 + 6a_3x + 12a_4x^2 + \alpha_1(\tilde{a}_0 + \tilde{a}_1x + \tilde{a}_2x^2 + \tilde{a}_3x^3 + \tilde{a}_4x^4)$$

$$+ \alpha_2(\tilde{b}_0 + \tilde{b}_1x + \tilde{b}_2x^2 + \tilde{b}_3x^3 + \tilde{b}_4x^4)]dx = 0 \qquad (3\text{-}76)$$

If equations (3-74) through (3-76) are integrated and evaluated between (η) and ($-\eta$), the expressions for a_2, a_3, and a_4 can be found.

$$a_2 = -\frac{1}{2}(\alpha_1\tilde{a}_0 + \alpha_2\tilde{b}_0) - \frac{\eta^2}{6}(\alpha_1\tilde{a}_2 + \alpha_2\tilde{b}_2) - \frac{\eta^4}{10}(\alpha_1\tilde{a}_4 + \alpha_2\tilde{b}_4)$$

$$- 2a_4\eta^2 \qquad (3\text{-}77)$$

$$a_3 = -\frac{1}{6}(\alpha_1\tilde{a}_1 + \alpha_2\tilde{b}_1) - \frac{\eta^2}{10}(\alpha_1\tilde{a}_3 + \alpha_2\tilde{b}_3) \qquad (3\text{-}78)$$

$$a_4 = -\frac{1}{12}(\alpha_1\tilde{a}_2 + \alpha_2\tilde{b}_2) - \frac{\eta^2}{14}(\alpha_1\tilde{a}_4 + \alpha_2\tilde{b}_4) \qquad (3\text{-}79)$$

where the terms on the right hand side are evaluated from a previous iterate.

Similar expressions could be found for the coefficients of the second group by applying the same procedure. If this is done, one has the following results

$$b_0 = \frac{\phi_2^r + \phi_2^\ell}{2} - b_2\eta^2 - b_4\eta^4 \tag{3-80}$$

$$b_1 = \frac{\phi_2^r - \phi_2^\ell}{2\eta} - b_3\eta^2 \tag{3-81}$$

$$b_2 = -\frac{1}{2}(\beta_1\tilde{a}_0 + \beta_2\tilde{b}_0) - \frac{\eta^2}{6}(\beta_1\tilde{a}_2 + \beta_2\tilde{b}_2) - \frac{\eta^4}{10}(\beta_1\tilde{a}_4 + \beta_2\tilde{b}_4)$$

$$- 2b_4\eta^2 \tag{3-82}$$

$$b_3 = -\frac{1}{6}(\beta_1\tilde{a}_1 + \beta_2\tilde{b}_1) - \frac{\eta^2}{10}(\beta_1\tilde{a}_3 + \beta_2\tilde{b}_3) \tag{3-83}$$

$$b_4 = -\frac{1}{12}(\beta_1\tilde{a}_2 + \beta_2\tilde{b}_2) - \frac{\eta^2}{14}(\beta_1\tilde{a}_4 + \beta_2\tilde{b}_4) \tag{3-84}$$

The iterative process is carried out the same as the one mentioned for the second order polynomial with the exception that initial values for a_3, b_3, a_4, and b_4 should also be specified.

One can show that the coefficients of the fourth order polynomial can reduce to the coefficients of the second, and third order polynomials. For the second order polynomial, a_3, a_4, b_3, and b_4 are set equal to zero and the following equations would result

$$a_0 = \frac{\phi_1^r + \phi_1^\ell}{2} - a_2\eta^2$$

$$a_1 = \frac{\phi_1^r - \phi_1^\ell}{2\eta}$$

$$a_2 = -\frac{1}{2}(\alpha_1\tilde{a}_0 + \alpha_2\tilde{b}_0) - \frac{\eta^2}{6}(\alpha_1\tilde{a}_2 + \alpha_2\tilde{b}_2)$$

$$b_0 = \frac{\phi_2^r + \phi_2^\ell}{2} - b_2\eta^2$$

$$b_1 = \frac{\phi_2^r - \phi_2^\ell}{2\eta}$$

$$b_2 = -\frac{1}{2}(\beta_1\tilde{a}_0 + \beta_2\tilde{b}_0) - \frac{\eta^2}{6}(\beta_1\tilde{a}_2 + \beta_2\tilde{b}_2)$$

which are exactly the same coefficients that were found for the second order polynomial.

For the third order polynomial, a_4 and b_4 are set equal to zero.

$$a_0 = \frac{\phi_1^r + \phi_1^\ell}{2} - a_2\eta^2$$

$$a_1 = \frac{\phi_1^r - \phi_1^\ell}{2\eta} - a_3\eta^2$$

$$a_2 = -\frac{1}{2}(\alpha_1\tilde{a}_0 + \alpha_2\tilde{b}_0) - \frac{\eta^2}{6}(\alpha_1\tilde{a}_2 + \alpha_2\tilde{b}_2)$$

$$a_3 = -\frac{1}{6}(\alpha_1\tilde{a}_1 + \alpha_2\tilde{b}_1) - \frac{\eta^2}{10}(\alpha_1\tilde{a}_3 + \alpha_2\tilde{b}_3)$$

$$b_0 = \frac{\phi_2^r + \phi_2^\ell}{2} - b_2\eta^2$$

$$b_1 = \frac{\phi_2^r - \phi_2^\ell}{2\eta} - b_3\eta^2$$

$$b_2 = -\frac{1}{2}(\beta_1\tilde{a}_0 + \beta_2\tilde{b}_0) - \frac{\eta^2}{6}(\beta_1\tilde{a}_2 + \beta_2\tilde{b}_2)$$

$$b_3 = -\frac{1}{6}(\beta_1\tilde{a}_1 + \beta_2\tilde{b}_1) - \frac{\eta^2}{10}(\beta_1\tilde{a}_3 + \beta_2\tilde{b}_3)$$

which are exactly the same coefficients that were found for the third order polynomial.

D. Interface Condition

The interface condition between two nodes is shown in Figure 3-5. It is required by the continuity of flux at the interface that ϕ_i^r be equal to ϕ_{i+1}^{ℓ} at any interface.

$$\phi_i^r = \phi_{i+1}^{\ell} \tag{3-85}$$

Two new parameters, namely ψ_i^r and ψ_{i+1}^{ℓ}, are defined such that they satisfy the following finite difference equations at any interface

$$\frac{\phi_i^r - \psi_i^r}{\theta_i} = \left.\frac{d\phi_i}{dx}\right|_{\text{interface}} \tag{3-86}$$

$$\frac{\psi_{i+1}^{\ell} - \phi_{i+1}^{\ell}}{\theta_{i+1}} = \left.\frac{d\phi_{i+1}}{dx}\right|_{\text{interface}} \tag{3-87}$$

where θ is a distance parameter that is chosen arbitrarily. Also, $\frac{d\phi}{dx}$ depends on the order of the polynomial that is being used. The fourth order polynomial for the first neutron group is written here. Similar expressions could be written for lower order polynomials by setting the appropriate higher order coefficients equal to zero.

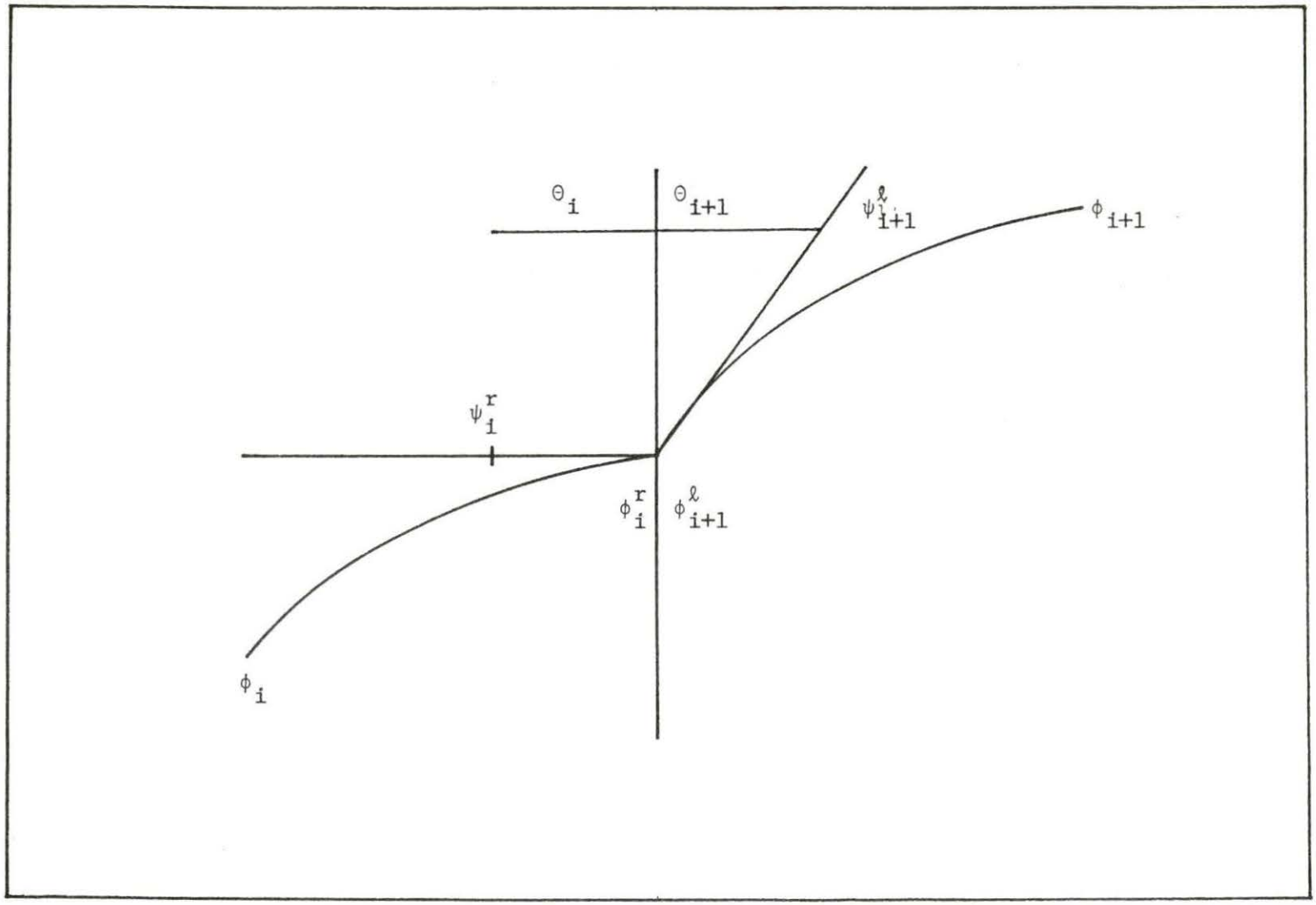

Figure 3-5 Assumed flux profiles at the interface

$$\left.\frac{d\phi_i^r}{dx}\right|_{x=\eta_i} = a_1 + 2a_2x + 3a_3x + 4a_4x^3\Big|_{x=\eta_i} \tag{3-88}$$

where the coefficients a_1 through a_4 in equation (3-88) are the coefficients which were evaluated for node i.

$$\left.\frac{d\phi_{i+1}^{\ell}}{dx}\right|_{x=-\eta_{i+1}} = a_1 + 2a_2x + 3a_3x^2 + 4a_4x^3\Big|_{x=-\eta_{i+1}} \tag{3-89}$$

and the coefficients a_1 through a_4 in equation (3-89) are the coefficients which were evaluated for node i+1. To find a new ϕ_i^r for the next iteration, the continuity of the current for the finite difference equation is applied at the interface. It is required that J_i^r be equal to J_{i+1}^{ℓ} at any iteration.

$$J_i^r = J_{i+1}^{\ell} \tag{3-90}$$

where reference [1] gives an expression for the current

$$J = -D\frac{d\phi}{dx} \tag{3-91}$$

Substituting equation (3-91) into (3-90), one has

$$-D_i\left.\frac{d\phi_i}{dx}\right|_i = -D_{i+1}\left.\frac{d\phi_{i+1}}{dx}\right|_{i+1} \tag{3-92}$$

and substituting equations (3-86) and (3-87) into (3-92) would result in the following expression

$$D_i\left(\frac{\phi_i^r - \psi_i^r}{\theta_i}\right) = D_{i+1}\left(\frac{\psi_{i+1}^{\ell} - \phi_{i+1}^{\ell}}{\theta_{i+1}}\right) \tag{3-93}$$

solving for ϕ_i^r from equation (3-93) one has

$$\phi_i^r = \frac{D_i\psi_i^r + D_{i+1}\psi_{i+1}^{\ell}}{D_i + D_{i+1}} \tag{3-94}$$

where ψ_i^r and ψ_{i+1}^{ℓ} are found from the previous iteration by using equations (3-86) and (3-87). Because of the continuity of flux at the interface (equation 3-85), equation (3-94) is also used to calculate ϕ_{i+1}^{ℓ}.

$$\phi_i^r = \phi_{i+1}^{\ell} = \frac{D_i\psi_i^r + D_{i+1}\psi_{i+1}^{\ell}}{D_i + D_{i+1}} \tag{3-95}$$

E. Boundary Conditions

The boundary condition is shown in Figure 3-6. For the boundary node i, the homogenous boundary condition

$$D_i \left.\frac{d\phi_i^r}{dx}\right|_{\text{boundary}} = -\tau\phi_i^r\Big|_{\text{boundary}} \tag{3-96}$$

can be used to find ϕ_i^r

$$\phi_i^r = -\frac{D_i}{\tau}\left.\frac{d\phi_i^r}{dx}\right|_{x=\eta_i} \tag{3-97}$$

The value of $\frac{d\phi_i^r}{dx}$ for the fourth order polynomial is

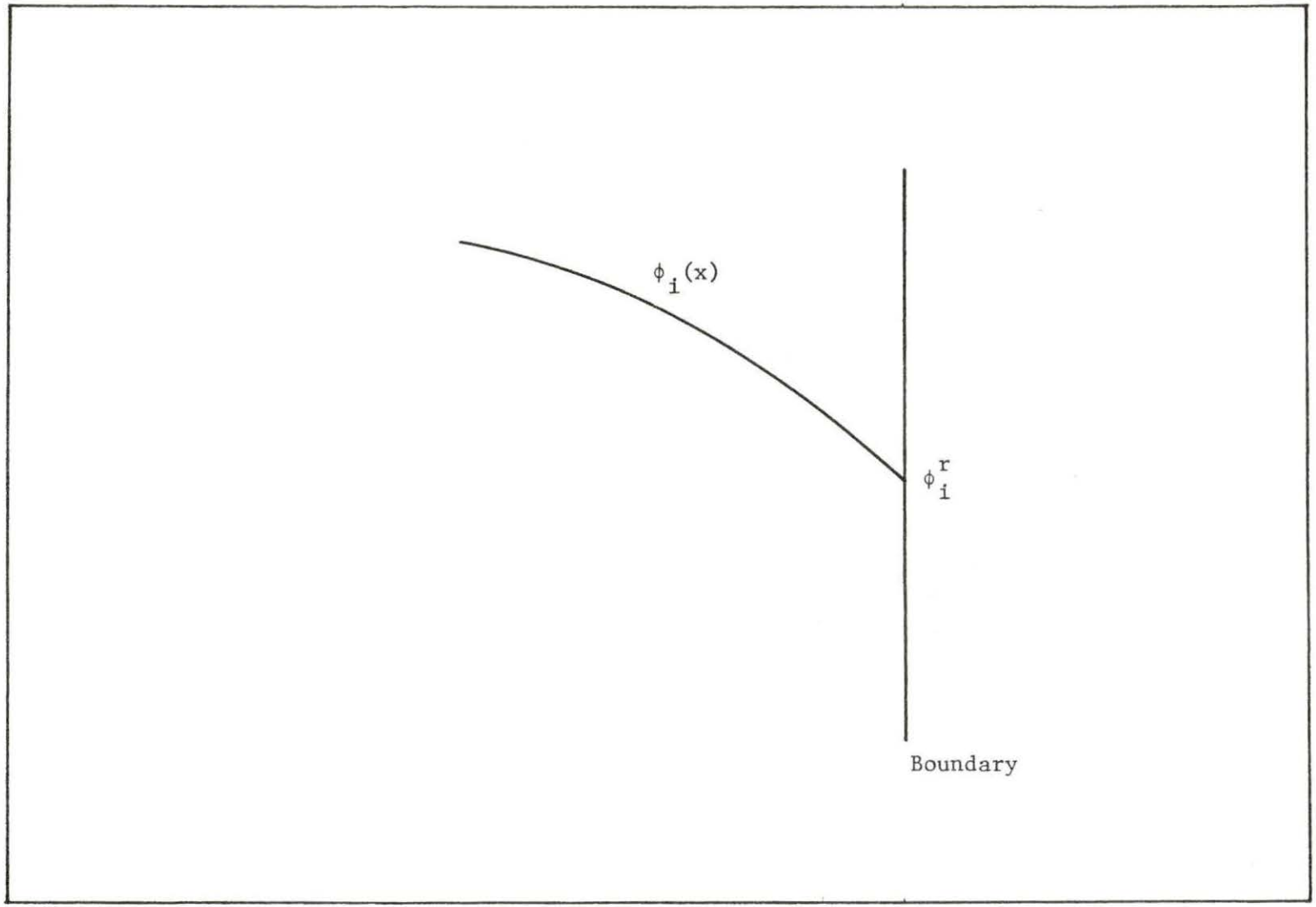

Figure 3-6 Assumed flux profile at the boundary

$$\left.\frac{d\phi_i^r}{dx}\right|_{x=\eta_i} = a_1 + 2a_2x + 3a_3x^2 + 4a_4x^3\Big|_{x=\eta_i} \tag{3-88}$$

where the coefficients a_1 through a_4 are the coefficients which were evaluated for node i.

If the outer boundary is a free surface, then the vacuum boundary condition can be used. For this case, τ would be expressed in terms of the transport mean free path, λ_{tr}.

$$\tau = \frac{3}{2}\frac{D}{\lambda_{tr}} \tag{3-98}$$

where

$$\lambda_{tr} = 3D \tag{3-99}$$

Therefore, equation (3-98) becomes

$$\tau = \frac{1}{2} \tag{3-100}$$

If the transport correction is taken into account, the vacuum boundary condition would be

$$\tau = \frac{1}{3(0.7104)} \tag{3-101}$$

If the outer boundary is not a free surface, then τ can be varied for a given albedo boundary condition (τ=0 is a symmetric boundary). The albedo boundary condition is given by reference [6] as the ratio between the current out of the reflecting region to the current into the reflecting region.

$$\alpha = \frac{J_{out}}{J_{in}} = \frac{J^-}{J^+} \tag{3-102}$$

The partial currents J^-, and J^+ are also given in [6]

$$J^+ = \frac{\phi_i^r}{4} - \frac{\lambda_{tr}}{6}\frac{d\phi_i^r}{dx} \tag{3-103}$$

$$J^- = \frac{\phi_i^r}{4} + \frac{\lambda_{tr}}{6}\frac{d\phi_i^r}{dx} \tag{3-104}$$

where λ_{tr} is given by equation (3-99). If equations (3-103) and (3-104) are inserted into equation (3-102), an expression for the albedo would result

$$\alpha = \frac{\frac{\phi_i^r}{4} + \frac{\lambda_{tr}}{6}\frac{d\phi_i^r}{dx}}{\frac{\phi_i^r}{4} - \frac{\lambda_{tr}}{6}\frac{d\phi_i^r}{dx}} \tag{3-105}$$

Equation (3-105) is rewritten as follows

$$\alpha = \frac{1 + \frac{2}{3}\frac{\lambda_{tr}}{\phi_i^r}\frac{d\phi_i^r}{dx}}{1 - \frac{2}{3}\frac{\lambda_{tr}}{\phi_i^r}\frac{d\phi_i^r}{dx}} \tag{3-106}$$

Equation (3-99) is inserted into equation (3-106)

$$\alpha = \frac{1 + 2\frac{D}{\phi_i^r}\frac{d\phi_i^r}{dx}}{1 - 2\frac{D}{\phi_i^r}\frac{d\phi_i^r}{dx}} \tag{3-107}$$

The expression for the homogenous boundary condition, equation (3-96) is used to find an expression for τ

$$\tau = -\frac{D_i}{\phi_i^r}\frac{d\phi_i^r}{dx} \tag{3-108}$$

If equation (3-108) is inserted into equation (3-107), one has

$$\alpha = \frac{1 - 2\tau}{1 + 2\tau} \tag{3-109}$$

The expression for τ is

$$\tau = \frac{1}{2}\left(\frac{1-\alpha}{1+\alpha}\right) \tag{3-110}$$

If the transport correction is taken into account, the expression for τ is

$$\tau = \frac{1}{3(0.7104)} \left(\frac{1-\alpha}{1+\alpha}\right) \tag{3-111}$$

F. Convergence Criterias

The solution technique used for developing a code suited for the finite element nodal model is the relaxation method. The relaxation method is described by reference [7]

$$X_i^{(K)} = \bar{X}_i^{(K)}\, w + (1-w)\, X_i^{(K-1)} \tag{3-112}$$

where $X_i^{(K-1)}$ is the present value of a given node, and $\bar{X}_i^{(K)}$ is the value calculated by the numerical method. The value predicted by the relaxation method for $X_i^{(K)}$ is the value actually used. Also in the expression given for $X_i^{(K)}$, "i" denotes the position of the node, "K" denotes the iteration number in the iteration process, and "w" is called the "relaxation parameter." The parameter "w" determines the speed of convergence and is chosen to speed convergence.

The relaxation method was applied to the following parameters

1. The coefficients of a chosen polynomial.

$$a_i^{(K)} = \bar{a}_i^{(K)}\, w + (1-w)\, a_i^{(K-1)} \qquad i = 0, 1, 2, 3, 4 \tag{3-113}$$

2. The flux and the interface conditions

$$\phi_i^{(K)} = \bar{\phi}_i^{(K)} w + (1-w)\phi_i^{(K-1)} \tag{3-114}$$

$$\frac{d\phi_i^{(K)}}{dx} = \frac{\phi_i^{(K)} - \psi_i^K}{\Theta} \tag{3-115}$$

where Θ and ψ were discussed in part D of this chapter.

3. The neutron source

$$S_i^{(K)} = \bar{S}_i^{(K)} w + (1-w) S_i^{(K-1)} \tag{3-116}$$

For one dimensional steady state conditions with only two neutron groups, the neutron source becomes

$$S = \frac{\sum_{i=1}^{I} (\nu\Sigma_{f1}\phi_1 + \nu\Sigma_{f2}\phi_2)_i \Delta V_i}{\sum_{i=1}^{I} \Delta V_i} \tag{3-117}$$

where the summation is taken over all the nodes.

G. Computer Code and Results

A computer program called ONODE was developed by Rohach [8] which is a one dimensional two group neutron code. The code has the capability to be used for second, third, and fourth order polynomials. A flow chart of the code is given in Figure 3-7. The ONODE code has been applied to a one dimensional version of the Benchmark problem [9] using second, third, and fourth order polynomials. In the one dimensional model with symmetric boundary conditions, the fuel loading pattern is shown in Figure 3-8. The

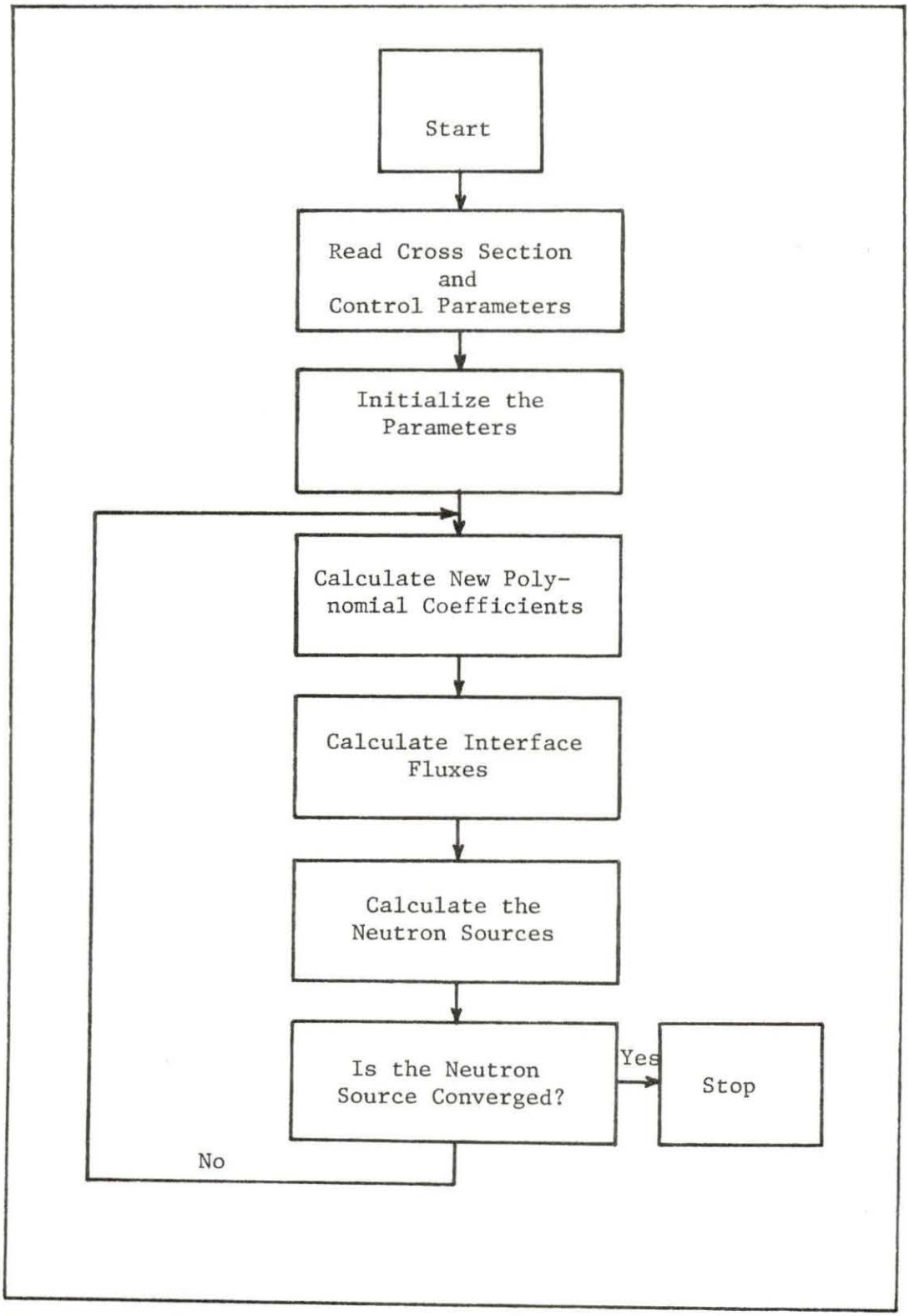

Figure 3-7 Flow chart of the ONODE code

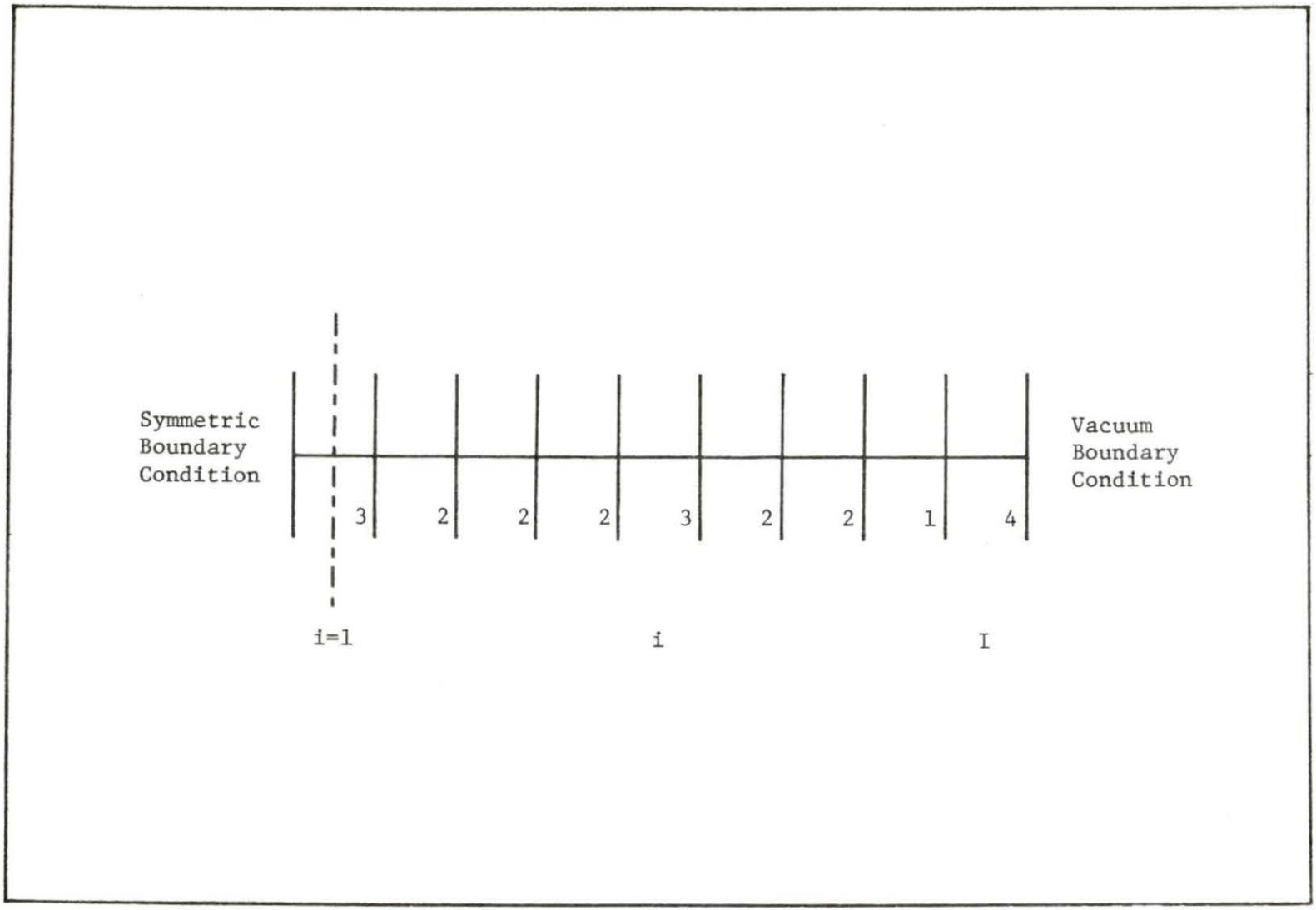

Figure 3-8 Fuel loading pattern for the one dimensional model

cross section data used for the fuel types in Figure 3-8 are given in Table 3-1, and are taken from the Benchmark problem.

Table 3-1 Benchmark Fuel Parameters

Material	Region	D_1	D_2	$\Sigma_{1\to2}$	Σ_{a1}	Σ_{a2}	$\nu\Sigma_{f2}$
Fuel 1	1	1.5	0.4	0.02	0.01	0.08	0.135
Fuel 2	2	1.5	0.4	0.02	0.01	0.085	0.135
Fuel 2 & Control	3	1.5	0.4	0.02	0.01	0.13	0.135
Reflector	4	2.0	0.3	0.04	0.0	0.01	0.0

A fine mesh finite difference diffusion theory calculation (1 cm per mesh point) is used as the reference calculation. Figure 3-9 illustrates the fast and thermal flux distributions calculated using fine mesh diffusion theory. One can note the large flux dips in the two control assemblies and the thermal flux peaking in the reflector. Several results of the ONODE code will be discussed.

The second order polynomial was first used to approximate the flux distributions. The fast and thermal flux distributions of the second order polynomial along with the flux distributions of the fine mesh diffusion theory are shown in Figure 3-10. Two significant points can be noted in the thermal flux comparison of the code and

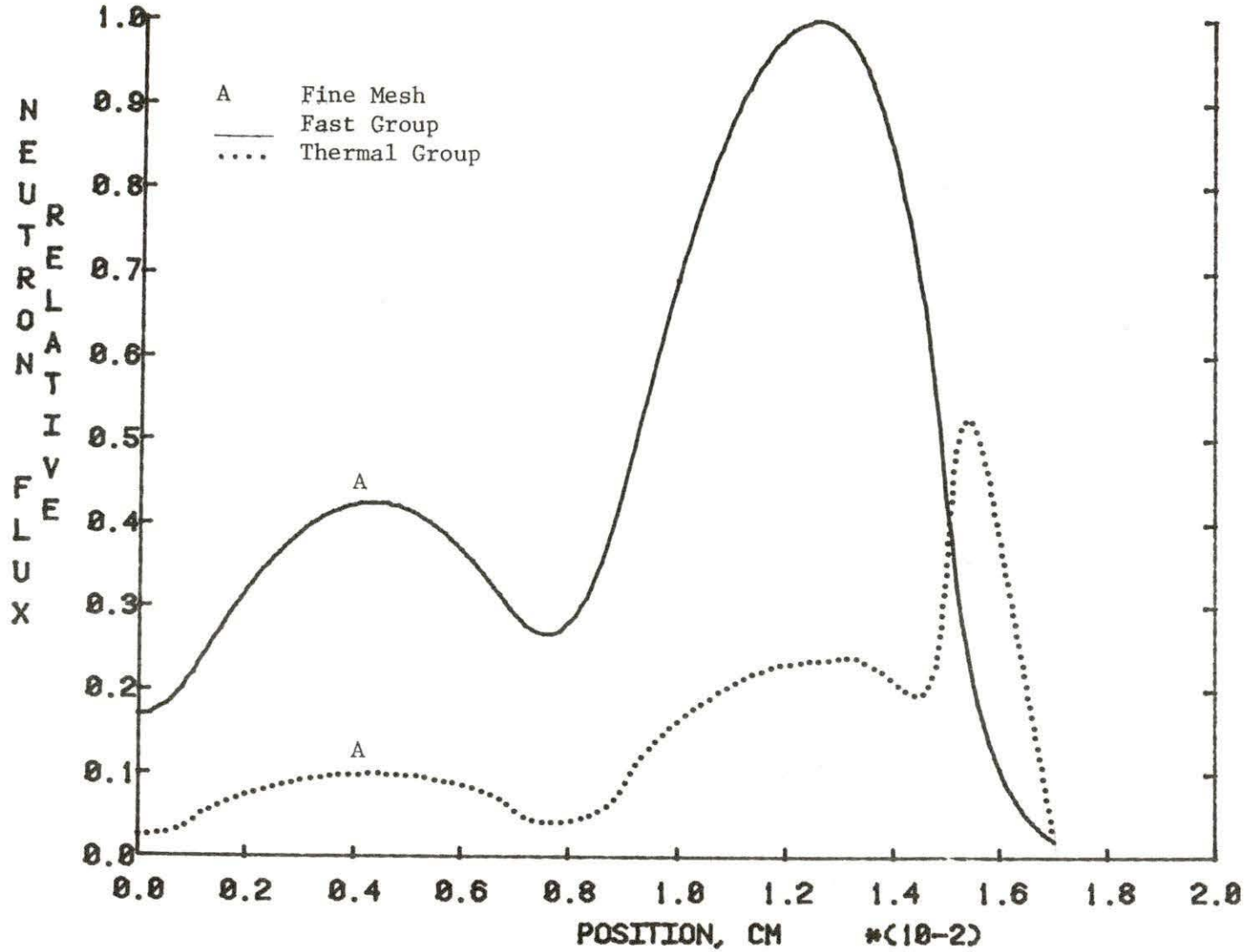

Figure 3-9 Fast and thermal flux of a fine mesh diffusion theory

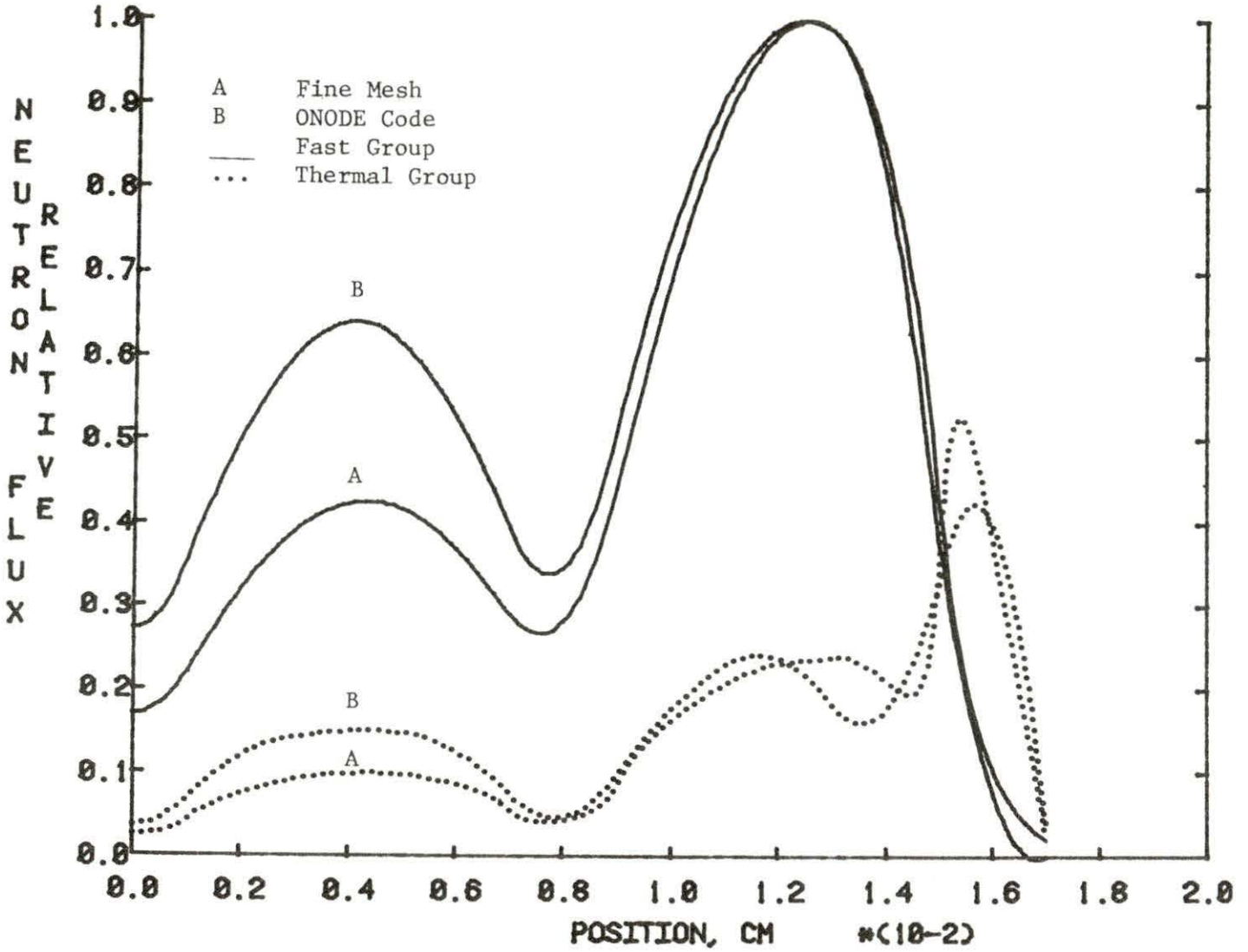

Figure 3-10 Fast and thermal flux comparison for a second order polynomial

the fine mesh diffusion theory. First, the technique cannot accurately predict the thermal flux peaking in the reflector. In addition, the second order polynomial is not adequate to predict the flux in the core node next to the reflector. This former problem is blamed on the shape of the flux in the reflector. The latter problem is due to inaccurate prediction of neutron leakage at core-reflector interface. An attempt was made to resolve these discrepancies by using two nodes per fuel assembly in the outer fuel assembly and the reflector assembly. Figure 3-11 shows the fast and thermal flux distributions of the fine mesh diffusion theory and the second order polynomial using two nodes in the outer two nodes. A thermal flux comparison in Figure 3-11 shows that the thermal flux shape has improved only at the outer nodes and not in the core. An attempt was made at replacing the reflector with a vacuum boundary condition at the core-reflector interface. Figure 3-12 is a comparison of the fast and thermal fluxes of the fine mesh diffusion theory and the second order polynomial without the reflector. It is noted that the thermal flux shape has improved but not to a degree of satisfaction.

The third order polynomial was then used to approximate the flux distribution and hopefully resolve some of the problems encountered with the second order polynomial. The fast and thermal flux distributions of the third order polynomial along with the

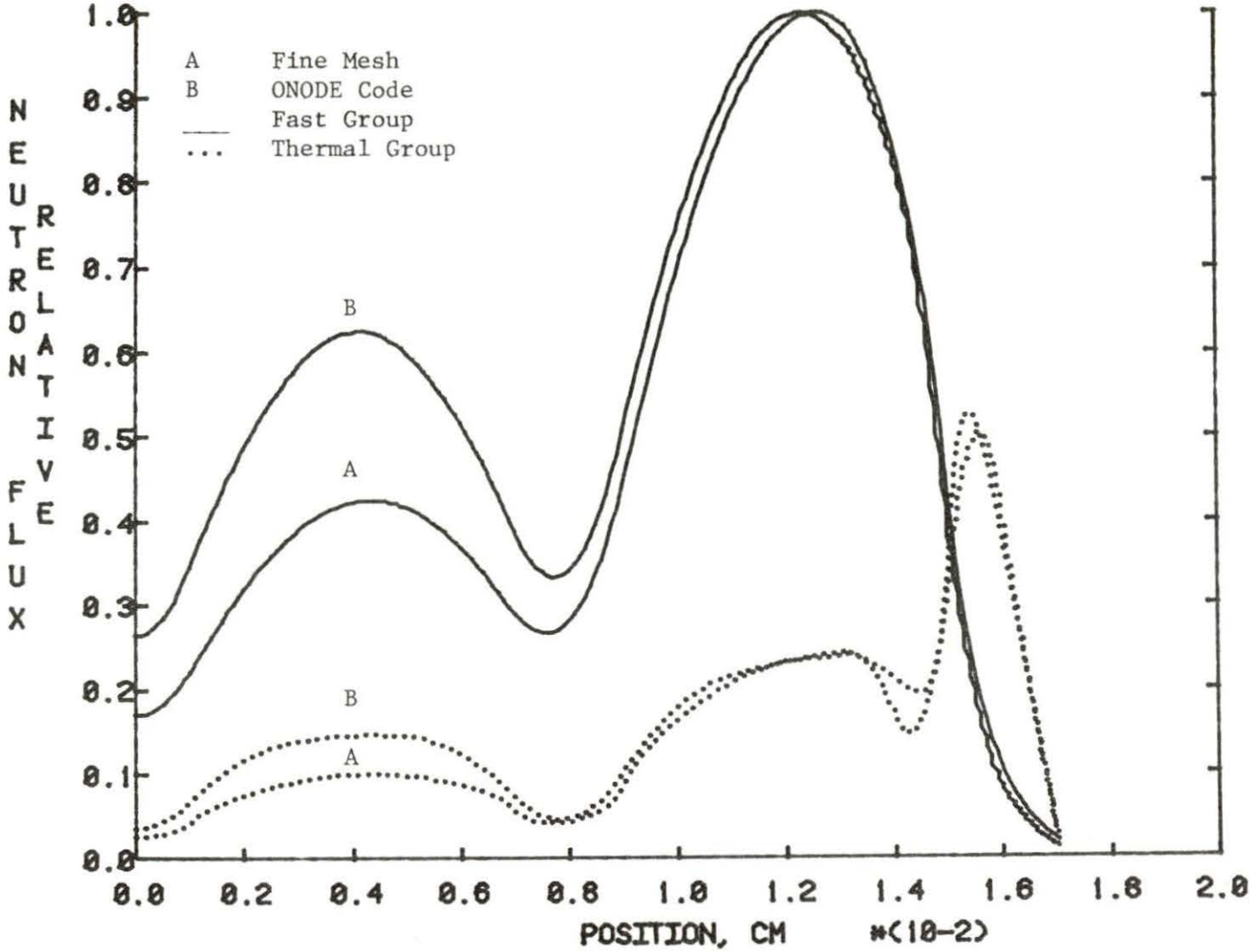

Figure 3-11 Fast and thermal flux comparison for a second order polynomial. Four nodes in the outer two nodes

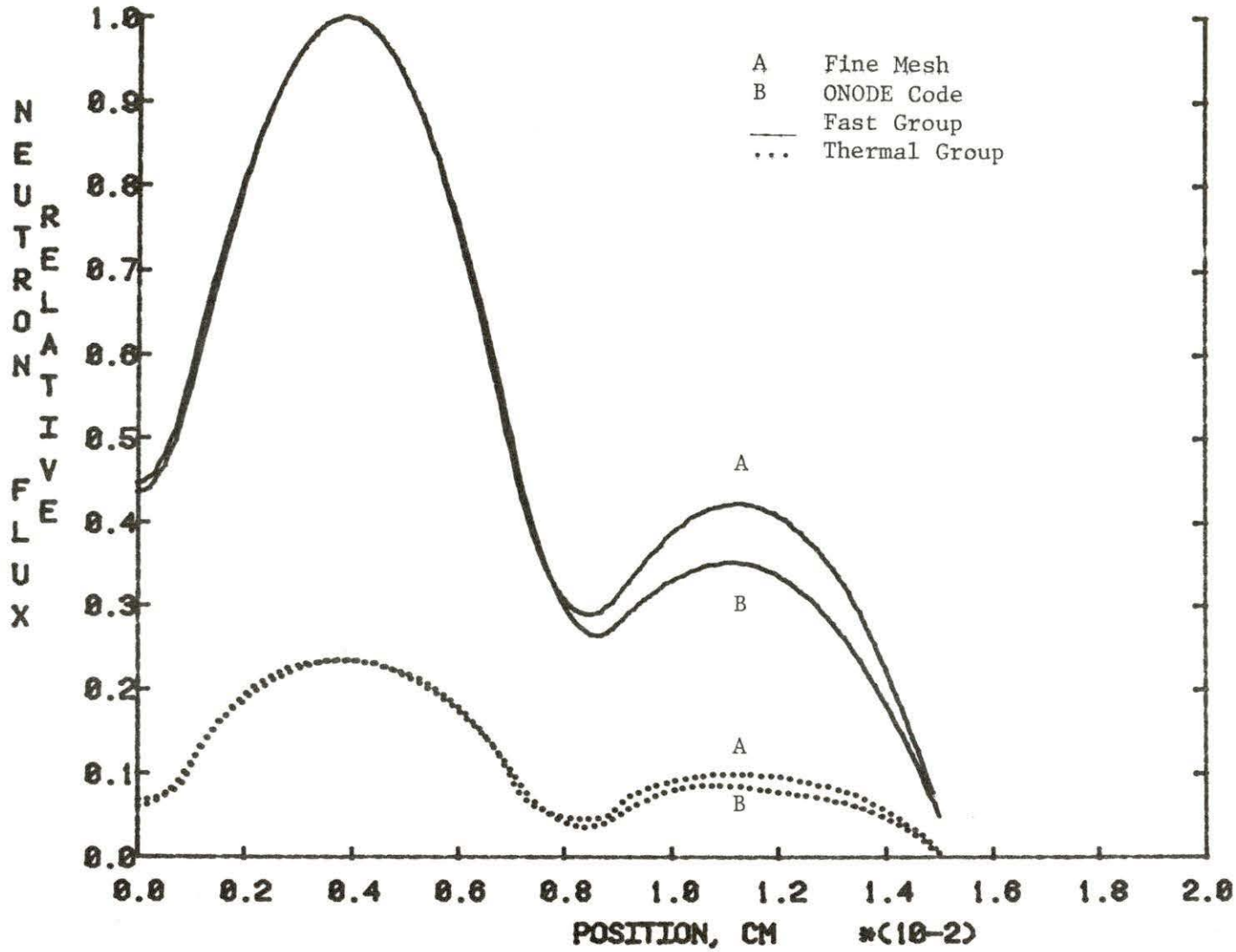

Figure 3-12 Fast and thermal flux comparison for a second order polynomial without a reflector

flux distributions of the fine mesh diffusion theory are shown in Figure 3-13. By comparing the thermal flux of the code and the fine mesh diffusion theory, one can observe that the thermal flux peak in the reflector was better predicted using a third order polynomial. It should also be noted that although the thermal flux comparison is quite good at some nodes, the third order polynomial is not adequate to predict the flux in the core. Since the shape of the thermal flux at the node next to the reflector is not satisfactory, two nodes per fuel assembly in the outer fuel assembly and the reflector assembly was used. Figure 3-14 shows the fast and thermal flux distributions of the fine mesh diffusion theory and the third order polynomial using two nodes in the outer two nodes. A thermal flux comparison in Figure 3-14 shows that not only the thermal flux shape has improved in the reflector and the node next to it, but also a better flux agreement is observed. Figure 3-15 is a comparison of the fast and thermal fluxes of the fine mesh diffusion theory and the third order polynomial with no reflector. It is observed that very good agreement between the fluxes exists in Figure 3-15. Therefore, the third order polynomial may be adequate in the core when there is no reflector.

The fourth order polynomial was then used to approximate the flux distributions. The fast and thermal flux distributions of the fourth order polynomial along with the flux distributions of the

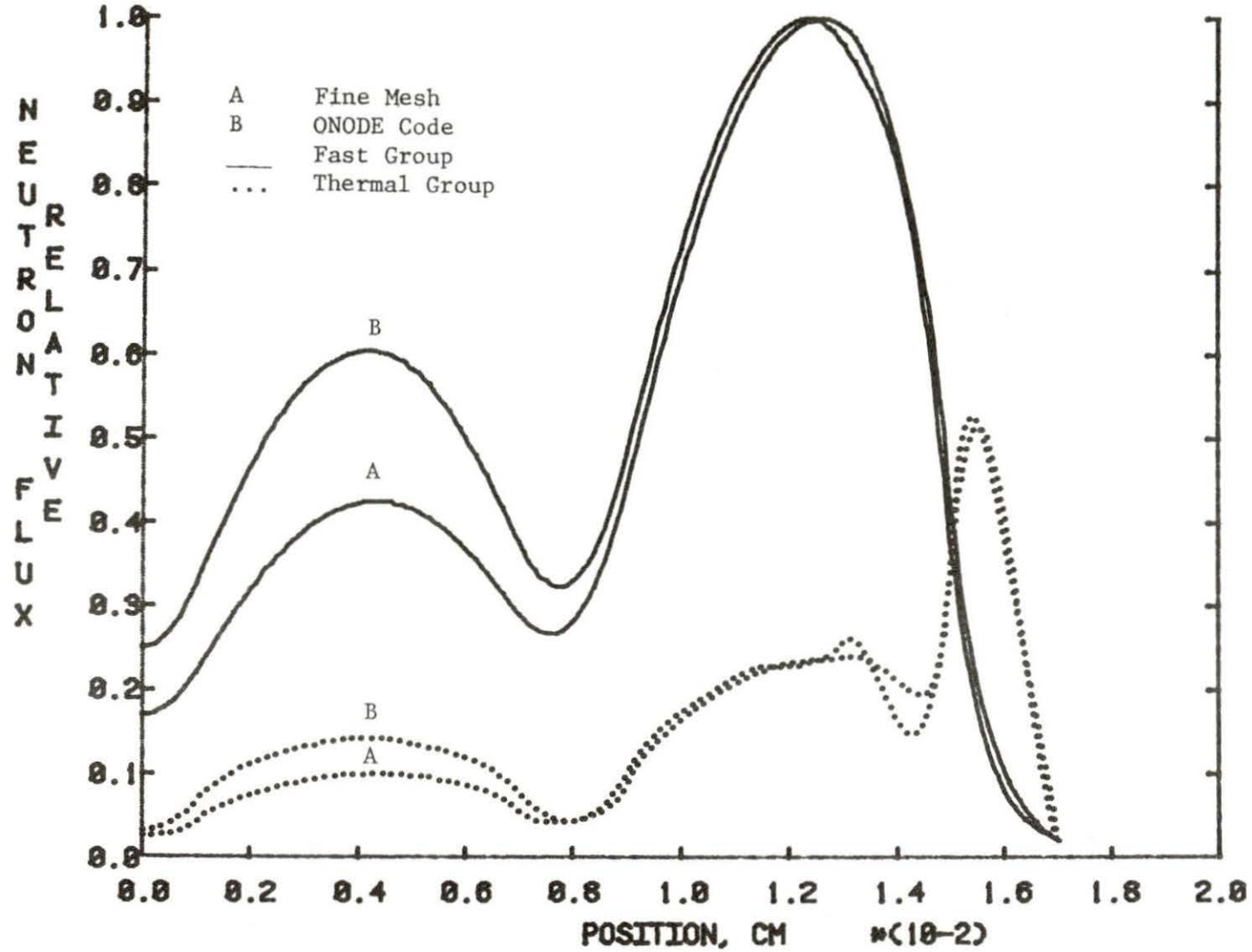

Figure 3-13 Fast and thermal flux comparison for a third order polynomial

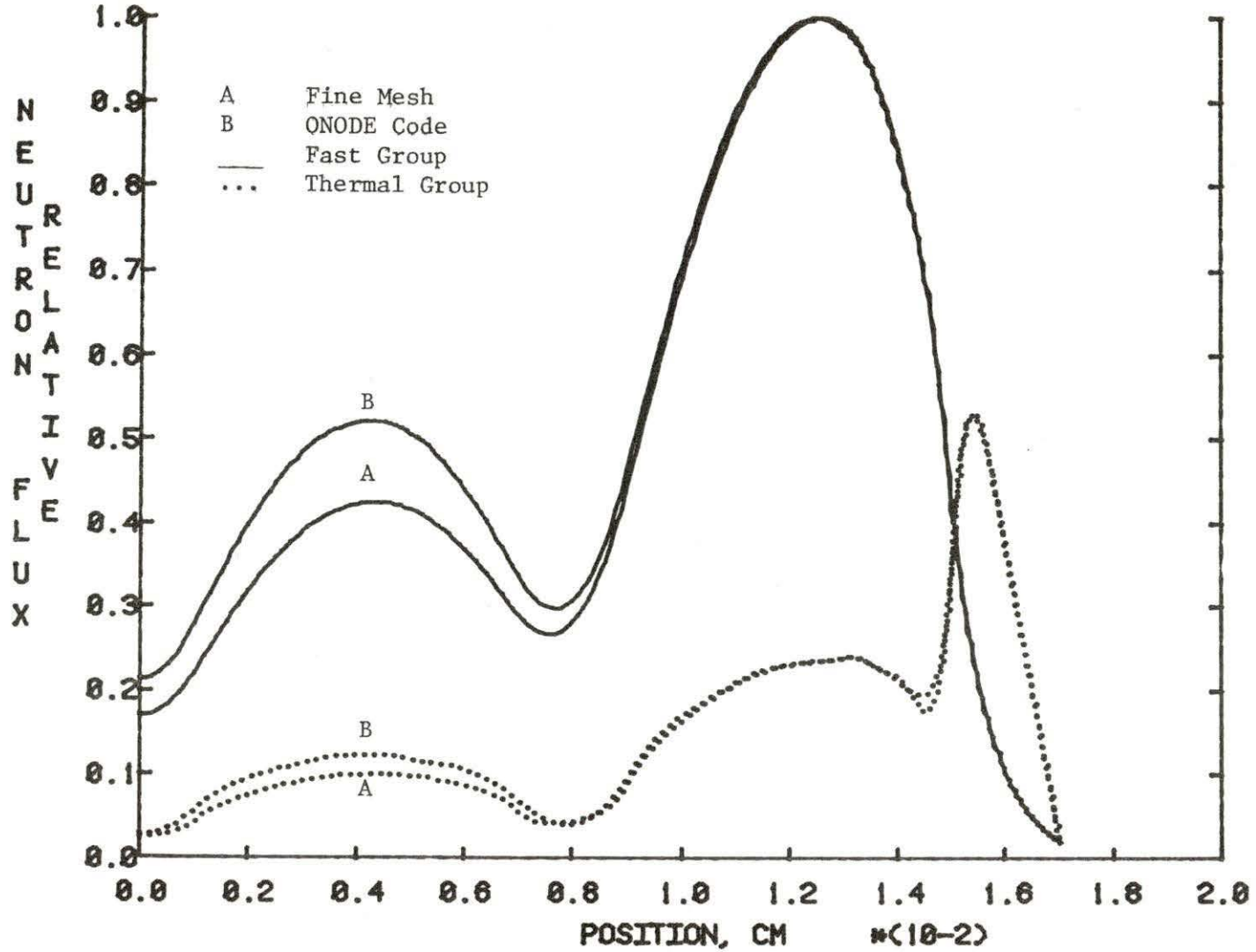

Figure 3-14 Fast and thermal flux comparison for a third order polynomial. Four nodes in the outer two nodes

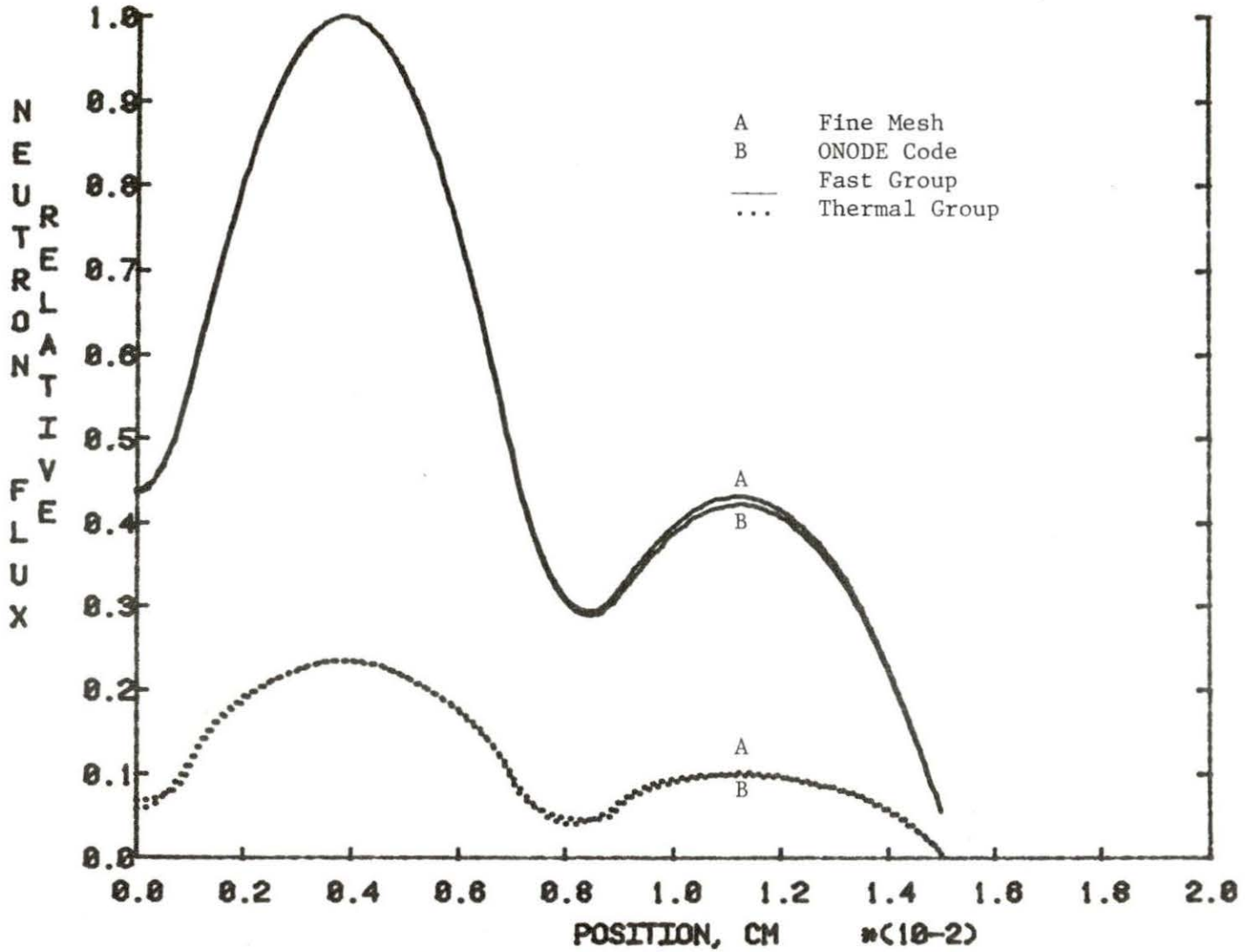

Figure 3-15 Fast and thermal flux comparison for a third order polynomial without a reflector

fine mesh theory are shown in Figure 3-16. Excellent agreement is attained with this order of polynomial. Figure 3-17 shows the fast and thermal flux distributions of the fine mesh diffusion theory and the fourth order polynomial using two nodes in the outer two nodes. A thermal flux comparison in Figure 3-17 shows that the flux shape in the reflector and the node next to it is better than the one in Figure 3-16. But it should be noted that extra nodes are not needed since the flux agreement in Figure 3-16 is very good. Figure 3-18 is a comparison of the fast and thermal fluxes of the fine mesh diffusion theory and the fourth order polynomial with no reflector. Again excellent agreement is observed between the fluxes.

Figure 3-19 shows the eigenvalue convergence of the fourth order polynomial versus the number of iterations. The eigenvalue oscillates at low iteration numbers but converges as the number of iterations increases. Benghanam [2] indicates that the interface relaxation parameter governs the oscillation shown in the eigenvalue curve (Figure 3-19). Benghanam also indicates that the interface relaxation parameter should be under-relaxed to prevent the oscillation at low iteration numbers. Benghanam also found out that the source relaxation parameter should be over-relaxed in order to increase the convergence of the system.

One can note the fast and thermal flux comparisons to be quite good in some nodes and not so accurate in others for the polynomials

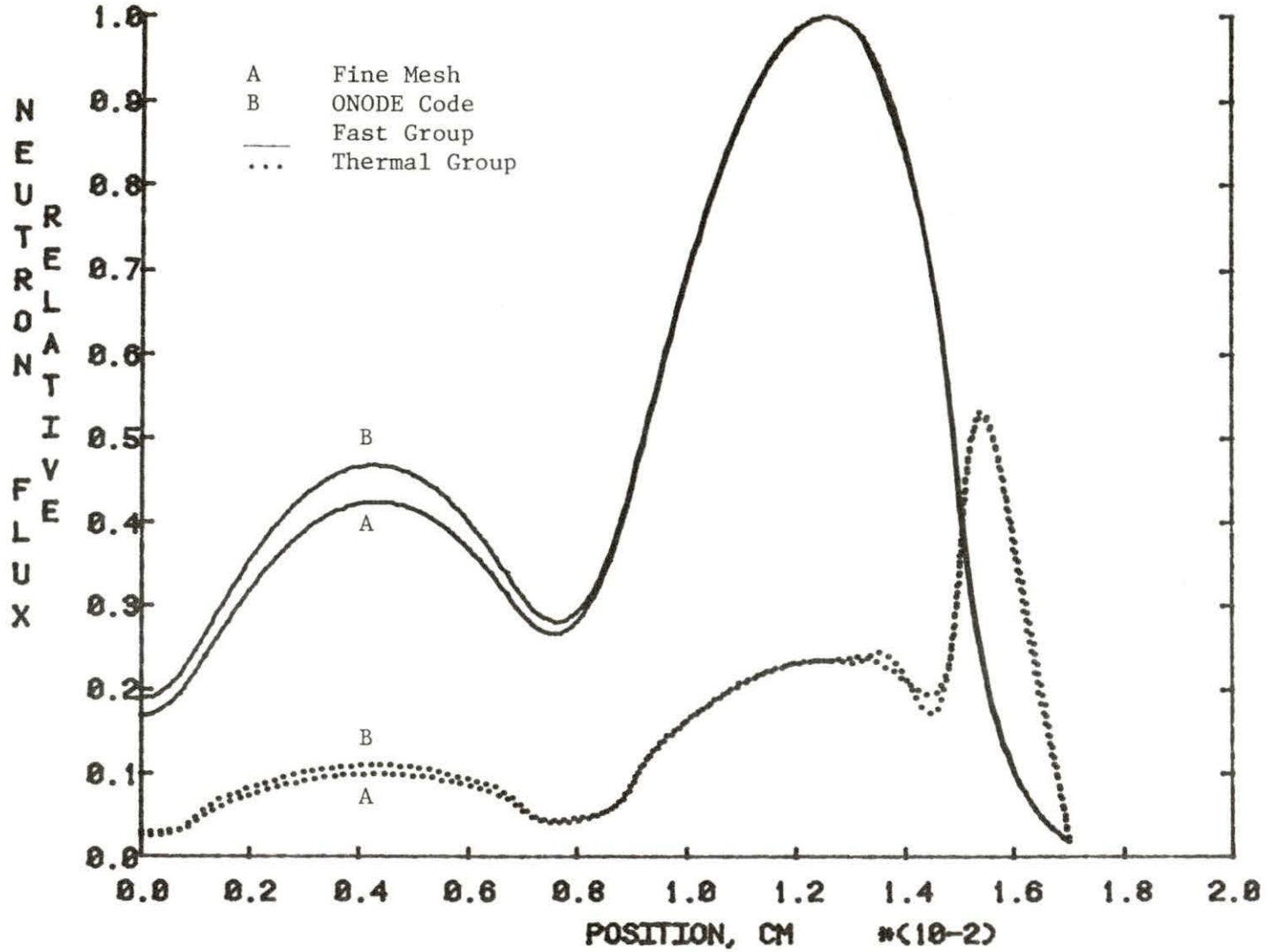

Figure 3-16 Fast and thermal flux comparison for a fourth order polynomial

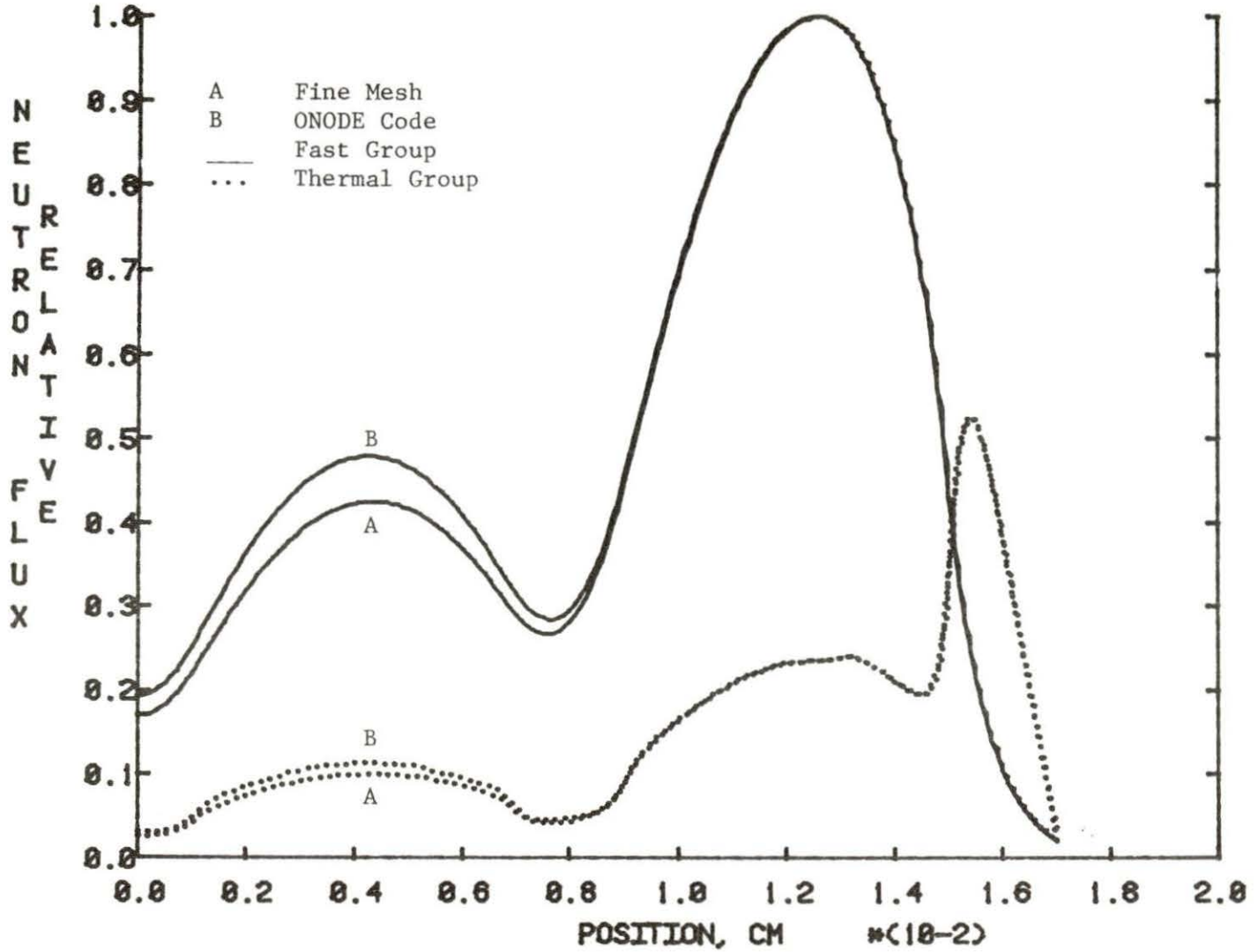

Figure 3-17 Fast and thermal flux comparison for a fourth order polynomial. Four nodes in the outer two nodes

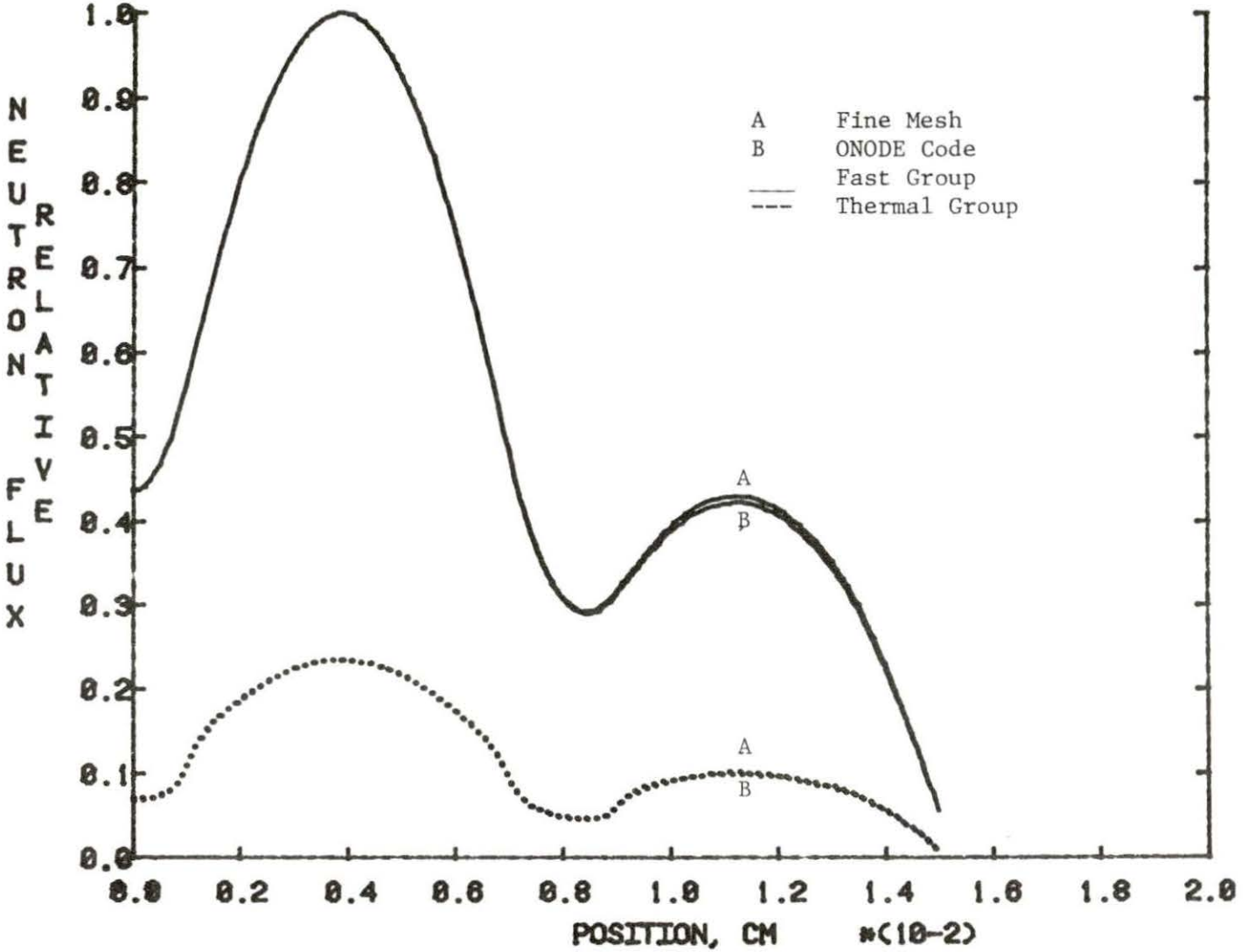

Figure 3-18 Fast and thermal flux comparison for a fourth order polynomial without a reflector

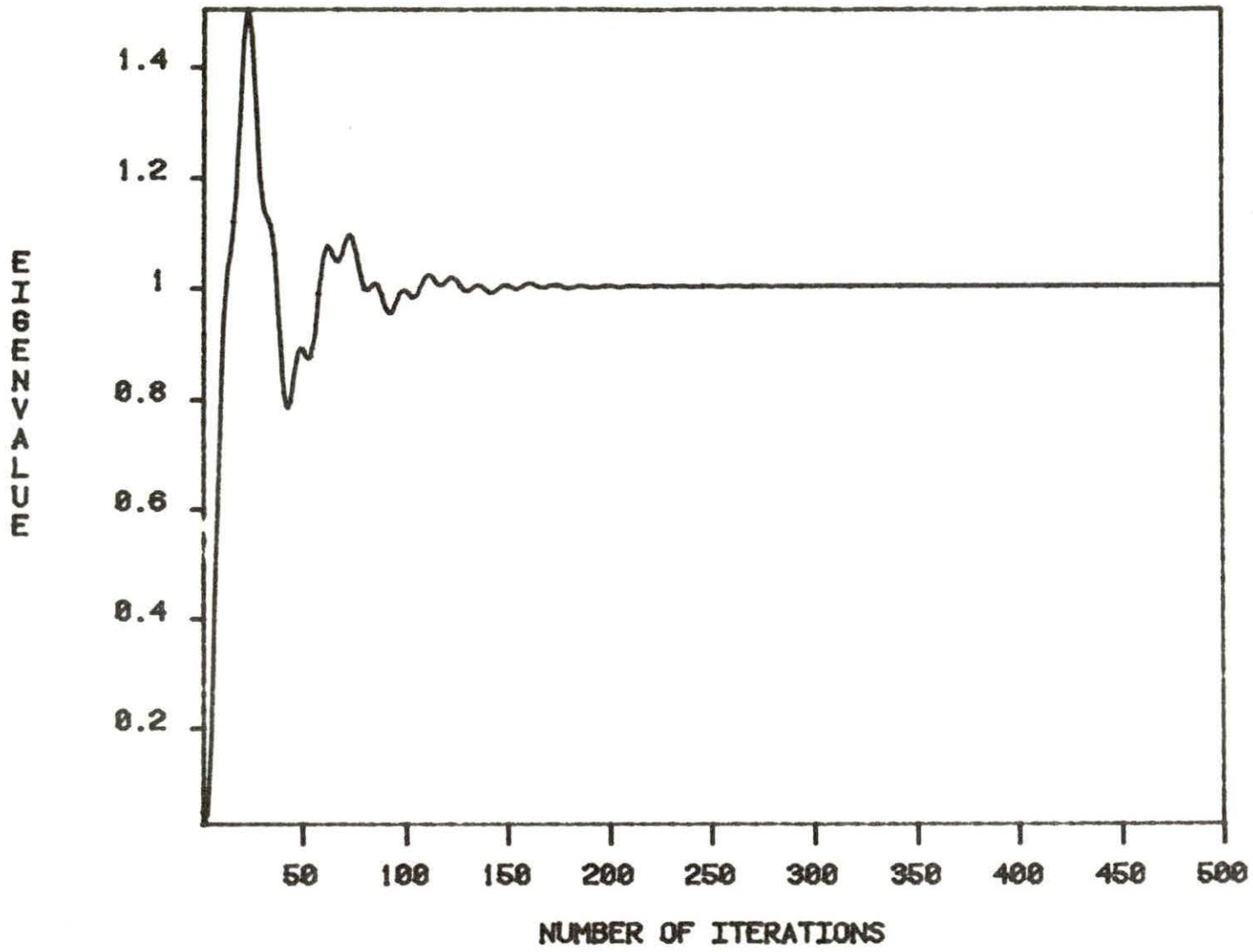

Figure 3-19 Eigenvalue convergence for a fourth order polynomial

mentioned above. This is due to the normalization process that was used. Since both the fast and thermal flux distributions are normalized to the highest point on the fast flux distribution curve, this flux agreement is seen in some nodes. If other normalization processes are used, flux disagreement would decrease in some nodes and increase in other's.

Figure 3-20 shows the neutron current is indeed continous along the core for the fourth order polynomial. The continuity of the current was used in the interface condition for every iteration and is an important criteria in calculating the flux at the interfaces along the core.

Figures 3-21 and 3-22 show the spatial neutron balance for the fourth order polynomial using a second order fit. Since the polynomial is not an exact solution and is only an approximation, the minimization process which is described by equation (3-67) is used. The areas between the two curves in both Figure 3-21 and 3-22 are minimized to insure the best fit to the flux using this order of polynomial.

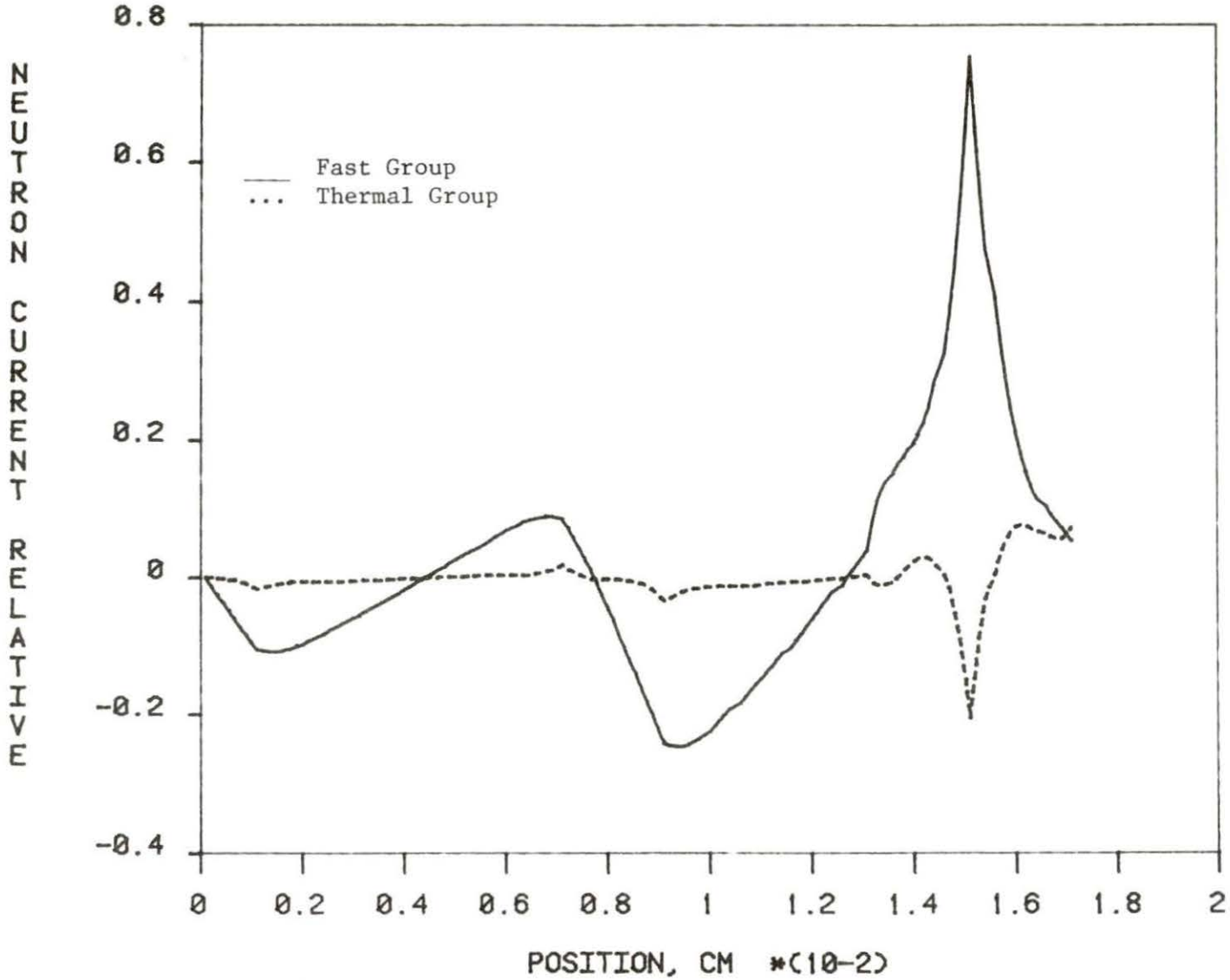

Figure 3-20 Current-continuity across the core for a fourth order polynomial

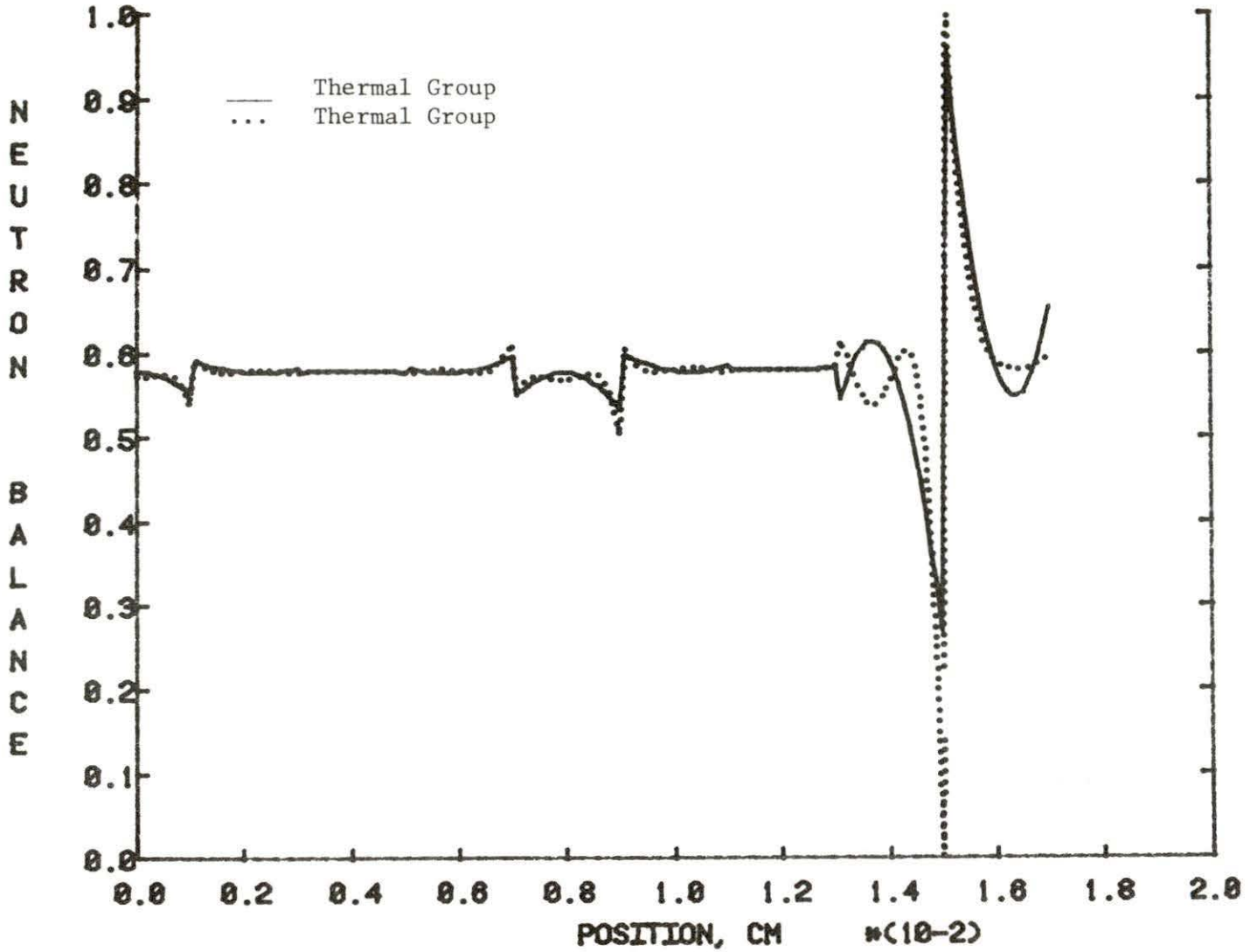

Figure 3-21 Spatial neutron balance for the thermal group using a fourth order polynomial

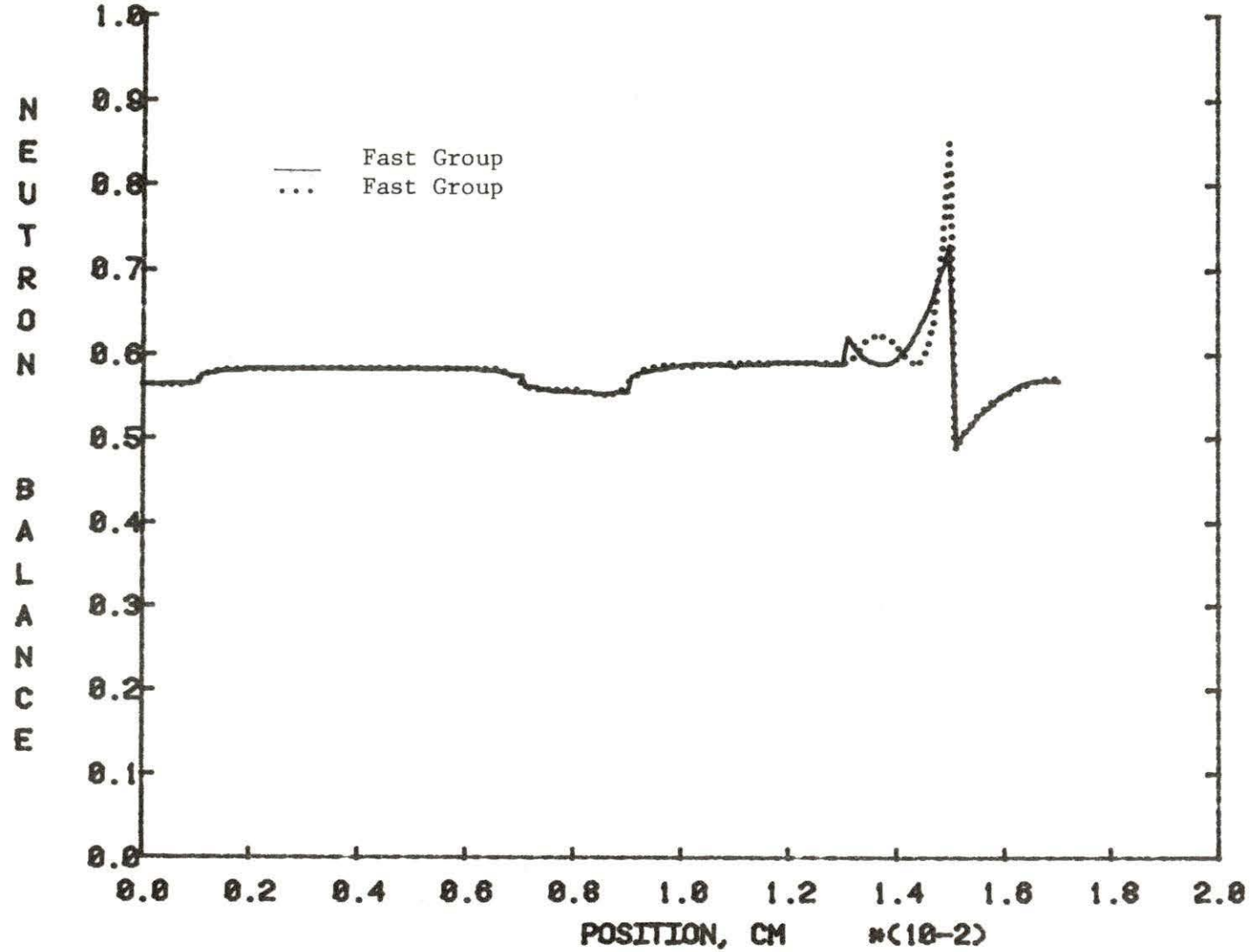

Figure 3-22 Spatial neutron balance for the fast group using a fourth order polynomial

IV. THEORETICAL DEVELOPMENT OF THE ONE DIMENSIONAL FINITE ELEMENT NODAL MODEL FOR THE MULTI-GROUP NEUTRON DIFFUSION EQUATIONS

The multigroup diffusion equation has the following form [1]

$$-\nabla.[D_g \nabla\phi_g(r)] + \Sigma_{ag}\phi_g(r) + \phi_g(r)\sum_{g'=g+1}^{G} \Sigma_s^{g\to g'} -$$

$$\sum_{\substack{g'=1 \\ g'\neq g}}^{g-1} \Sigma_s^{g'\to g}\phi_{g'}(r) - \frac{1}{\lambda}\chi_g \sum_{g'=1}^{G} \nu\Sigma_{fg'}\phi_{g'}(r) = 0 \qquad (4\text{-}1)$$

where the terms in equation (4-1) were discussed in Chapter 3.

If one assumes that the diffusion coefficient in equation (4-1) would stay constant for each group over a homogenous region, the following equation would result

$$- D_g \nabla^2\phi_g(r) + \Sigma_{ag}\phi_g(r) + \phi_g(r)\sum_{g'=g+1}^{G} \Sigma_s^{g\to g'} -$$

$$\sum_{\substack{g'=1 \\ g'\neq g}}^{g-1} \Sigma_s^{g'\to g}\phi_{g'}(r) - \frac{1}{\lambda}\chi_g \sum_{g'=1}^{G} \nu\Sigma_{fg'}\phi_{g'}(r) = 0 \qquad (4\text{-}2)$$

Equation (4-2) is then divided by $(-D_g)$

$$\nabla^2\phi_g(r) - \frac{1}{D_g}\Sigma_{ag}\phi_g(r) - \frac{1}{D_g}\phi_g(r)\sum_{g'=g+1}^{G} \Sigma_s^{g\to g'} +$$

$$\frac{1}{D_g}\sum_{\substack{g'=1 \\ g'\neq g}}^{g-1} \Sigma_s^{g'\to g}\phi_{g'}(r) + \frac{1}{\lambda}\frac{\chi_g}{D_g}\sum_{g'=1}^{G} \nu\Sigma_{fg'}\phi_{g'}(r) = 0 \qquad (4\text{-}3)$$

Equation (4-3) is much easier to deal with numerically if it is cast into matrix form. With this understanding equation (4-3) is written as

$$\nabla^2[\phi_g] + [M][\phi_g] + \frac{1}{\lambda}[F][\phi_g] = 0 \tag{4-4}$$

where [M] is a GXG lower diagonal matrix defined by

$$[M] = \frac{1}{D_g}\left[-\Sigma_{ag} - \sum_{g'=g+1}^{G} \Sigma_s^{g\to g'} + \sum_{\substack{g'=1 \\ g'\neq g}}^{g-1} \Sigma_s^{g'\to g}\right] \tag{4-5}$$

and [F] is the GXG fission matrix defined by

$$[F] = \frac{1}{D_g}[\chi_g][\nu\Sigma_{fg}]^T \tag{4-6}$$

where $[\chi_g]$ is a G-element column vector, and $[\nu\Sigma_{fg}]^T$ is a G-element row vector, the transpose of the column vector $[\nu\Sigma_{fg}]$.

For one dimensional steady state conditions, the multigroup diffusion equation for a given node becomes

$$\frac{d^2}{dx^2}[\phi_g] + [M][\phi_g] + \frac{1}{\lambda}[F][\phi_g] = 0 \tag{4-7}$$

Therefore, it is desired to solve equation (4-7) using the finite element nodal model.

A. Fourth-Order Polynomial

As it was observed in the previous chapter, the second and third order polynomials can be obtained from the fourth order polynomial solution. Therefore, only the fourth order polynomial is considered here.

The assumption here is that the flux in each node and neutron group can be expressed in the form of a fourth order polynomial

$$[\phi_g(x)] = [C_0] + [C_1]x + [C_2]x^2 + [C_3]x^3 + [C_4]x^4 \qquad (4\text{-}8)$$

where [C] is a GX1 matrix corresponding to the respective coefficient and neutron group. The polynomial in equation (4-8) has five unknowns for each neutron group. Therefore, five conditions are needed for each neutron group to define the flux in equation (4-8).

The first assumption is that the fluxes at the right and left of a given node for each neutron group are known. Therefore, as it is shown in Figure 3-2, the following equations would result from this assumption

$$[\phi_g^{\ell}] = [\phi_g(-\eta)] = [C_0] - [C_1]\eta + [C_2]\eta^2 - [C_3]\eta^3 + [C_4]\eta^4 \qquad (4\text{-}9)$$

$$[\phi_g^{r}] = [\phi_g(\eta)] = [C_0] + [C_1]\eta + [C_2]\eta^2 + [C_3]\eta^3 + [C_4]\eta^4 \qquad (4\text{-}10)$$

Equations (4-9) and (4-10) are added and subtracted and the coefficients $[C_0]$ and $[C_1]$ are found

$$[C_0] = \frac{[\phi_g^r] + [\phi_g^\ell]}{2} - [C_2]\eta^2 - [C_4]\eta^4 \tag{4-11}$$

$$[C_1] = \frac{[\phi_g^r] - [\phi_g^\ell]}{2\eta} - [C_3]\eta^2 \tag{4-12}$$

But $[C_2]$, $[C_3]$, and $[C_4]$ are still unknown to completely define the polynomial. Therefore, three other conditions for each group is needed.

The second derivative of equation (4-8) is

$$\frac{d^2[\phi_g(x)]}{dx^2} = 2[C_2] + 6[C_3]x + 12[C_4]x^2 \tag{4-13}$$

Equation (4-13) as well as (4-8) are then inserted into equation (4-7). Since the polynomial solutions are only approximations, the equations are not equal to zero. Therefore, let

$$2[C_2] + 6[C_3]x + 12[C_4]x^2 + \{[M] + \frac{1}{\lambda}[F]\}\{[\tilde{C}_0] + [\tilde{C}_1]x$$

$$+ [\tilde{C}_2]x^2 + [\tilde{C}_3]x^3 + [\tilde{C}_4]x^4\} = [g(x)] \tag{4-14}$$

where $[g(x)]$ is a GXG matrix which is assumed to be a function of x only and is defined by the left hand side of equation (4-14).

Now rewrite equation (4-14) as

$$2[C_2] + 6[C_3]x + 12[C_4]x^2 + [f(x)] = [g(x)] \tag{4-15}$$

where

$$[f(x)] = \{[M] + \frac{1}{\lambda}[F]\}\{[\tilde{C}_0] + [\tilde{C}_1]x + [\tilde{C}_2]x^2 + [\tilde{C}_3]x^3 + [\tilde{C}_4]x^4\}$$

and is assumed to be known from a previous iterate.

The minimization process described in Chapter 3 is again applied to the integral of $[g^2(x)]$ with respect to $[C_2]$, $[C_3]$, and $[C_4]$ to determine these coefficients respectively.

$$\left[\int_{-\eta}^{\eta} g^2(x)dx \right] \tag{4-16}$$

The minimization process is carried out by differentiating equation (4-16) with respect to $[C_2]$, $[C_3]$, and $[C_4]$ and the results would then be set equal to zero and hence, one can calculate these coefficients. By the use of Leibnitz rule, one has

$$\left[\int_{-\eta}^{\eta} g(x) \frac{\partial g(x)}{\partial C_2} \right] \tag{4-17}$$

$$\left[\int_{-\eta}^{\eta} g(x) \frac{\partial g(x)}{\partial C_3} \right] \tag{4-18}$$

$$\left[\int_{-\eta}^{\eta} g(x) \frac{\partial g(x)}{\partial C_4} \right] \tag{4-19}$$

where $\left[\frac{\partial g(x)}{\partial C_2}\right]$, $\left[\frac{\partial g(x)}{\partial C_3}\right]$, and $\left[\frac{\partial g(x)}{\partial C_4}\right]$ are found from equation (4-15).

$$\left[\frac{\partial g(x)}{\partial C_2}\right] = [2] \tag{4-20}$$

$$\left[\frac{\partial g(x)}{\partial C_3}\right] = [6x] \tag{4-21}$$

$$\left[\frac{\partial g(x)}{\partial C_4}\right] = [12x^2] \tag{4-22}$$

Equations (4-20) through (4-22) along with equation (4-14) are then inserted into equations (4-17) through (4-19) to give

$$\int_{-\eta}^{\eta} \{2[C_2] + 6[C_3]x + 12[C_4]x^2 + \{[M] + \frac{1}{\lambda}[F]\}\{[\tilde{C}_0] + [\tilde{C}_1]x + [\tilde{C}_2]x^2 + [\tilde{C}_3]x^3 + [\tilde{C}_4]x^4\}\}dx = 0 \tag{4-23}$$

$$\int_{-\eta}^{\eta} x\{2[C_2] + 6[C_3]x + 12[C_4]x^2 + \{[M] + \frac{1}{\lambda}[F]\}\{[\tilde{C}_0] + [\tilde{C}_1]x + [\tilde{C}_2]x^2 + [\tilde{C}_3]x^3 + [\tilde{C}_4]x^4\}\}dx = 0 \tag{4-24}$$

$$\int_{-\eta}^{\eta} x^2\{2[C_2]x + 6[C_3]x + 12[C_4]x^2 + \{[M] + \frac{1}{\lambda}[F]\}\{[\tilde{C}_0] + [\tilde{C}_1]x + [\tilde{C}_2]x^2 + [\tilde{C}_3]x^3 + [\tilde{C}_4]x^4\}\}dx = 0 \tag{4-25}$$

If equations (4-23) through (4-25) are integrated and evaluated between $(-\eta)$ and (η), the coefficients $[C_2]$, $[C_3]$, and $[C_4]$ are found.

$$[C_2] = \{[M] + \frac{1}{\lambda}[F]\}\{-\frac{1}{2}[\tilde{C}_0] - \frac{1}{6}\eta^2[\tilde{C}_2] - \frac{1}{10}\eta^4[\tilde{C}_4]\} - 2\eta^2[C_4] \quad (4\text{-}26)$$

$$[C_3] = \{[M] + \frac{1}{\lambda}[F]\}\{-\frac{1}{6}[\tilde{C}_1] - \frac{1}{10}\eta^2[\tilde{C}_3]\} \quad (4\text{-}27)$$

$$[C_4] = \{[M] + \frac{1}{\lambda}[F]\}\{-\frac{1}{12}[\tilde{C}_2] - \frac{1}{14}\eta^2[\tilde{C}_4]\} \quad (4\text{-}28)$$

where the terms on the right hand sides are evaluated from a previous iterate.

In summary, for the multigroup neutrons, the following system of equations were used

$$[\phi_g(x)] = [C_0] + [C_1]x + [C_2]x^2 + [C_3]x^3 + [C_4]x^4 \quad (4\text{-}8)$$

where the coefficients are found using the following system of equations

$$[C_0] = \frac{[\phi_g^r] + [\phi_g^\ell]}{2} - [C_2]\eta^2 - [C_4]\eta^4 \quad (4\text{-}11)$$

$$[C_1] = \frac{[\phi_g^r] - [\phi_g^\ell]}{2\eta} - [C_3]\eta^2 \quad (4\text{-}12)$$

$$[C_2] = \{[M] + \frac{1}{\lambda}[F]\}\{-\frac{1}{2}[\tilde{C}_0] - \frac{1}{6}\eta^2[\tilde{C}_2] - \frac{1}{10}\eta^4[\tilde{C}_4]\} - 2\eta^2[C_4] \quad (4\text{-}26)$$

$$[C_3] = \{[M] + \frac{1}{\lambda}[F]\}\{-\frac{1}{6}[\tilde{C}_1] - \frac{1}{10}\eta^2[\tilde{C}_3]\} \tag{4-27}$$

$$[C_4] = \{[M] + \frac{1}{\lambda}[F]\}\{-\frac{1}{12}[\tilde{C}_2] - \frac{1}{14}\eta^2[\tilde{C}_4]\} \tag{4-28}$$

The iterative technique resembles the one described for the two neutron group. Here, the matrix [M] and [F] are nuclear data and are known. At the beginning of the process $[\phi_g^r]$, $[\phi_g^\ell]$, $[C_0]$, $[C_1]$, $[C_2]$, $[C_3]$, and $[C_4]$ are assumed to be known for every neutron group. New coefficients are found using equations (4-11) through (4-12), and (4-26) through (4-28). New interface fluxes are found for every neutron group using the interface conditions. Using the new fluxes, one can find new coefficients, and the process is continued until convergence occurs.

Lower order of polynomials can be obtained by setting the appropriate higher order coefficients equal to zero. Therefore, for the second order polynomial $[a_3]$, and $[a_4]$ are each set equal to the zero vector and for the third order polynomial $[a_4]$ is set equal to the zero vector.

The interface condition and the boundary conditions are similar to the ones described in the previous chapter. The relaxation method was applied to the following parameters

1. The coefficients of a chosen polynomial.

$$[C_i]^{(K)} = [\bar{C}_i]^{(K)}\, w + (1-w)[C_i]^{(K-1)} \quad i=0,1,2,3,4 \tag{4-29}$$

2. The flux and the interface conditions.

$$[\phi_i]^{(K)} = [\bar{\phi}_i]^{(K)}\, w + (1-w)[\phi_i]^{(K-1)} \tag{4-30}$$

$$\frac{d[\phi_i]^{(K)}}{dx} = \frac{[\phi_i]^{(K)} - [\psi_i]^{(K)}}{\theta_i} \tag{4-31}$$

where θ and ψ were described in the previous chapter.

3. The neutron source.

$$S_i^{(K)} = \bar{S}_i^{(K)}\, w + (1-w)\, S_i^{(K-1)} \tag{4-32}$$

where the neutron source is defined by

$$S = \frac{\sum_{i=1}^{I} \sum_{g=1}^{G} (\nu\Sigma_{fg}\phi_g)\Delta V_i}{\sum_{i=1}^{I} \Delta V_i} \tag{4-33}$$

B. Computer Code and Results

The computer code ONODE [9] was expanded to handle multigroup neutrons. The modified ONODE code is called ONODEM and has the same flow chart as the one in Figure 3-8. The ONODEM code has been applied to a one dimensional slab using three neutron group. Two different fuel loading patterns are used, where pattern A is shown in Figure 4-1, and pattern B in Figure 4-2. The cross section data used for the fuel types in the two different fuel patterns are

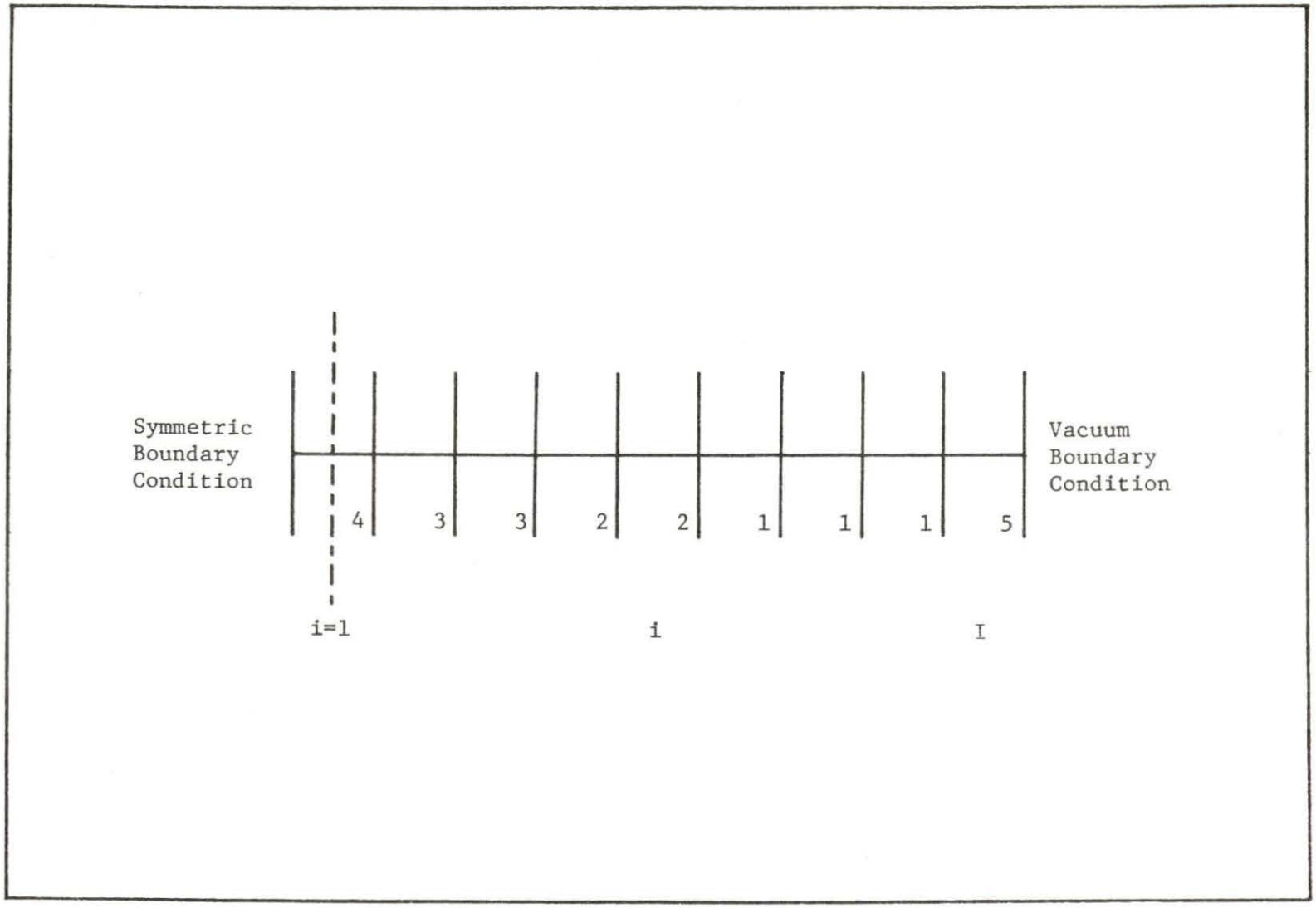

Figure 4-1 Fuel loading pattern A for the one dimensional model

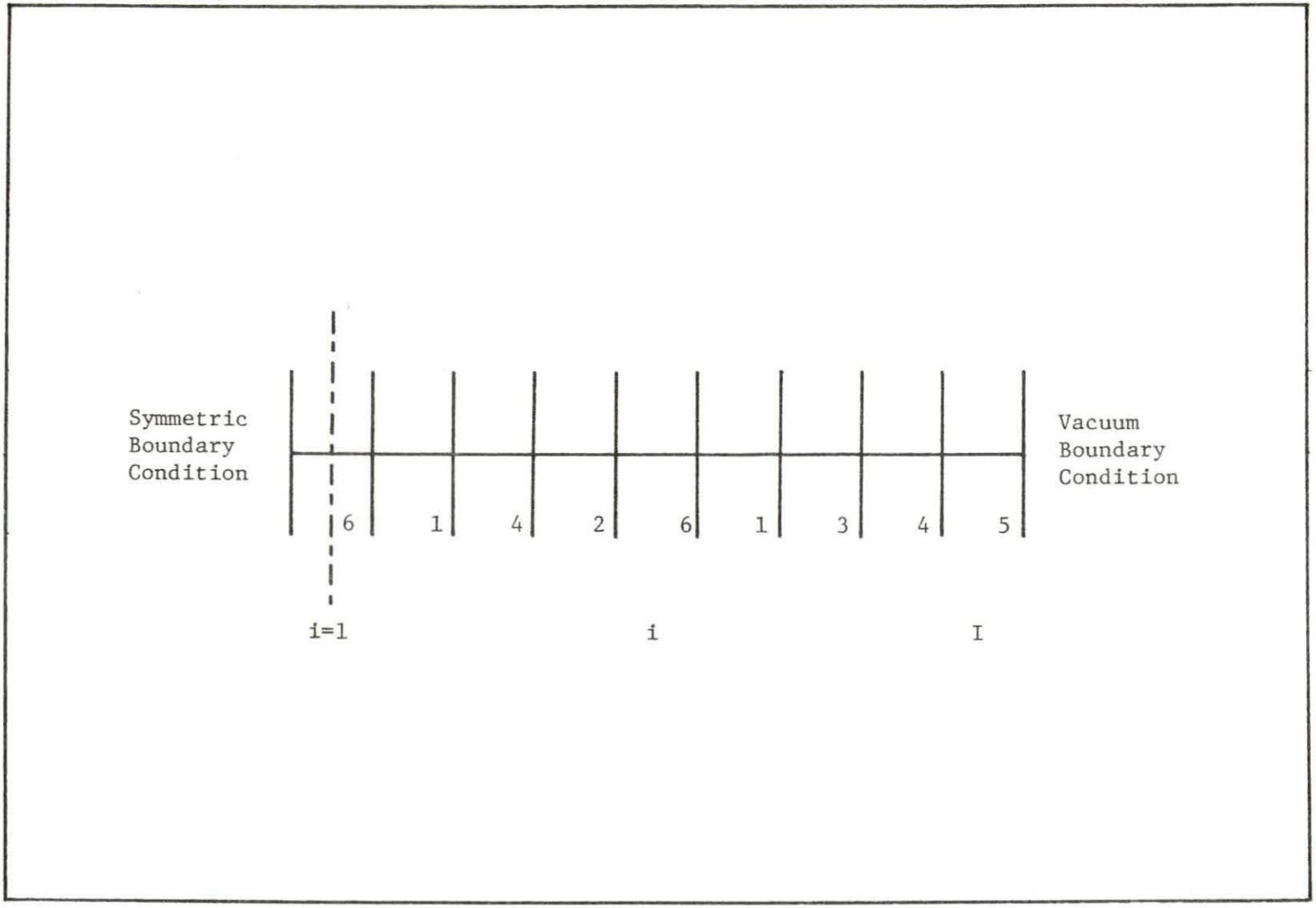

Figure 4-2 Fuel loading pattern B for the one dimensional model

given in Table 4-1 and have been generated at Iowa State University. A fine mesh finite difference diffusion theory calculation (1 cm per mesh point) is used as the reference calculations for the two fuel loading patterns. The convergence of the fine mesh was set equal to 1E-09 in all of the calculations.

Figure 4-3 illustrates the fast, intermediate, and thermal flux distributions calculated using fine mesh diffusion theory for pattern A. One can note the large thermal flux peaking in the reflector. After 111 iterations, a k_{eff} of 1.05560 was obtained. Figure 4-4 shows the flux distributions of the fine mesh and results of the ONODEM code using a second order polynomial. A k_{eff} of 1.055236 and a convergence of 3.3436E-09 was attained at 500 iterations for this order of polynomial. As it is observed, the second order polynomial is not adequate to predict the flux peak in the reflector and the node next to it. Since only fuel is used in pattern A, it appears that a second order polynomial is adequate to predict the flux inside the slab where no reflector and control is used. This is best shown in Figure 4-5 where the reflector was replaced with a vacuum boundary condition. Excellent agreement is observed using this order of polynomial with the fine mesh. The convergence of the system in Figure 4-5, was 4.30159E-09 at 500 iterations, and a k_{eff} of 1.05346 was obtained.

Table 4-1 Nuclear Fuel Data

	Fuel Type #1	Fuel Type #2	Fuel Type #3	Fuel Type #4	Reflector #5	Fuel and Control #6
Enrichment	2.6%	2.8%	3.0%	3.2%	--	3.2%
D_1	0.180E+01	0.180E+01	0.180E+01	0.180E+01	0.286E+01	0.180E+01
D_2	0.803E+00	0.804E+00	0.805E+00	0.806E+00	0.817E+00	0.789E+00
D_3	0.259E+00	0.259E+00	0.258E+00	0.258E+00	0.237E+00	0.357E+00
Σ_{a1}	0.350E-02	0.347E-02	0.345E-02	0.342E-02	0.191E-03	0.632E-02
Σ_{a2}	0.297E-01	0.293E-01	0.287E-01	0.283E-01	0.577E-03	0.660E-01
Σ_{a3}	0.970E-01	0.937E-01	0.898E-01	0.861E-01	0.870E-02	0.999E-01
$\nu\Sigma_{f1}$	0.418E-02	0.413E-02	0.407E-02	0.401E-02	0.000	0.433E-01
$\nu\Sigma_{f2}$	0.126E-01	0.118E-01	0.110E-01	0.102E-01	0.000	0.129E-01
$\nu\Sigma_{f3}$	0.142E+00	0.134E+00	0.126E+00	0.118+00	0.000	0.143E+00
$\Sigma^s_{1\to2}$	0.328E-01	0.328E-01	0.328E-01	0.328E-01	0.510E-01	0.335E-01
$\Sigma^s_{1\to3}$	0.000	0.000	0.000	0.000	0.000	0.000
$\Sigma^s_{2\to3}$	0.496E-01	0.498E-01	0.507E-01	0.502E-01	0.114E+00	0.496E-01

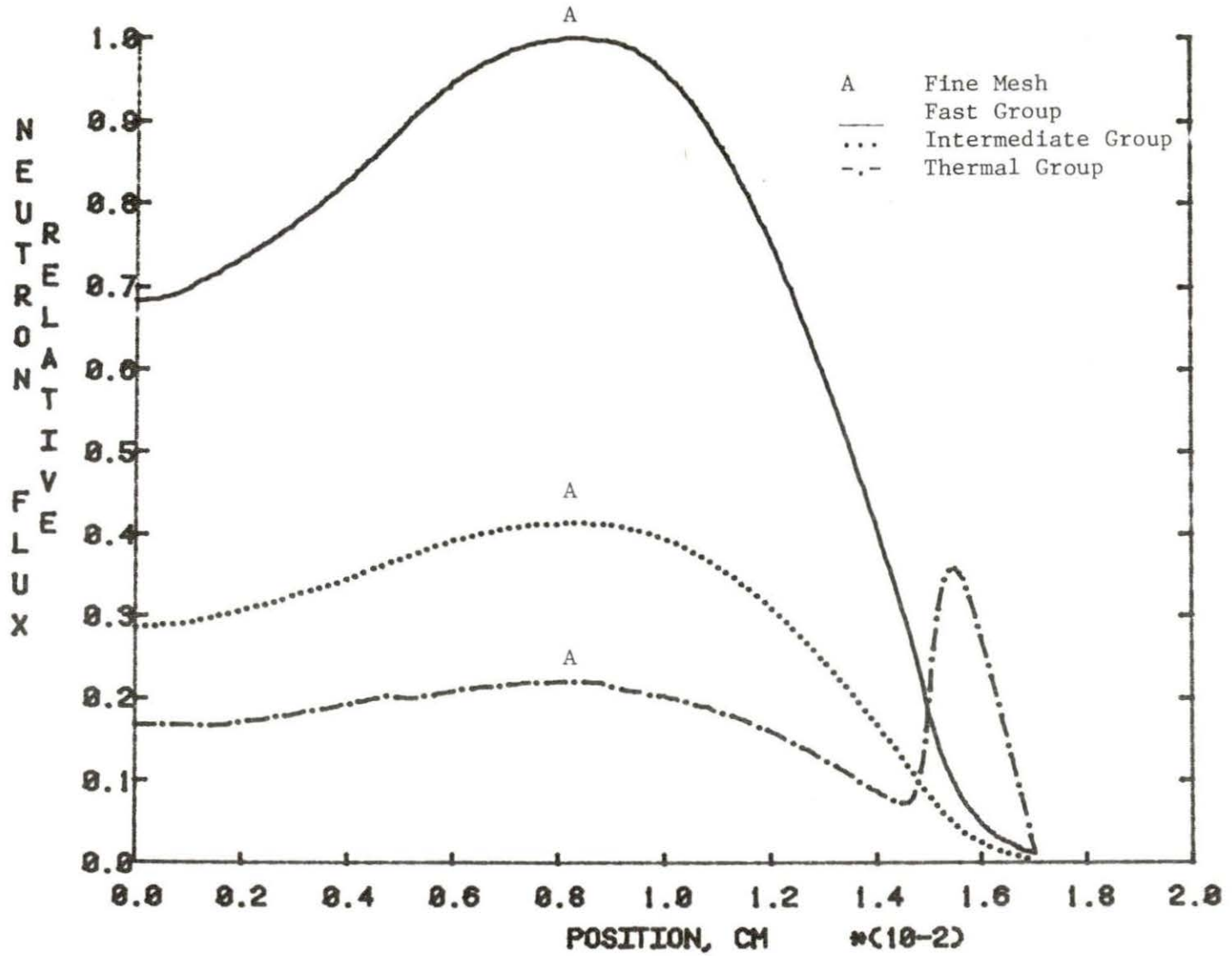

Figure 4-3 Flux distributions of a fine mesh diffusion theory for pattern A

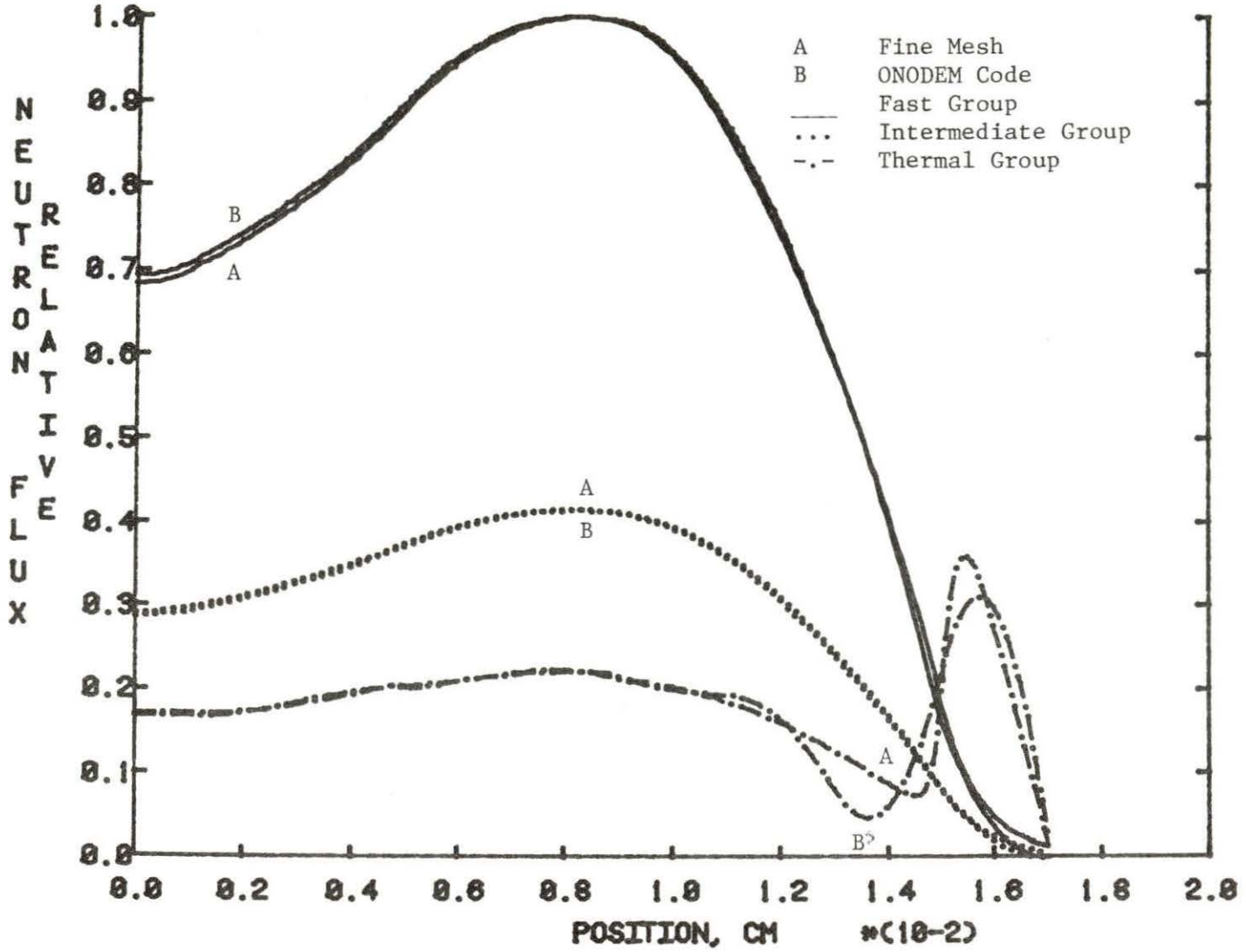

Figure 4-4 Flux distribution comparisons for a second order polynomial for pattern A

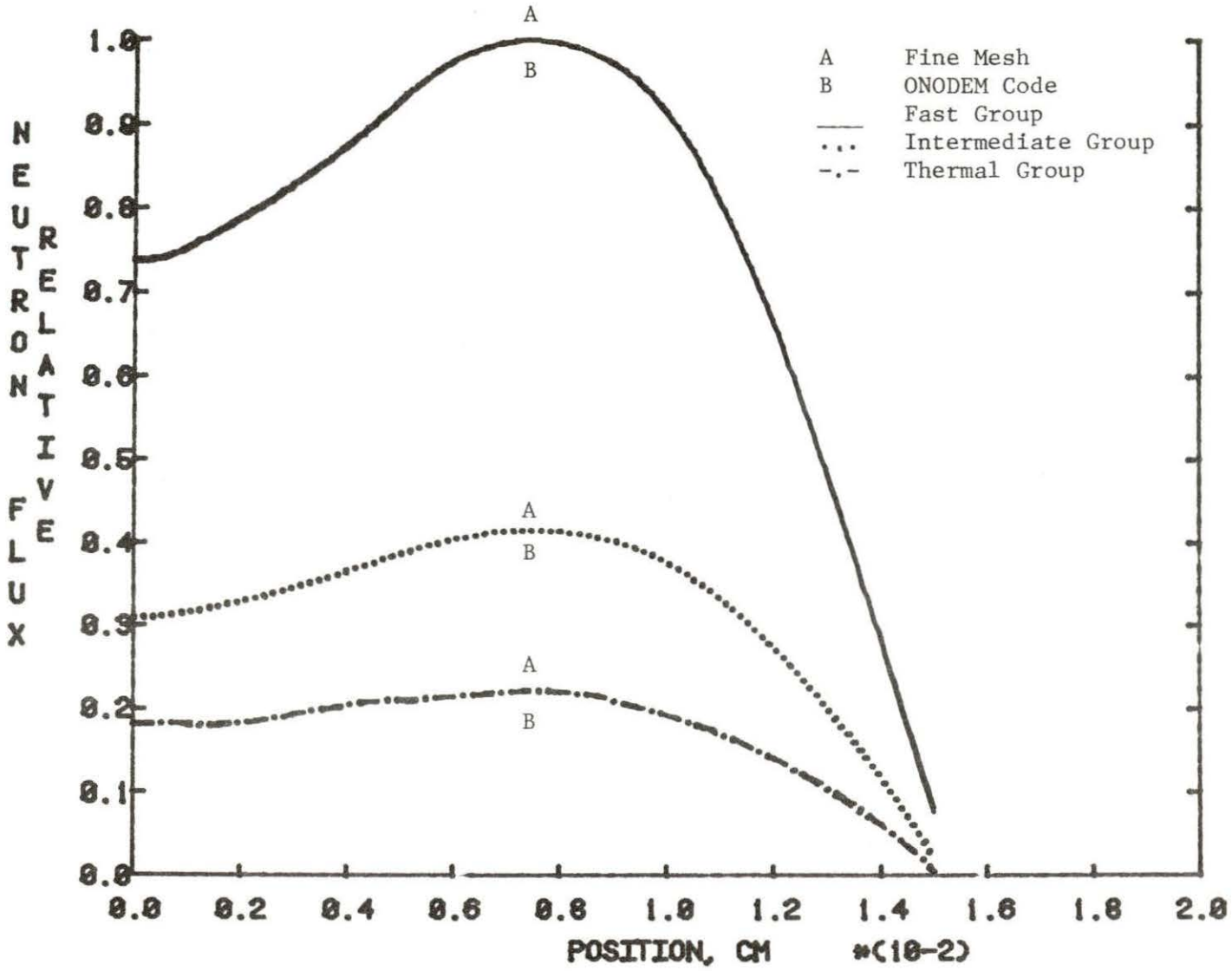

Figure 4-5 Flux distribution comparisons for a second order polynomial for pattern A without a reflector

The third order polynomial was then used to approximate the flux distributions for pattern A and hopefully resolve the thermal flux discrepancies in the reflector and the node next to it. Figure 4-6 shows the flux distributions of the fine mesh and results of ONODEM using a third order polynomial. A K_{eff} of 1.055317 and a convergence of 6.3238E-09 was attained at 500 iterations for this order of polynomial. As one can observe the system's k_{eff} using this order of polynomial is closer to the k_{eff} of the fine mesh and the flux agreement is very good inside the core. The flux peak in the reflector and the node next to it is also better predicted using this order of polynomial. But from the standpoint of power calculations the flux disagreement is still high in the reflector and the node next to it.

The fourth order polynomial was then used to approximate the flux distributions for pattern A. Figure 4-7 shows the flux distributions of the fine mesh calculations and results of the ONODEM code using a fourth order polynomial. Excellent agreement is observed between the fluxes, but still there seems to be a small tilt in the thermal flux at the node next to the reflector. This problem is solved if one uses two nodes per fuel assembly in the outer fuel assembly and the reflector assembly. Figure 4-8 shows the flux distributions of the fine mesh and the fourth order poly-

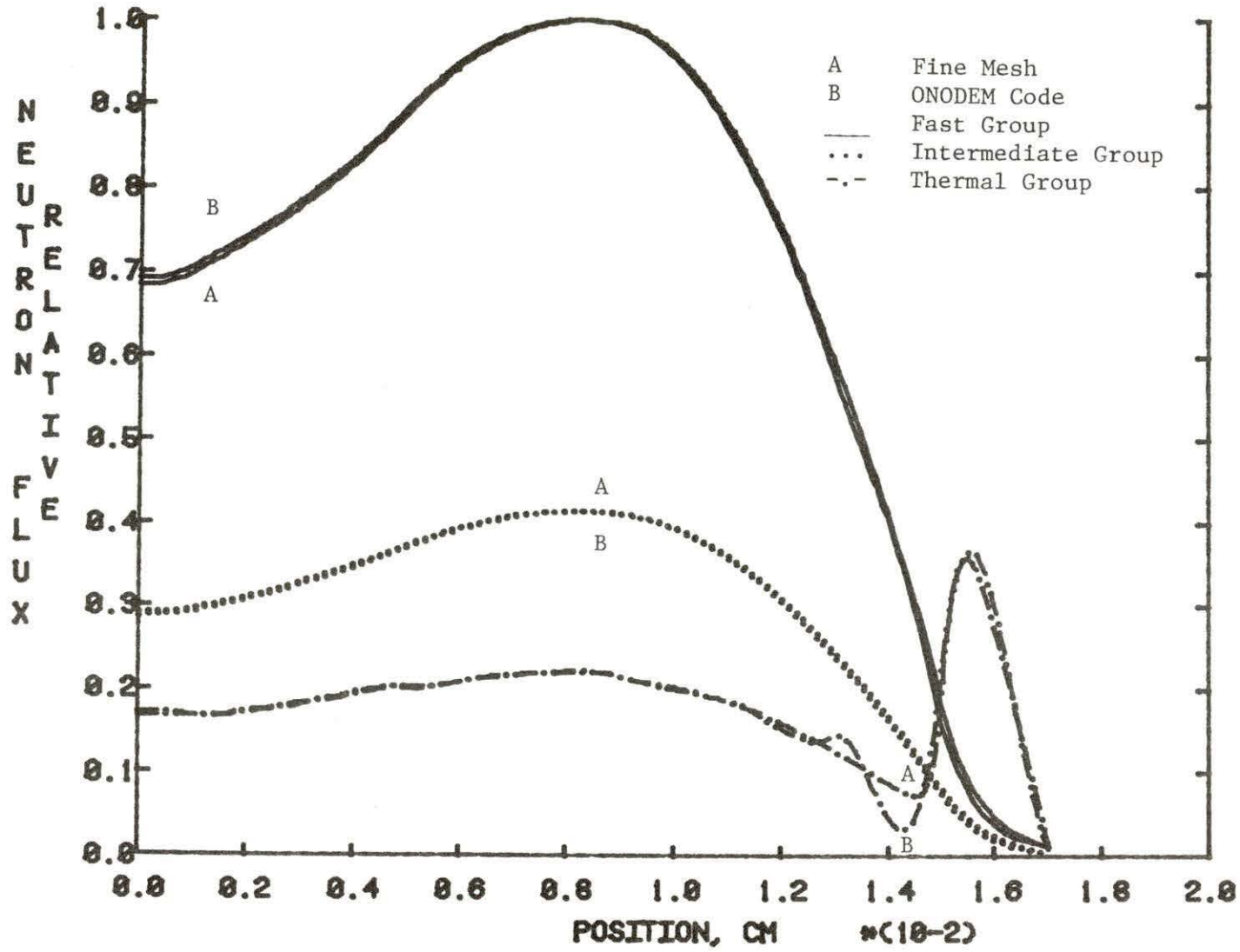

Figure 4-6 Flux distribution comparisons for a third order polynomial for pattern A

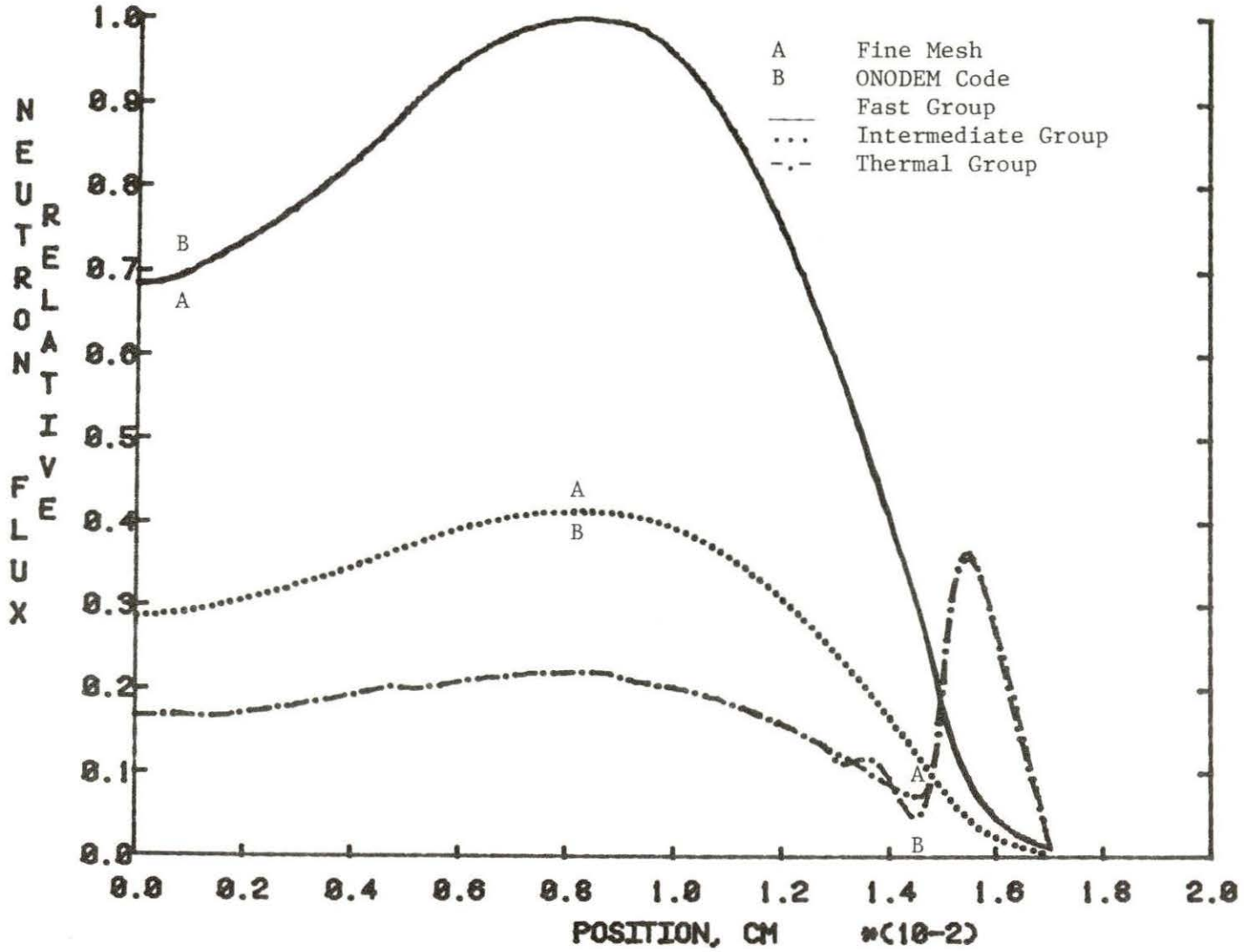

Figure 4-7 Flux distribution comparisons for a fourth order polynomial for pattern A

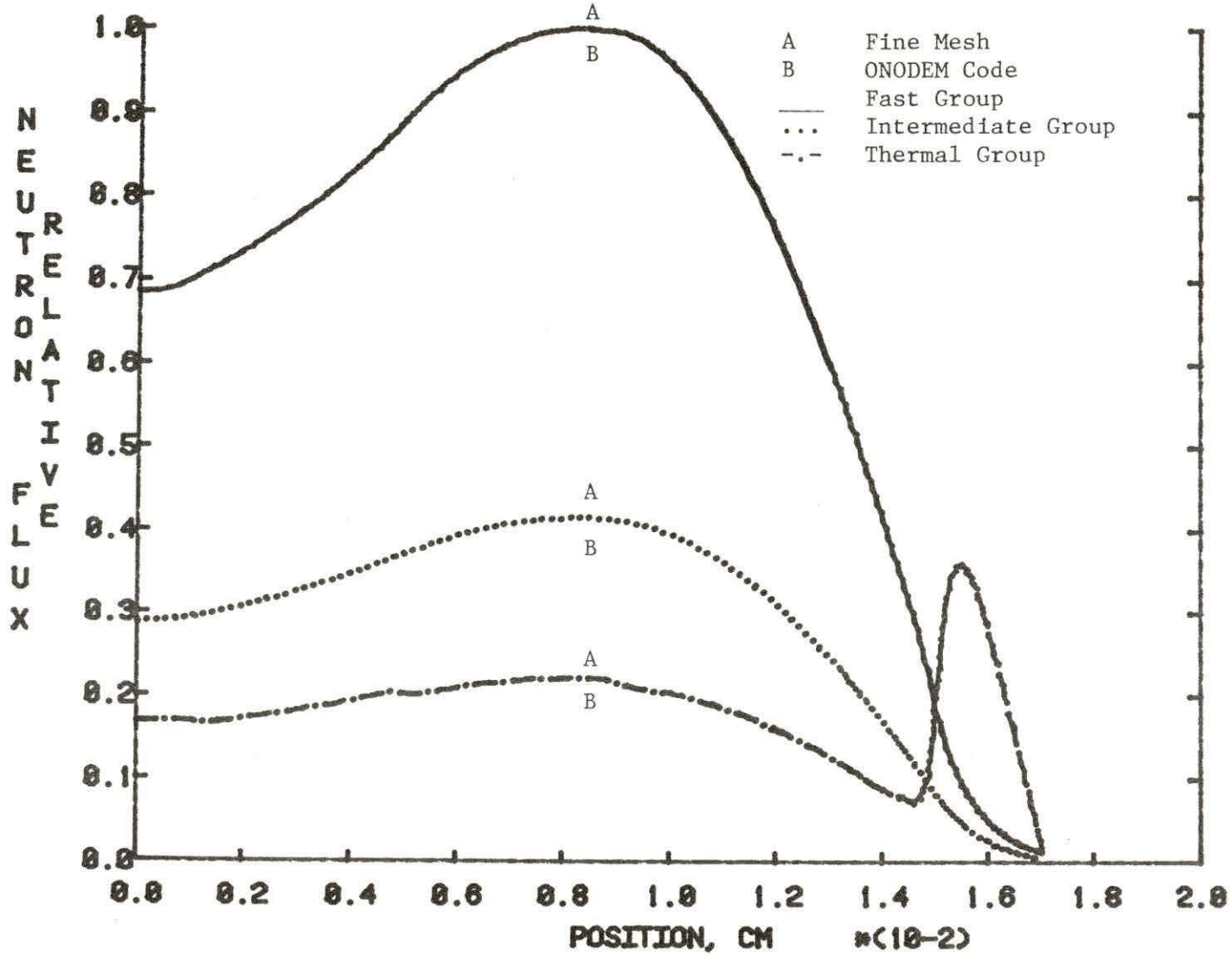

Figure 4-8 Flux distribution comparison for a fourth order polynomial. Four nodes in the outer two nodes for pattern A

nomial using two nodes in the outer two nodes. The flux agreement is excellent.

A k_{eff} of 1.05424 and a convergence of 9.6037E-06 was attained at 500 iterations for the fourth order polynomial. Figure 4-9 shows the eigenvalue convergence of the system. As it is observed from this figure, the eigenvalue oscillates and it appears that the number of iterations is not enough. Therefore, the number of iterations was increased to 1,000, doing so resulted in a k_{eff} of 1.055530 and a convergence of 7.8728E-08. The convergence and k_{eff} have improved using a large number of iterations. But using 1,000 iterations is not practical and hence, Benghanam [2] suggested a set of optimized relaxation parameters. Using the suggested relaxation parameters, a k_{eff} of 1.055520 and a convergence of 9.70419E-09 was attained at 500 iterations. Figure 4-10 shows the eigenvalue convergence of the fourth order polynomial using the optimized relaxation parameters. A better result is observed in Figure 4-10 than the one in Figure 4-9.

Pattern B in Figure 4-2 was then used to compare the ONODEM results and the fine mesh. The reactivity change due to fuel and control is 6.61% $\frac{\Delta k}{k}$. Figure 4-11 shows the flux distributions of the fine mesh. One can note the large flux dips in the two control assemblies, and the thermal flux peaking in the reflector.

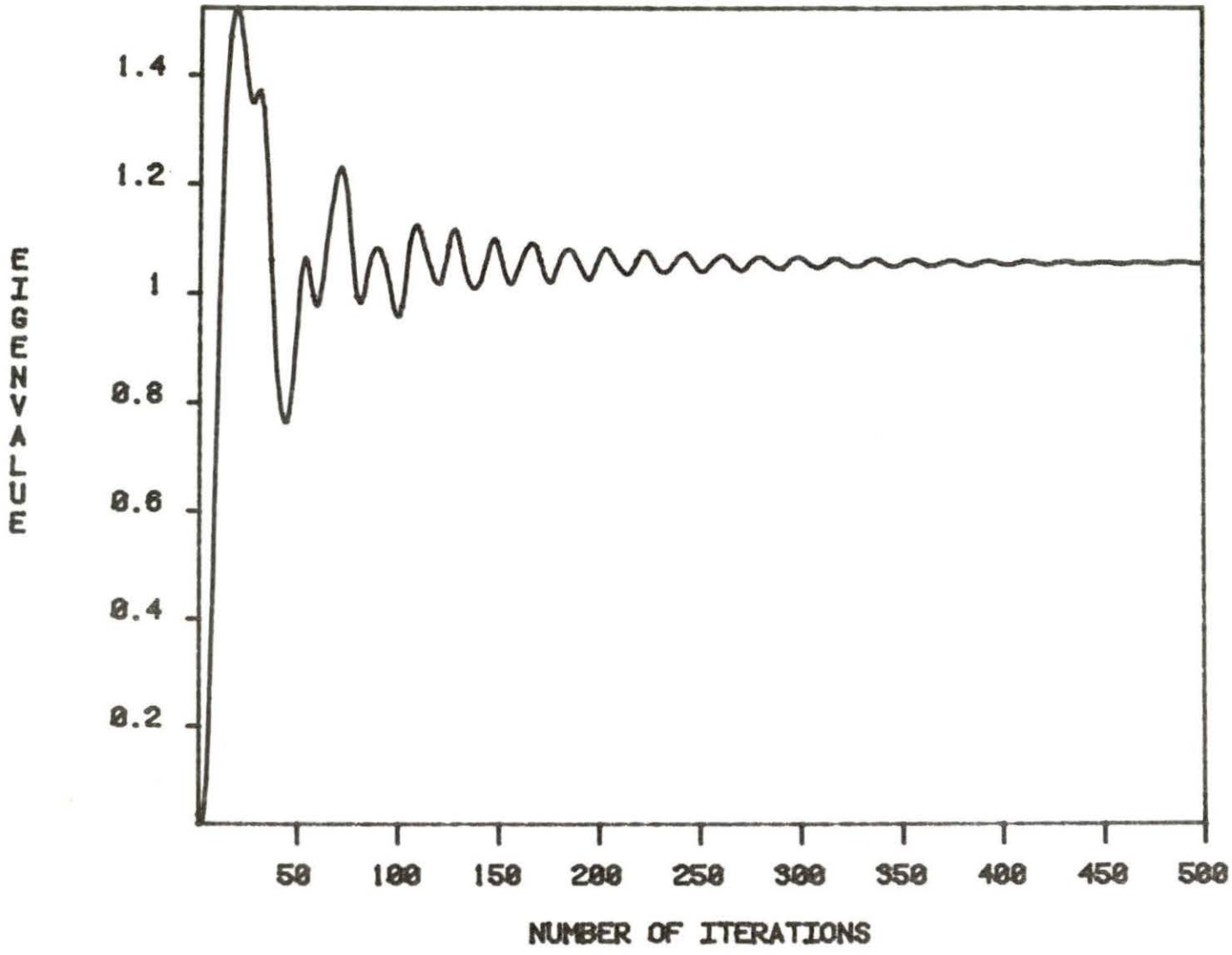

Figure 4-9 Eigenvalue convergence for a fourth order polynomial for pattern A

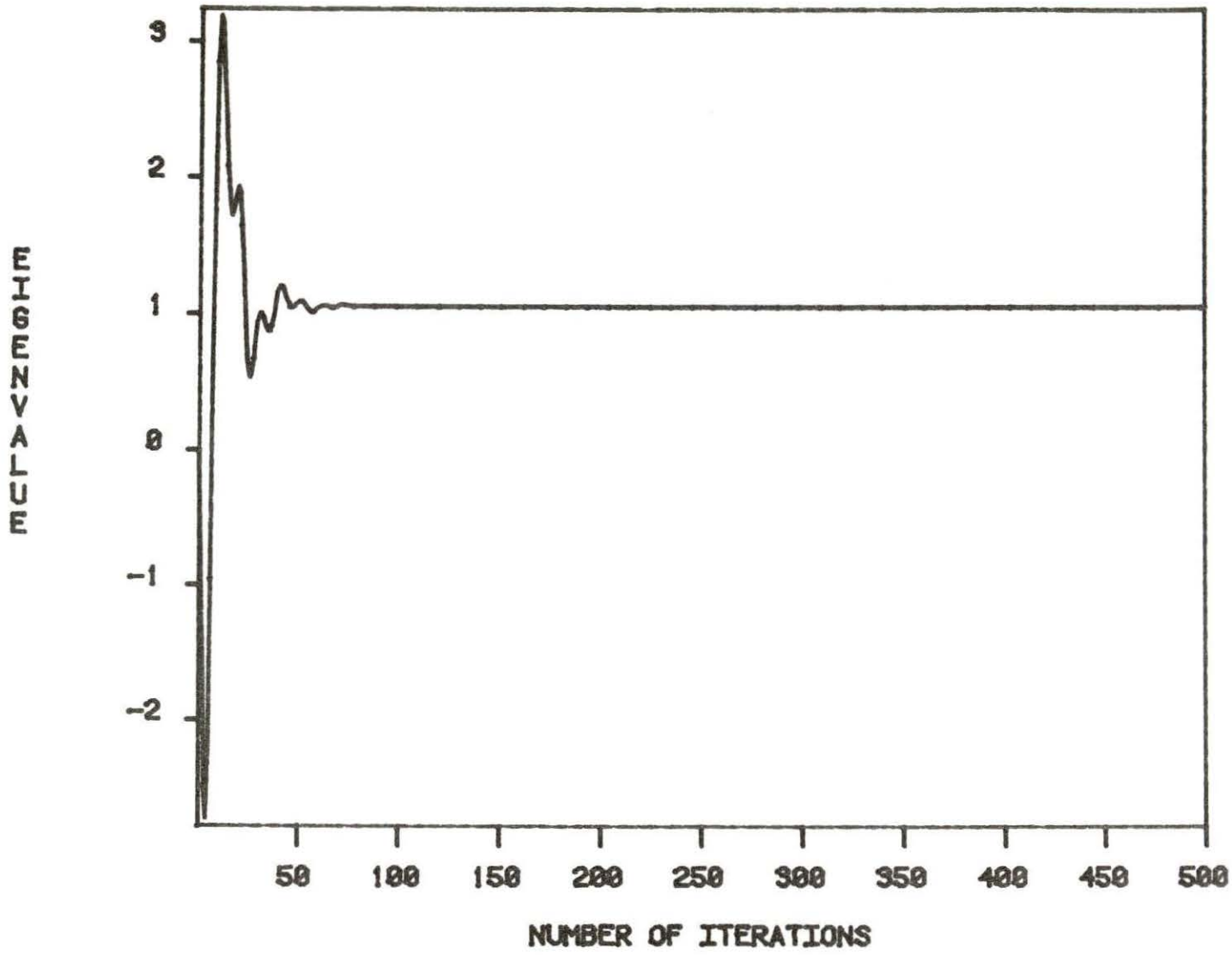

Figure 4-10 Eigenvalue convergence for a fourth order polynomial for pattern A. Using the optimized relaxation parameters

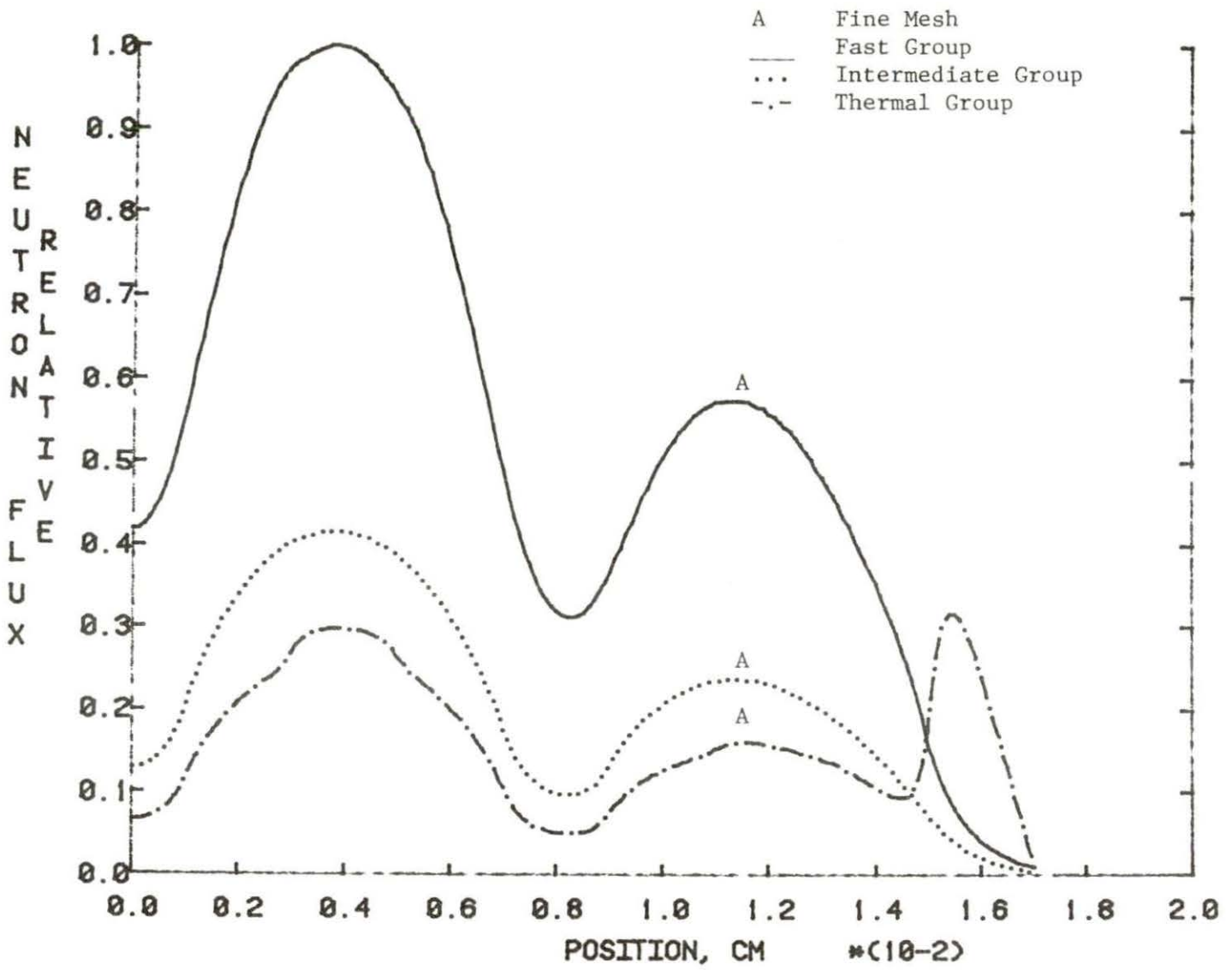

Figure 4-11 Flux distributions of a fine mesh diffusion theory for pattern B

A k_{eff} of 1.13533 was obtained after 118 iterations for the fine mesh calculation. Pattern B is used to investigate if the different polynomials used by ONODEM can handle large flux changes.

Figure 4-12 illustrates the flux distributions of the fine mesh and the ONODEM code using a second order polynomial. A k_{eff} of 1.135211 and a convergence of 7.74750E-06 was obtained at 500 iterations. As it can be observed, the second order polynomial is not adequate to predict the flux accurately. Although some agreement is seen in the large flux peak, it should not be mistaken that good flux agreement exists. The reason is because of the normalization process that was used to normalize every value with respect to the highest flux. Therefore, it appears that the second order polynomial is not adequate to predict the flux when control and reflector regions are present. One can observe the proof of this last statement by looking at Figure 4-13 where a second order fit was used for pattern B with the reflector replaced by a vacuum boundary condition.

The third order polynomial was then used for pattern B. Figure 4-14 shows the flux distributions of the fine mesh and ONODEM code using a third order polynomial. A k_{eff} of 1.136028 and a convergence of 2.9928E-06 was obtained for this order of polynomial. Better flux agreement is observed especially in the reflector but the flux agreement is still not satisfactory. It

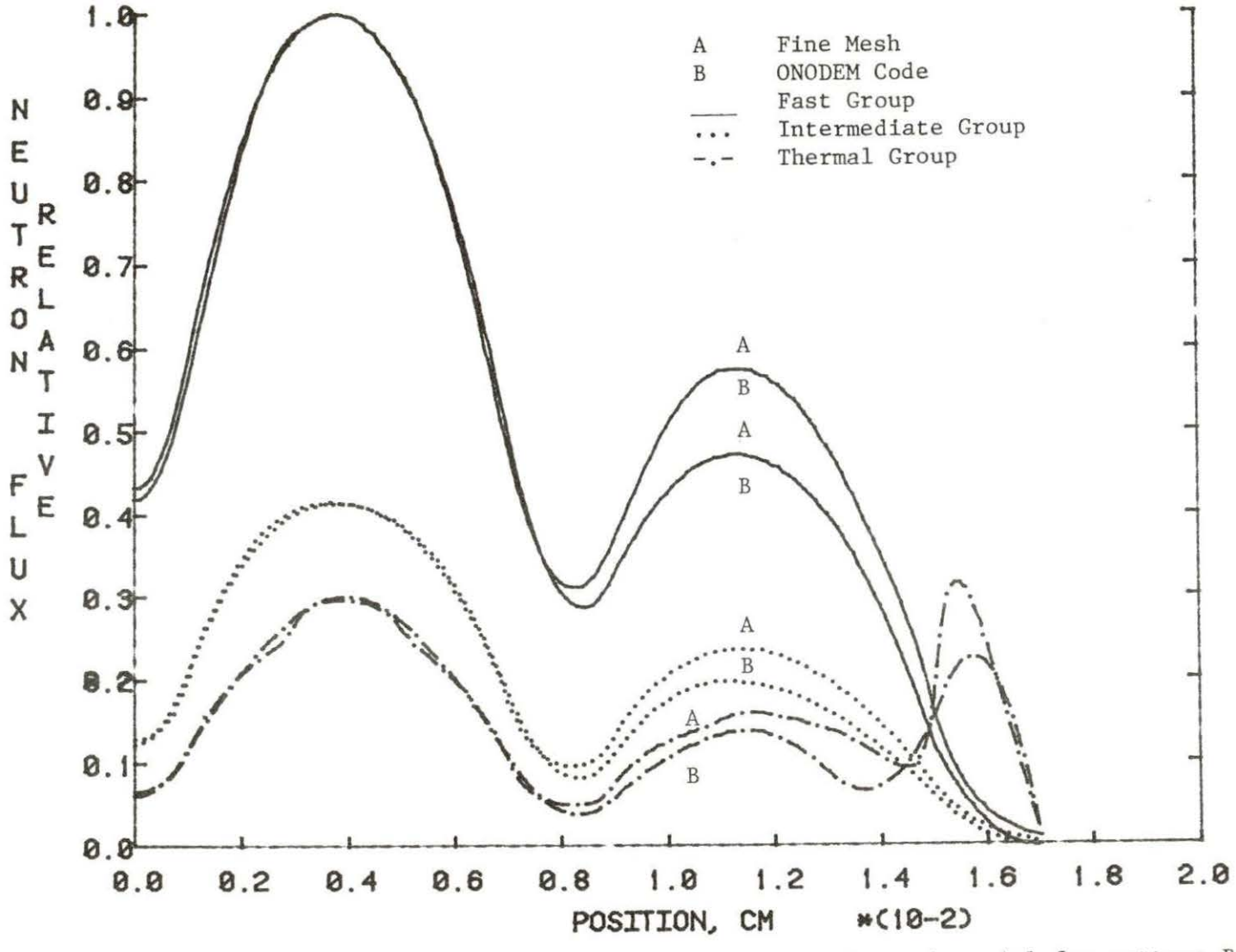

Figure 4-12 Flux distribution comparisons for a second order polynomial for pattern B

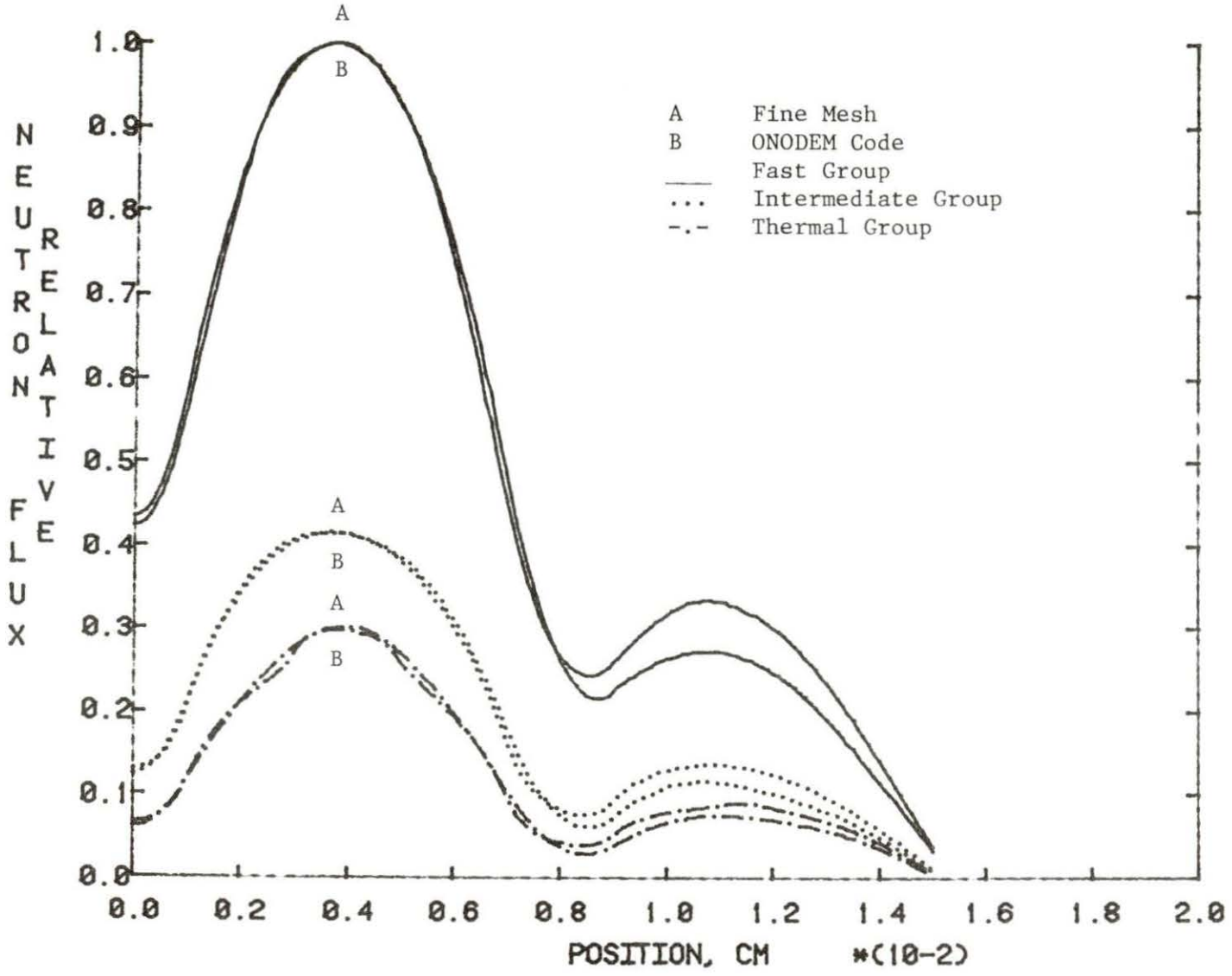

Figure 4-13 Flux distribution comparisons for a second order polynomial for pattern B without a reflector

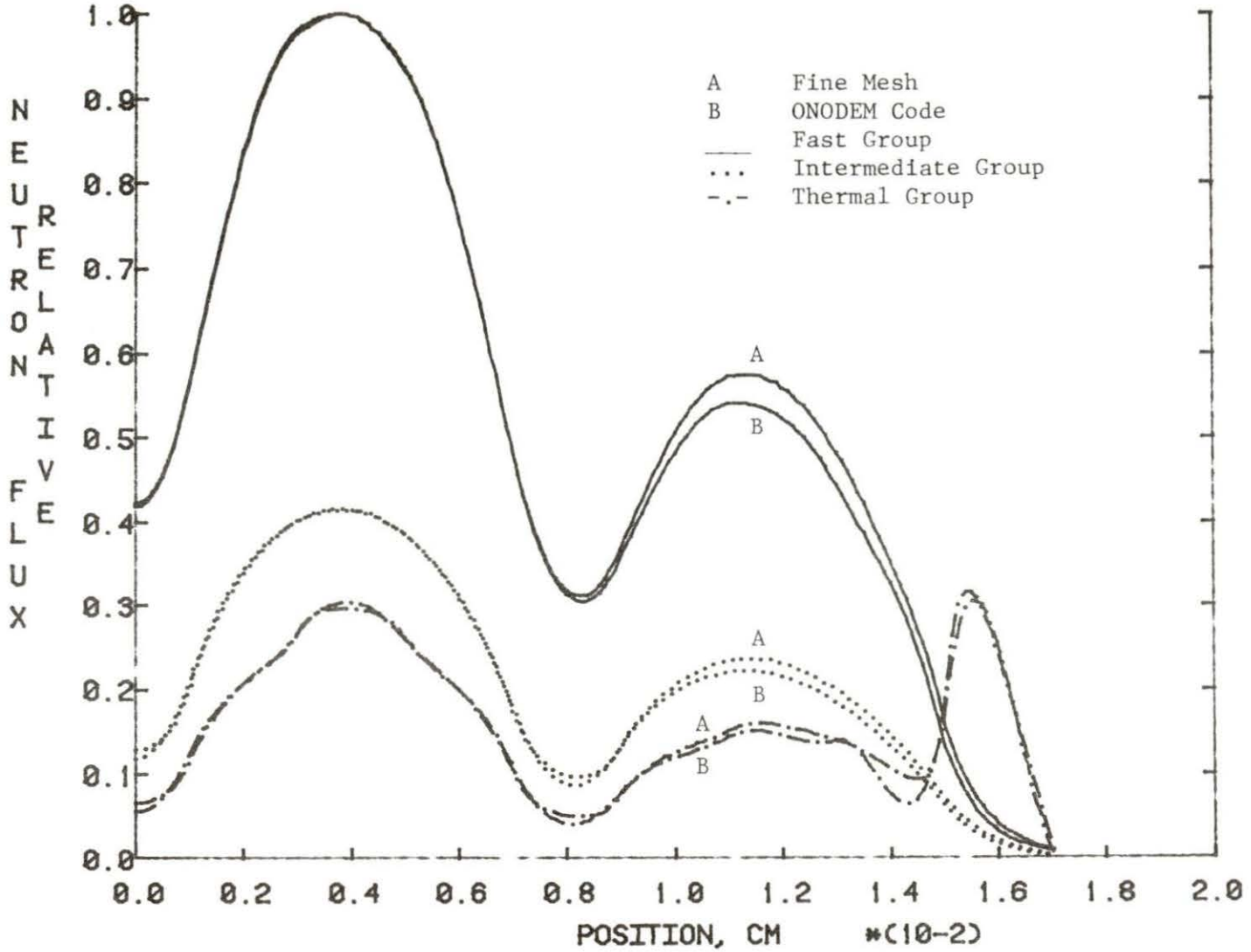

Figure 4-14 Flux distribution comparisons for a third order polynomial for pattern B

appears that the third order polynomial is adequate to approximate the flux for regions where fuel and control are used and not for a region where a reflector is present. This is exactly the case when one looks at Figure 4-15 where a third order fit was used for pattern B with the reflector replaced by a vacuum boundary condition. Excellent flux agreement is observed in Figure 4-15.

The fourth order polynomial was then used for pattern B with the hope that it resolves some of the problems encountered with second and third order polynomials. Figure 4-16 shows the flux distributions of the fine mesh and the ONODEM using a fourth order polynomial. Excellent agreement is observed between the flux distributions of the fine mesh and the ONODEM code. A k_{eff} of 1.124541 and a convergence of 1.339565E-04 was obtained at 500 iterations. The convergence is not at all acceptable and this is exactly the same problem that occurred for pattern A. Again, the suggested relaxation parameters [2] were used and a k_{eff} of 1.135388 and convergence of 0.286707E-06 was obtained. Therefore, it is concluded that a fourth order polynomial is capable of predicting the flux in any region of the slab providing optimum relaxation parameters are used.

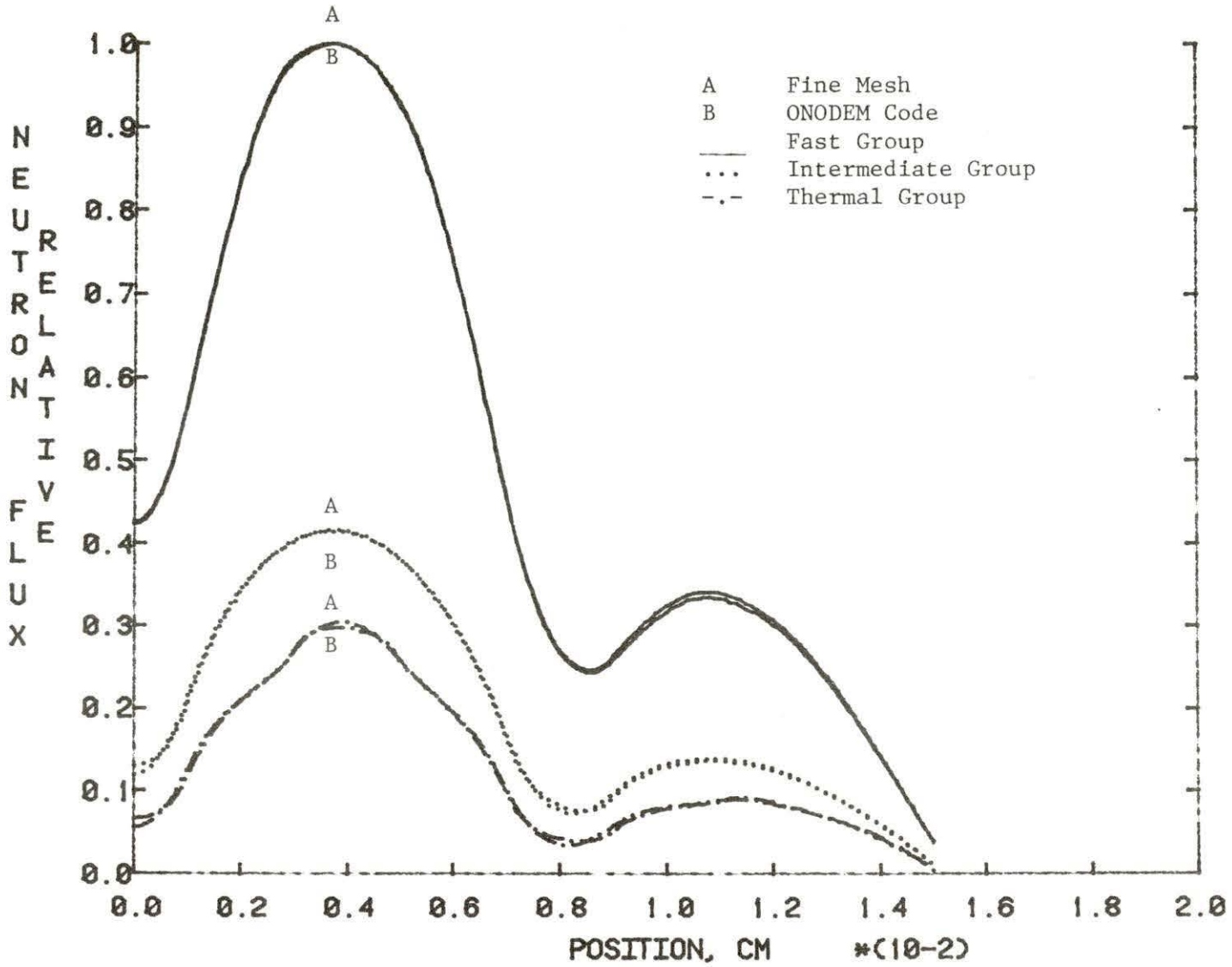

Figure 4-15 Flux distribution comparisons for a third order polynomial for pattern B without a reflector

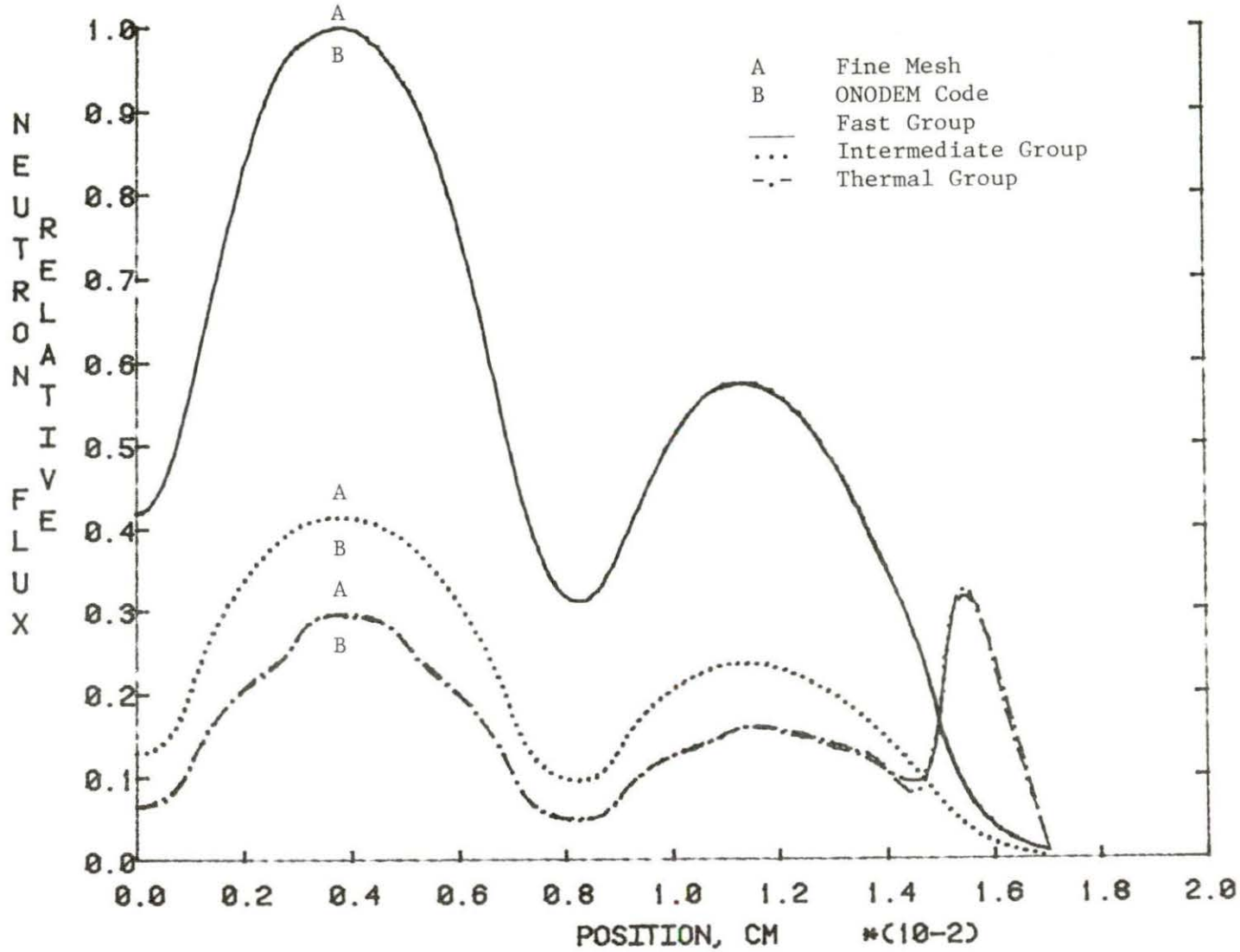

Figure 4-16 Flux distribution comparisons for a fourth order polynomial for pattern B

Figure 4-17 shows the neutron current along the core for the fourth order polynomial for pattern B. As it is observed, the current is indeed continuous along the core for the three neutron groups. The continuity of the current was used in the interface condition for every iteration and is an important criteria in calculating the flux at the interfaces along the core.

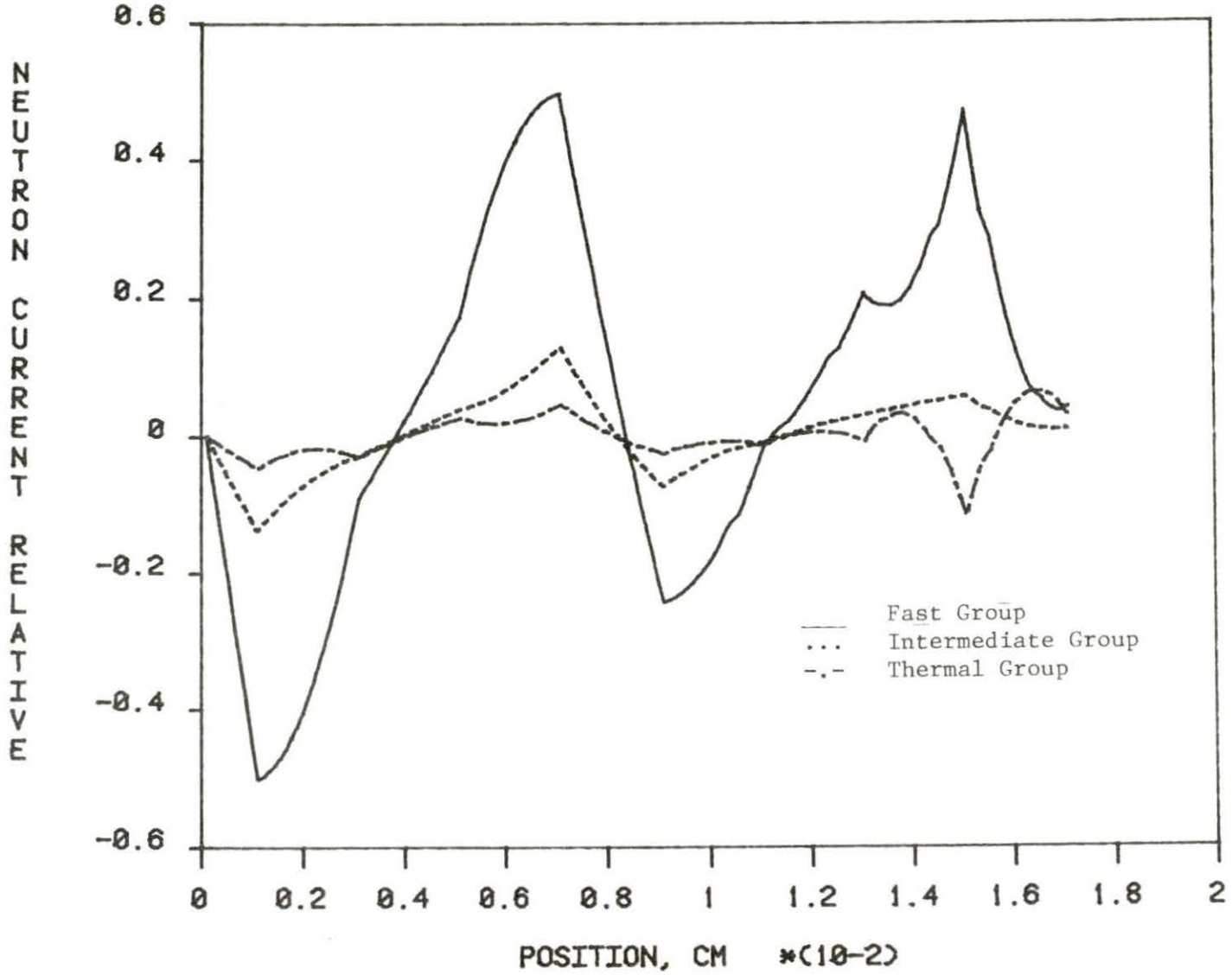

Figure 4-17 Current-continuity across the core for a fourth order polynomial for pattern B

V. SUMMARY AND CONCLUSIONS

The purpose of this study was to develop a one dimensional finite element nodal model suited for calculating the flux inside a reactor. The flux calculated from the model could in turn be used for calculating the power of the reactor. Since the power calculation precision does not need to be as detailed as other parameters of a reactor design, diffusion theory is adapted as the basis of calculating the flux.

The model is based upon polynomial expansion of the neutron flux within the node. Second, third, and fourth order polynomials were used and each have proven to be adequate depending on the region of the reactor. The interface fluxes and node neutronic properties are used to evaluate the polynomial coefficients. Using these coefficients, one can calculate new fluxes and the process is continued until convergence is attained.

The second order polynomial was first used to approximate the flux. The second order polynomial is not adequate to approximate large flux changes. Also, the shape of the flux in the reflector and control nodes were not acceptable using this order of polynomial. On the other hand, it appears that the second order polynomial is capable of approximating the flux when only fuel regions are present.

The third order polynomial was then used to approximate the flux. The third order polynomial did a better job of approximating the

flux in the reflector and the control regions. When the reflector region was replaced by a vacuum boundary condition, excellent flux agreement was observed in the fuel and control regions. Therefore, it is concluded that the third order polynomial is adequate for approximating the flux in the fuel and control regions.

The fourth order polynomial was then investigated in approximating the flux. The fourth order polynomial is capable of approximating the flux in any region of the reactor provided that optimized relaxation parameters are used.

One dimensional finite element nodal model is not significant for practical use since the one dimensional fine mesh finite difference equation can be easily solved. However, certain properties of the model can be studied in the simpler one dimensional framework and then extended and tested in the more complicated two and three dimensions.

VI. SUGGESTIONS FOR FUTURE RESEARCH

The following suggestions are made for possible future research:

1. A mathematical technique should be developed to successfully predict the input relaxation parameters. This is an important area since the convergence of the system is heavily dependent on these parameters.
2. The model can be expanded into higher order polynomials. The main problem is the development of the coefficient formulas. However, once these formulas have been developed, very little additional computational time or computer storage is required.
3. Since the flux distributions and hence, the power distributions are given in terms of polynomials, the burnup history of each node can also be given in terms of polynomials. Hence, each node or assembly will have its individual set of burnup polynomial coefficients. If assemblies are shuffled or even stored in a fuel pool, the burnup polynomial coefficients will accompany a particular assembly. This is the advantage of expanding the polynomials over the individual nodes.
4. Expressions analogous to those of the one dimensional model can be developed for two and three dimensional models. If this is done, a two and three dimensional calculations should be performed and compared. If adequate agreement is obtained between

the two models, the two dimensional model should be used since it requires less computer time and hence, saving of funds could result.

VII. REFERENCES

1. H. W. Graves, Jr. Nuclear Fuel Management. John Wiley & Sons, New York, New York, 1979.

2. M. Benghanam. "Enhanced Convergence Technique for a One Dimensional Nodal Model," Unpublished M.S. Thesis, Iowa State University, Ames, Iowa, 1983.

3. A. F. Henry. Nuclear Reactor Analysis. The MIT Press, Cambridge, Massachusetts, 1975.

4. J. Askew. "Summary of the Meeting" in Calculation of 3-Dimensional Rating Distributions in Operating Reactors. Organization for Economic Cooperation and Development, Paris, 1979.

5. M. R. Wagner. "Current Trends in Multidimensional Static Reactor Calculations." Proceedings of the Conference on Computational Methods in Nuclear Engineering, April 1975.

6. J. R. Lamarsh. Nuclear Reactor Theory. Addison-Wesley Publishing Company, New York, New York, 1966.

7. R. L. Burden et al. Numerical Analysis. Prindle, Weber & Schmidt, Boston, Massachusetts, July, 1981.

8. A. F. Rohach. ONODE Code. Department of Nuclear Engineering, Iowa State University, Ames, Iowa, 1982.

9. Numerical Determination of the Space, Time, Angle, or Energy Distribution of Particles in an Assembly. Argonne Code: Benchmark Problem Book. Supplement 2. Argonne National Laboratory, Oak Ridge, Tennessee, June, 1977.

VIII. ACKNOWLEDGEMENTS

The author is indebted to his major professor, Dr. Alfred F. Rohach for his support, interest, suggestions, and encouragement during the various phases of this research. In addition, the author wishes to express his special appreciation to the Department of Nuclear Engineering for a departmental assistantship; to Mr. Mohammad Benghanam for many helpful suggestions and discussions during the time this study was performed; to Steven Sorrell for generating cross section data; and to Jo Sedore for typing this thesis.

Finally, the author wishes to thank his parents, Mr. and Mrs. Reza Feiz, for their continued support and encouragement.